Head Office: Università degli Studi di Padova

Department of Animal Medicine, Production and Health

Ph.D. COURSE IN: ANIMAL AND FOOD SCIENCE

SERIES XXXV

Application of spectroscopic techniques and chemometric approaches for authentication of animal food products

Coordinator: Prof.ssa Angela Trocino

Supervisor: Prof. Severino Segato

Ph.D. student: Ilaria Lanza

Declaration

I, Ilaria Lanza, certify that the work I am submitting is my own and has not been submitted for another degree, either at University of Padova or elsewhere. All external references and sources are clearly acknowledged and identified within the contents.

Abstract

Nowadays, food quality assessment has become a topic of huge importance for both the consumer and the industry along the whole supply chain. Globalisation has resulted in increasingly vulnerable and less transparent food supply chains with greater incidence of sophisticated food fraud especially economically motivated adulteration. With increasing complexity of food chains and hidden food fraud, the authentication of agri-food products has become necessary. There is a need to develop analytical methodologies to tackle authenticity concerns, reassure safety parameters and ensure product quality. This body of work regards different applications of NMR and NIR spectroscopic techniques to evaluate authenticity of agri-food products from animal origin. These spectroscopic techniques provide structural and physiochemical properties of the sample of interest and could play an important role in the assessment of food quality due to their high-throughput and rapidity especially when using portable devices. The large datasets that can be generated using the various spectroscopic techniques can be analysed through chemometrics to extract the maximum amount of meaningful information and to distinguish significant trends in the data.

This thesis is divided in four case studies (**Chapters 3, 4, 5** & **6**) with different experimental designs, specific aims, food matrices and chemometric applications but they all share a common goal - to determine the viability of those techniques for food authentication.

In **Chapter 3**, a bench-top and a portable NIR spectrometer are used to discriminate pyrrolizidine alkaloids (PAs) and their N-oxides (PANOs) in 60 contaminated dehydrated bee pollen samples. PAs/PANOs are secondary metabolites produced by plants as a chemical defence against herbivorous insects. They have been reported to cause toxicity in many animal species, including humans especially in the case of chronic exposure. Since the consumption of bee pollen as a food supplement and a health product has increased in recent years, there is a need for rapid detection of these natural toxins in food; a challenge that could be met by NIR spectroscopy. The main goal of this trial was to assess the feasibility of two NIR systems by means of a statistical modelling approach based on targeted canonical discriminant analysis (CDA). The application of CDA resulted in a modelling statistical approach that demonstrates the predictive capacity of NIR systems to

distinguish among the three quantitative PA/PANOs classes, especially for detection of those samples belonging to the low class, which corresponds to safe samples.

In **Chapter 4**, the feasibility of using bench-top and portable NIR spectrometers for discriminating chicken breast shelf life is explored since fresh chicken meat (and meat in general) is highly perishable, leading to rapid loss of freshness during storage. Given the relatively short shelf life, preservation of quality during refrigerated storage represents one of the main challenges for the poultry industry. For this reason, a fast, cost-effective and non-destructive quality control system to assess meat freshness is needed. The study evaluates the feasibility of using NIR spectrometers combined with multivariate statistical models to discriminate chicken breasts during a 14-day refrigeration period. Also, suitability of the portable instrument for real time, on-the-spot evaluations is explored. NIR spectroscopy showed reliable effectiveness to recognise a 7-day shelf life threshold of breasts, suitable for routine at-line application for screening of meat quality.

In **Chapter 5**, capability of a VIS/NIR and two NIR instruments (portable and bench-top) to discriminate among table eggs from quails fed with different inclusion levels of silkworm pupa meal was evaluated. Since insects represent an alternative to conventional protein and lipid feedstuffs for monogastric animals, they could provide strategic solutions to address some environmental and ethical concerns linked to animal production and sustainability, and represent a premium value by declaring a highly-marketable labelling designation. Both NIR benchtop and portable devices combined with PLS-DA, KNN and SVM successfully showed capacity to recognise in the eggs the inclusion of insect meal in layers diet while the VIS-NIR portable tool displayed worse predictive capacity. The portable NIR spectrometer had comparatively accurate classification to the benchtop instrument, highlighting the potential of hand-held NIR spectrometers in at-line monitoring of insect-based feed along the egg supply chain.

In **Chapter 6**, discriminant capacity of fatty acids and NMR metabolomic profiles of milk from three different forage-based dairy chains was tested. Forage may affect the environmental sustainability of a given dairy chain, the quality of milk and its suitability for high-value dairy products. For these reasons, the study was conducted to better understand the influence of the dietary forage proportion on the milk metabolomic profile for better understanding of the relationship between feeding system and the wide pool of biomarkers useful to authenticate the milk dairy chain. The outcomes showed that only a total replacement of maize silage with legume and grass hays in the cows' diet led to a significant change in the milk metabolomic profile. A low-level FA and NMR data fusion coupled with

a CDA chemometric approach has been shown to improve the predictive performance of the supervised CDA discriminant model of milk samples from diverse ensiled or dried forage-based feeding systems.

Our findings suggest that both NIR and NMR spectroscopic techniques are effective methods for the authentication and analysis of the studied food products. Implementation of such methods in routine authentication analysis while keeping the costs low and the performance level high can open up the potential for further incorporation of NMR and NIR technologies in food analysis.

List of Commonly used Abbreviations

^{1}H NMR	Proton Nuclear Magnetic Resonance
CDA	Canonical Discriminant Analysis
EMA	Economically Motivated Adulteration
FS	Forage Source
GC-MS	Gas Chromatography-Mass Spectrometry
KNN	K-nearest Neighbour
LC–MS/MS	Liquid Chromatography coupled to Tandem Mass Spectrometry
MCC	Matthew Correlation Coefficient
ML	Machine Learning
MVSA	Multivariate Statistical Analysis
NIR	Near-infrared
NIRS	Near-infrared Spectroscopy
NMR	Nuclear Magnetic Resonance
PANOs	Pyrrolizidine Alkaloids N-oxides
PAPs	Processed Animal Proteins
PAs	Pyrrolizidine Alkaloids
PCA	Principal Component Analysis
PLS-DA	Partial Least Squares-Discriminant Analysis
RF	Random Forest
SVM	Support Vector Machine
VIP	Variable Importance in Projection

Acknowledgments

At the end of this journey I would to express my gratitude, by briefly mentioning the people whose contribution helped me cross the finish line.

First and foremost, I am extremely grateful to my supervisor Professor Severino Segato, who believed in my ability giving me the opportunity to undertake this journey which proved to be very stimulating and rewarding. Thank you for guiding me along my Ph.D. journey, for your tutelage, and for always being available and patient.

My gratitude extends to the University of Padova for the funding opportunity to undertake my studies at the Department of Animal Medicine, Production and Health.

I would like to acknowledge Professor Flaviana Gottardo and Professor Giulio Cozzi for their useful feedback and support in shaping experimental methods and critiquing results.

Thanks should also go to Dr Lorenzo Serva and M.Sc. Barbara Contiero for their technical support and advice. Your extensive experience and knowledge of the field of statistics was fundamental to this work and highly appreciated.

Thank you to Professor Tom O'Callaghan for the research opportunity at the School of Food and Nutritional Science at University College Cork, Ireland. Even if my period abroad was not directly connected to my Ph.D. project, the opportunity to visit and work with such a great institution in the field of dairy science has educated me further and gave me more knowledge of the analytical techniques useful for the drafting of this thesis.

Heartfelt thanks to my close friends and family who were with me throughout the Ph.D. A huge thanks to my family, especially to my parents Elisabetta and Andrea for giving me roots and wings and for the constant support throughout my journey.

Last but not least, thanks to my partner Shane for always believing in me even when I do not; for being my biggest fan and for your tremendous understanding and support these last few months. Thanks for being part of my life.

Index

CHAPTER 1
Introduction

1.1 Food quality

In the past, food was produced close to the place of consumption, whereas nowadays, globalisation has increased the length of the "farm to fork" food chain, highlighting the importance of food quality (Lineback et al., 2009). Food quality has become a central issue in the public debate, in food policy, in industry and in today's food economics, but its objective description is a very challenging task (Petrescu et al., 2020). The term, a complex and multi-dimensional concept, refers to a range of attributes and factors that are mainly related to sensory traits, shelf life, ethics, nutrition, authenticity, freshness of food and properties associated with microbiological and technological parameters. Food quality has both a subjective and objective dimension. Subjective quality pertains to the experience of the consumer, framed by consumer expectations, perceptions, and acceptance ('fitness for consumption'). Objective quality pertains to measurable characteristics inherent to the product, physicochemical attributes typically explored by food technologists. At the core of the economic importance of food is the relationship between the subjective and objective quality of food. Food quality can only be a competitive parameter for producers when consumer expectations and desires are translated into physical product characteristics that are recognized by the consumer (Grunert, 2005).

Globalisation has resulted in increasingly vulnerable and less transparent food supply chains. As a result, food quality assessment has become of huge importance for both the consumer and the industry along all the whole supply chain, from the raw material to the final product. Increasing demand for food, globalisation of the supply chain, constant integrity challenges, ambiguous definitions, and lack of specific guidance are some of the factors that have resulted in a greater incidence of sophisticated food fraud (Robson et al., 2021; Valand et al., 2020). Food fraud is an umbrella term for intentional practices committed for extracting economic profits through consumer deception, defined as "any suspected intentional action by businesses or individuals for the purpose of deceiving purchasers and gaining undue advantage therefrom, in violation of the rules referred to in Article 1(2) of Regulation (EU) 2017/625". The rising threat of food fraud, including the more defined subcategory of economically motivated adulteration is gaining recognition and concern among consumers,

Food Business Operators (FBO's) and governments and necessitates a constant investigation of food to safeguard quality and safety. In particular, high-value food commodities (**Table 1**) such as meat, dairy products, alcoholic beverages, oils, bee products, spices, coffee and tea are vulnerable to fraudulent economically motivated adulteration (EMA) due to the potential for economic gain (Galvin-King et al., 2018). In fact, the global estimated value of food frauds each year ranges from 10 to 40 billion US dollars affecting 1% of the global food industry (U.S. Food & Drug Administration, 2022).

Table 1. Different types of deliberate adulterants in food products.

Food product	Adulterants	Purpose/Fraud type
Ghee	Vanaspati, anatta, & oleomargarine	To make more yellow
Milk	Water, skim milk	To increase volume
Condensed milk	Paneer, khoya	To give rich texture
Butter	Vegetable oil, anatta, banana, oleomargarine	To increase volume & make yellowish
Milk	Water	Diluition
Minced lamb meat	Duck minced meat	To increase weight
Minced chicken meat	Carrageenan solution	To increase weight
Ice cream	Starch, rice powder or wheat flour	To thicken cream
Tea leaves	Black/Bengal gram dal husk with colour	To add colour
Red wine	Juice of blueberries	To attract/produce deep blue precipitate with lead acetate
Seafood products	Substitution of a more valuable species by a cheaper one	Substitution
Sugar	Chalk powder	To increase amount
Oils	Rancid oil	To increase volume
Common salt	White powdered stone,chalk	To increase amount
Honey	Molasses, cane sugar	To increase volume
Wheat	Ergot (poisonous fungus)	To increase weight

Modified from literature (Choudhary et al., 2020; Tibola et al., 2018; Zhang et al., 2019; Zheng et al., 2019)

Food fraud is a serious offence that jeopardizes food integrity and undermines consumer confidence in government regulatory mechanisms and food industries. It can prevent consumers from making informed decisions and leads to unfair competition with considerable long-term economic consequences. However, the fight against food fraud is hindered by a lack of a harmonised and consistent definition of the term due to the range of

different categories of fraud (Robson et al., 2021). For this reason, globally recognised standardised processes and adequate policing of the supply chains and the food industry are necessary to deter, mitigate and prevent any food fraud. With increasing complexity of food chains and hidden food fraud, the authentication of agri-food products has become necessary. The determination of food authenticity is an important surveillance measure for the official bodies in charge of labeling and for the industries controlling and testing the quality and traceability of raw materials and finished products (Lohumi et al., 2015; McVey et al., 2021). If a sample could be traced along the supply chain from raw material to final product, its authenticity can be insured. During authentication, it is necessary that the description of the food on the label is in compliance with the regulations (Selamat et al., 2021) in relation to composition, origin (species, geographical or genetic) and production method (conventional, organic, traditional procedures, free range or processing technologies) (Danezis et al., 2016b) (**Fig. 1**). Since food safety legislation has become more stringent in modern times, there is a need to develop analytical methodologies to tackle authenticity concerns, reassure safety parameters and ensure product quality (Kritikou et al., 2022; Valand et al., 2020)

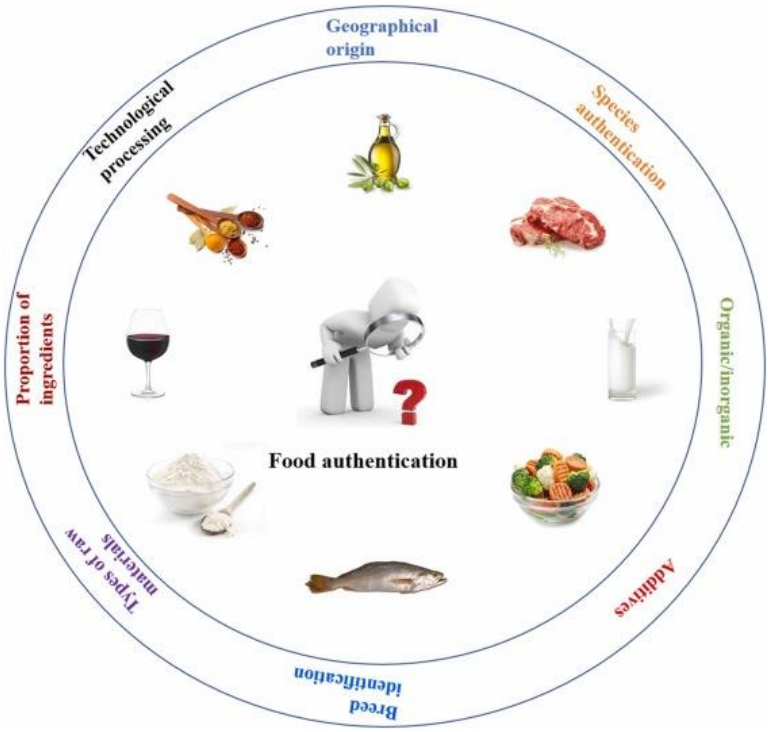

Fig. 1. Food product features analyzed by the authentication process (Saadat et al., 2022).

1.2 Analytical techniques for the evaluation of food quality

The growing concern about food quality worldwide has resulted in a rapid growth and expansion of authentication procedures through the implementation of reliable and efficient technologies to ensure compliance with national laws, international standards and other directives (Selamat et al., 2021). A range of physical and chemical methodologies have been developed and established for the investigation of authenticity of agri-food commodities, on-farm practices and food processing conditions. At the beginning of the 20th century, food quality was determined using a range of destructive, labor-intensive and time-consuming approaches, with modest analytical performance, that have evolved nowadays into powerful, novel analytical techniques (Cifuentes, 2012; Tümsavaş et al., 2013). To keep up with modern demands of food authentication there is a constant need to develop instruments with enhanced analytical accuracy, precision, robustness, lower detection limits, and higher sample throughput (Cifuentes, 2012), opposite to time-inefficient and resource-intensive conventional methods of analysis. Furthermore, authentication control can rarely be completed using a single method, there is no '*one size fits all'* methodology. Each technique provides specific information about the sample or components in question based on a specific physical-chemical interaction and each has its own positive and negative attributes when applied to food analysis. A comprehensive strategy incorporating several complementary analytical approaches is often required (Cifuentes, 2012; McVey et al., 2021).

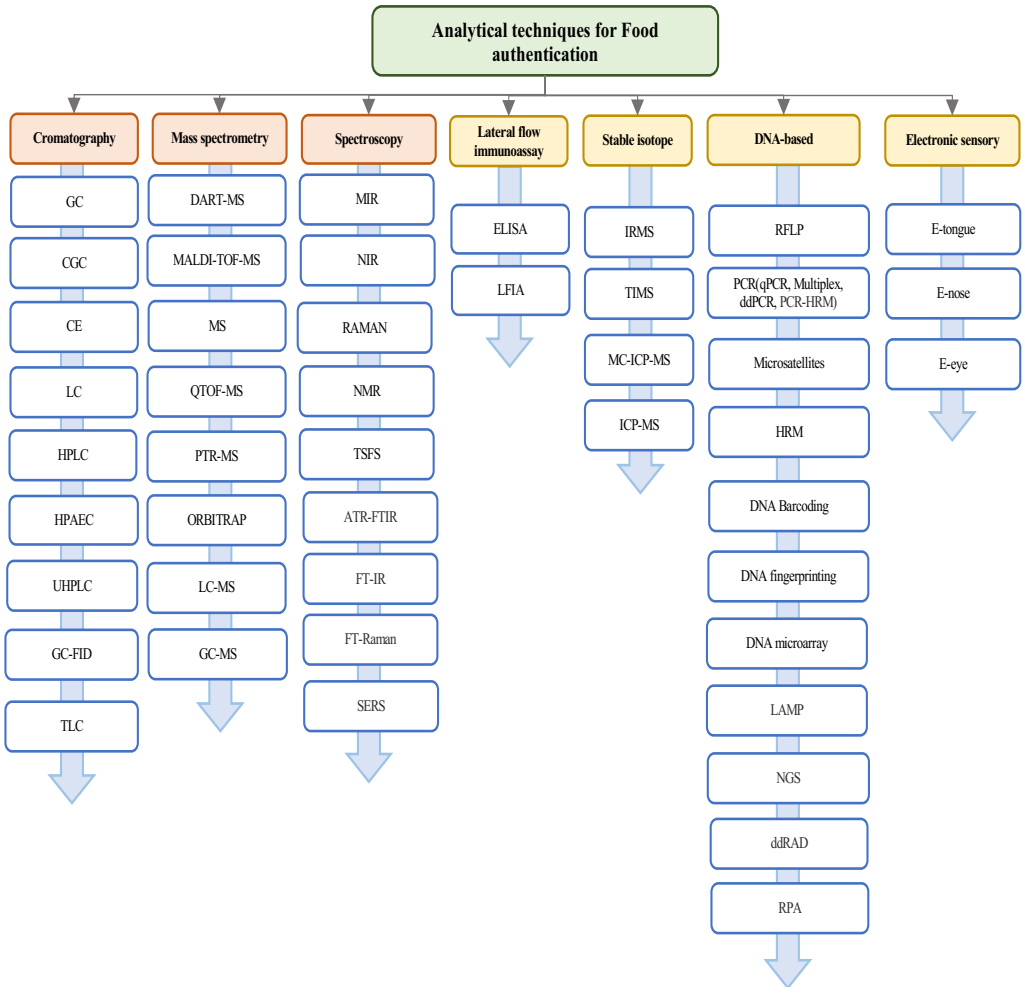

Fig. 2. Overview of different analytical techniques used for food analysis.

The analytical methods suitable for the authentication and characterisation of food products are based on a variety of chemical, physicochemical and physical methods, mainly targeted and non-targeted-based approaches (**Fig. 2**). Despite the different development history, theory and range of technical equipment (Tumanov, 1984) each method shares a common approach; namely, that a certain food matrix is investigated with at least one analytical technique for data acquisition and subsequently one or more chemometric approaches for statistical evaluation (Riedl et al., 2015). Several analytical techniques and combinations of techniques within chromatography (e.g., hyphenated techniques), spectrometry, and spectroscopy have been used to identify and detect emerging fraudulent trends in various food products especially the ones with high market price per volume/weight (**Fig. 3**). There are many analytical instruments useful for food analysis and thus large volumes of raw data can be generated for samples of interest. However, the raw data in and of itself, is not informative – it must be processed in order to extract meaningful and useful information that

can then be interpreted by the researcher and used to build models that can aid in the understanding the sample in question (De Araújo Gomes et al., 2022).

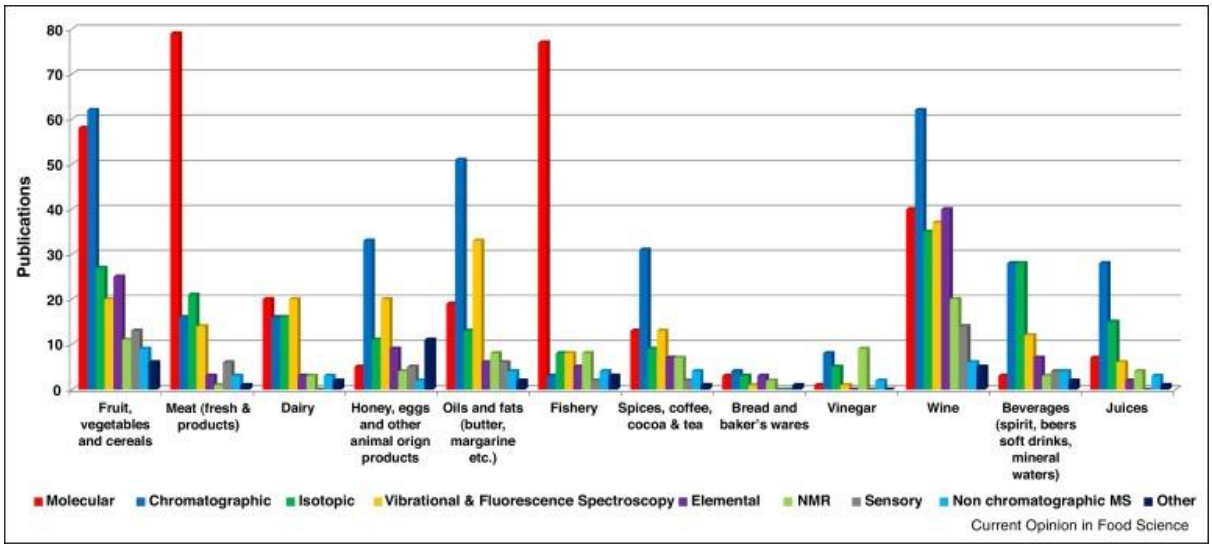

Fig. 3. Analytical techniques preferred in relation to specific food commodities (Danezis et al., 2016a).

In recent years, the number of publications concerning analytical methods for food authentication has grown exponentially as reported in **Fig. 3** (Danezis et al., 2016a); and in relation to food fingerprint analysis, spectroscopic and spectrometric-based studies are most reported (Cubero-Leon et al., 2018; Medina et al., 2019). For the purposes of the thesis, an in-depth discussion on nuclear magnetic resonance and infra-red techniques is presented in **Sections 1.3** and **1.4**.

1.2.1 Targeted vs non-targeted techniques

The analytical methods for authentication are classified into several types (**Fig. 4**). They can search for markers related to a particular adulteration of the product that are not naturally present in the food, and then compare them with threshold limits often established by specification rules or regulations. They can point to a targeted analysis of analytes naturally present in food or they can simultaneously measure a range of analytes/markers (non-targeted) and compare these profile (fingerprint) with authentic reference sample databases (Donarski et al., 2019).

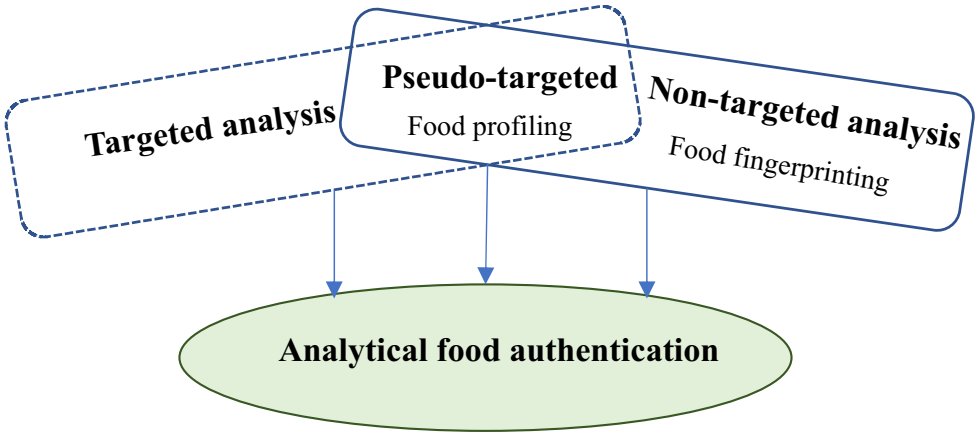

Fig. 4. Targeted versus non-targeted analytical food authentication.

Targeted approaches usually allow the precise and accurate detection of marker compounds linked directly or indirectly to the authentication issue. Targeted approaches involve the monitoring of *a priori* selected metabolites that are known to be directly related to the characteristics under investigation. The analytical targets are chemically or biologically characterised before data acquisition and then compared to reference data (legal limit or threshold value/database) (Ballin & Laursen, 2019) and are followed by univariate statistical analysis. In classical targeted analysis, validation is well defined, comprising the whole procedure from sampling or sample preparation to statistical evaluation of the acquired data (Riedl et al., 2015). Even though they enable the lowering of the analytes' detection limits (up to sub ppt-levels) in complex matrices, the extraction procedures are often very complex and expensive (Kaufmann et al., 2015). Focusing on a narrow group of targeted analytes, these approaches provide limited information about the product, incapable of providing an overall picture of samples' chemical composition making it unsuitable for identifying different adulterants that have potentially been added to the food (Cavanna et al., 2018; Daglia et al., 2014). This example of complexity epitomizes the inadequacy of several targeted methods into routine analysis and food surveillance, underlining the importance of using methods that instead are able to detect different classes of compounds at the same time (Ballin & Laursen, 2019).

Profiling analysis (pseudo-targeted) is a multi component analysis targeting a group of metabolic products or a specific class of compounds. Profiling often provides increased classification power and is richer in information when compared to targeted-based method. The profile can be used to calculate a value to be tested against a threshold limit, or it can be

used for comparison to a database much in the same way as a non-targeted analytical approach. As an indirect authentication procedure, the obtained data are usually investigated using multivariate data analysis (Ballin & Laursen, 2019).

Non-targeted analysis, also referred to as "fingerprinting", globally studies the metabolite fingerprint itself measuring a range of unspecified analytes/markers, not known *a priori*, to gain a comprehensive insight into the composition of the sample. Then, a comparison of the profile is made to reference data in order to reveal possible adulterations. Non-targeted analytical analysis is typically much more demanding when compared to classical targeted approaches since the workflow requires multivariate statistical models and subsequent model validation in order to guarantee reliability of the data and to allow a conclusion on the applicability of the analysis method (Riedl et al., 2015). Owing to the large number of features typically contained in non-targeted analyses, the classification models are enhanced and there is an increased chance that the chosen model/analysis is successful in accurately describing the data. Emerging technologies will enable parallel measurements of large number of targets increasing the accuracy and speed of data collection while decreasing the cost and allowing for measurements to be performed at the site of sample collection (Danezis et al., 2016a).

1.3 Nuclear magnetic resonance (NMR) spectroscopy

Nuclear magnetic resonance (NMR) is one of the most suitable methods to obtain "high-throughput" spectroscopic and structural information on a wide range of metabolites in various food products with high analytical precision (Danezis et al., 2016b). NMR spectroscopy leverages the fact that in the presence of a magnetic field, atomic nuclei absorb and emit electromagnetic radiation than can be detected to discern information about the physical and chemical properties of the material in question (Rusilowicz et al., 2014). NMR identifies the carbon-hydrogen framework in a sample according to the absorption of electromagnetic radiation, allowing for the characterisation of the compounds present (Farag et al., 2018). It is a non-destructive, highly-reproducible analytical method that can determine and quantify a large number of compounds simultaneously. Its high reproducibility enables a single NMR instrument to be used to conduct many different analyses without the need for additional calibration or adjustment specific to the material under analysis (Minoja & Napoli, 2014). This reduces both the time required for analysis and also the cost per sample. An additional benefit of NMR is that it can be used to gather

information from samples of all states of matter, although most food-related applications involve liquids and solids (Tang et al., 2019) (**Fig. 5**).

In food analysis two types of NMR are applied, low-resolution NMR (LR-NMR) and high-resolution NMR (HR-NMR) (Luykx & van Ruth, 2008). LR-NMR instruments (frequencies ranging 10–40 MHz), provide less detailed information than the high-resolution version due to a sensitivity loss that somewhat limits its applicability. However, LR-NMR is typically more accessible and versatile than HR-NMR since it is less expensive and easier to use (Azeredo et al., 2003). HR-NMR (frequencies above 100 MHz) is a spectroscopic technique commonly used in the field of food composition analysis (Consonni & Cagliani, 2022) since it can provide "high-throughput" spectroscopic and structural information on a wide range of molecular compounds. However, HR-NMR comes at a high cost – both in terms of the initial capital required to setup and the associated running costs (Luykx & van Ruth, 2008). The data gathered using NMR includes a diverse array of measurable parameters such as peak intensity, frequency (normalized to chemical shift), line shape, line width and relaxation times. This technique is an extremely powerful and useful tool that can give insight into molecular structures and to investigate foodstuffs at molecular scale (Eisenmann et al., 2016). Acquired NMR data needs to be processed before statistical analysis can be carried out (**Fig. 5**). The choice of preprocessing techniques depends on multiple factors, including: the nature of data, the focus of the investigation, and the analysis methods to be used. A single approach is not appropriate for all kinds of acquired data even within a particular NMR technique.

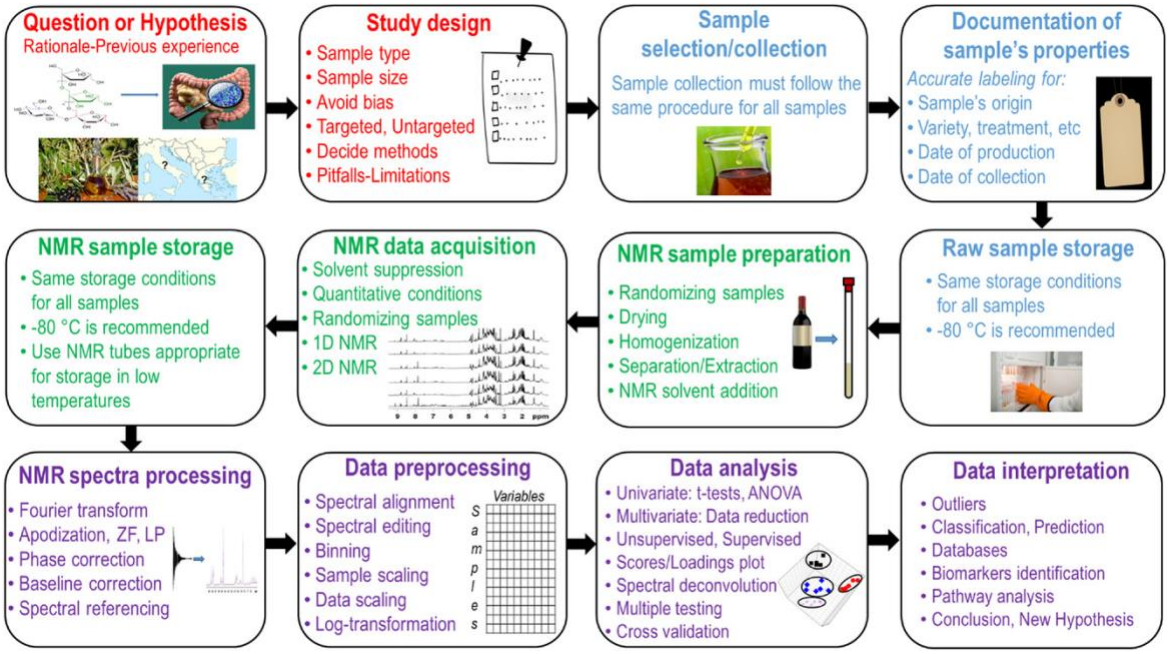

Fig. 5. Schematic representation of the workflow for the application of NMR-based metabolomics in food science (Hatzakis, 2019).

Despite its usefulness and power, NMR alone is not sufficient to describe precisely the constituents of food. Foods are very complex matrices consisting of hundreds or thousands of compounds that can and do interact with one another (Hatzakis, 2019; Tang et al., 2019). Also, these compounds can be affected by external factors such as processing, storage or transport. Often, NMR fails to capture these details and even more simply, NMR signal overlap can occur which results in the misidentification of compounds of interest (Hatzakis, 2019; Tang et al., 2019). The main disadvantage of NMR compared to other technologies used in food analysis is its relatively low sensitivity. The sensitivity of the experiment depends on the type of NMR probe used, the strength of the applied magnetic field, the type of the spectroscopic experiment (nucleus, pulse sequence, acquisition parameters) and the nature of the sample (Tang et al., 2019). Furthermore, advances in NMR technology (higher field magnets and cryogenically cooled probes that increase signal-to-noise ratios (SNR) are constantly being made in an effort to overcome any sensitivity concerns (Rusilowicz et al., 2014). With that said, an alternative, more efficient and holistic interpretation of the gathered spectral information needs to be applied. One such approach is food-based metabolomics, a member of the "foodomics" family (Cifuentes, 2009), where the data gathered using NMR and other analytical methods are combined with multivariate statistical analysis (MVSA) to fully characterise a food product as a whole, allowing for the collection of information the food's origin, quality, processing, storage history and sensory perception (Hatzakis, 2019).

Metabolomics can also be used to investigate what impact a specific nutritional approach has on metabolism and overall health (Hatzakis, 2019). The vast amount of information that can be derived from NMR data often requires a multivariate statistical protocol to effectively highlight the possible markers in quality assessment applications. Univariate methods can be used to identify individual variables that differ significantly between groups and are particularly useful when carrying out targeted studies (Rusilowicz et al., 2014). In addition, according to the type of investigation, metabolomic analysis can be performed using a targeted or an untargeted approach (Cagliani et al., 2017).

The use of NMR and MVSA in routine analysis allows for the simultaneous identification of a wide range of chemical compounds (Consonni & Cagliani, 2019) – an attribute that is particularly useful when trying to discern food origin and whether food fraud is at play. In fact, the coupling of chemometrics and NMR spectroscopy was a significant step forward in the field of food analysis. Chemometrics elevated NMR's status from a technique used only for compositional analysis to one that could be used to achieve a holistic and unbiased food assessment and explore interactions and relationships between chemical profile and food properties (Tang et al., 2019).

Some use cases of NMR combined with MVSA include for food authentication, quality control, geographical origin, production monitoring/improvement and sensory evaluation (Masetti et al., 2021; Tang et al., 2019). NMR combined with MVSA has been used for assessing the authenticity of certain food products such as wines (Amargianitaki & Spyros, 2017; Viskić et al., 2021), spirits (Fotakis & Zervou, 2016; Kuballa et al., 2018; Monakhova et al., 2012), coffee (Consonni et al., 2018), olive oils (Dais & Hatzakis, 2013) and vinegar (Nie et al., 2019; Wang et al., 2016), honey (Olawode et al., 2018), meat (Akhtar et al., 2021; Bertram & Ersen, 2004; Zanardi et al., 2015), fish (Erikson et al., 2012; Shumilina et al., 2016) and dairy (Consonni & Cagliani, 2008; Klein et al., 2012; Niero et al., 2022; Segato et al., 2019; Sundekilde et al., 2013; Tomassini et al., 2019). In these studies, NMR has been applied for the investigation of the metabolite profile of dairy products, in relation to different aspects such as feeding system, animal health, lactation stage, milk quality, geographical origin and cheese ripening process. NMR has proved to be a valuable contribute to the metabolite profiling, even if further applications of the technique in the field are still unexploited and suggested (Scano et al., 2019). In **Chapter 6** that follows, NMR with MVSA is used to authenticate bovine milk from different feeding systems and to better understand the influence of the dietary forage proportion.

1.4 Vibrational spectroscopy techniques

In recent years, a number of vibrational spectroscopic techniques have been developed that enable the determination of complex chemical information from the samples being scrutinised. The non-destructive techniques that have been developed can be used for the qualitative and quantitative evaluation of food fraud and food authenticity (Sun, 2009). These techniques include Fourier transform near-infrared (NIR), medium-infrared (MIR), Raman spectroscopy, terahertz spectroscopies and hyperspectral imaging (HIS) (Beć et al., 2020). Spectroscopic techniques operate over different and limited frequency ranges depending on the process being studied and the magnitude of the associated energy change (Lohumi et al., 2015) (**Fig. 6**). There are many instances where non-invasive techniques such as NIR, MIR, Raman spectroscopy and HIS have been used as analytical methods during routine analysis of food ingredients and products (Beć & Huck, 2019; Cattaneo & Stellari, 2019; Cozzolino, 2012; Kartheek et al., 2011; Qu et al., 2015). These techniques have the advantage of being non-destructive and have a relatively low analysis cost. Some advantages associated with non-destructive vibrational spectroscopy include: the need for minimal or no sample preparation, reagentless preparation, easy-to-use instrumentation, and, more recently, the availability of portable and inexpensive devices (Cozzolino, 2022). These spectroscopic techniques have been adopted for both qualitative and quantitative analysis of agriculture and food products, and have provided an alternative to other wet-chemical and time-consuming techniques (Cozzolino, 2022; Lohumi et al., 2015).

Infrared radiation (IR) spectroscopy leverages the fact that solids, liquids and gaseous samples can absorb some of the incoming infrared radiation at specific frequencies producing a spectral 'fingerprint' of the sample. The infrared spectrum can be divided into three distinct regions; near- (0.8–2.5 μm, 12,500–4000 cm^{-1}) incorporating both electronic and vibrational spectroscopy, mid- (2.5–25 μm, 4000–400 cm^{-1}) monitoring mainly molecular vibrations and far- (25–1000 μm, 400–10 cm^{-1}) infrared containing rotatory and vibrational movements (Ozaki, 2021). Infrared-based spectroscopic methods have been used to develop qualitative (pattern recognition) and quantitative (multivariate calibration) procedures for food analysis (Osborne, 2000). MIR fingerprints result from the stretching, bending and rotating vibrations of the molecules that absorb the IR radiation, while NIR spectra result from the complex overtones and high-frequency combinations of the shorter emitted wavelengths. Compared to MIR, NIR spectroscopy is more adequate for food

analysis as it requires less sample preparation and can be easily used for in-field and at-line analysis (De Marchi et al., 2018).

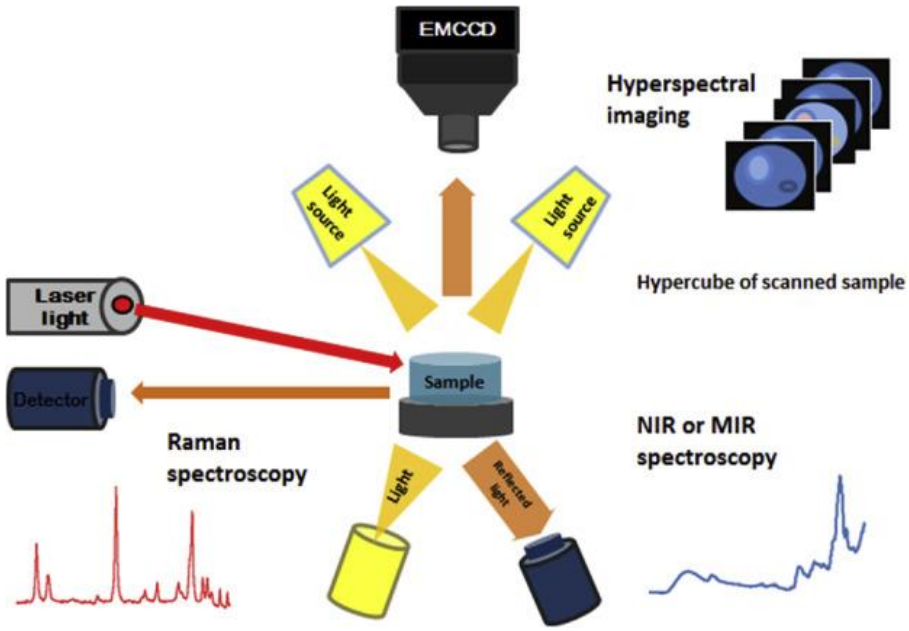

Fig. 6. Schematic diagram of typical vibrational spectroscopic techniques (Lohumi et al., 2015).

1.4.1 Near-infrared (NIR) spectroscopy

NIR spectroscopy (NIRS) involves the use of electromagnetic radiation to probe the vibrational degrees of freedom (DOFs) of molecules. This spectroscopic technique reveals molecular information of the sample being probed by measuring absorption bands resulting from overtones and combination excitations (Beć et al., 2020). NIR spectroscopic tools are comprised of a radiation source, wavelength selector/modulator, sample cell, detector, and signal processor (Esteve Agelet, 2011). Spectra can be recorded in reflection, transmission or interactance modes (**Fig. 8**), providing information related to the vibration behaviour of typical molecular bonds mainly C-H, O-H, and N-H (Lohumi et al., 2015; Nicolaï et al., 2007; Osborne, 2000).

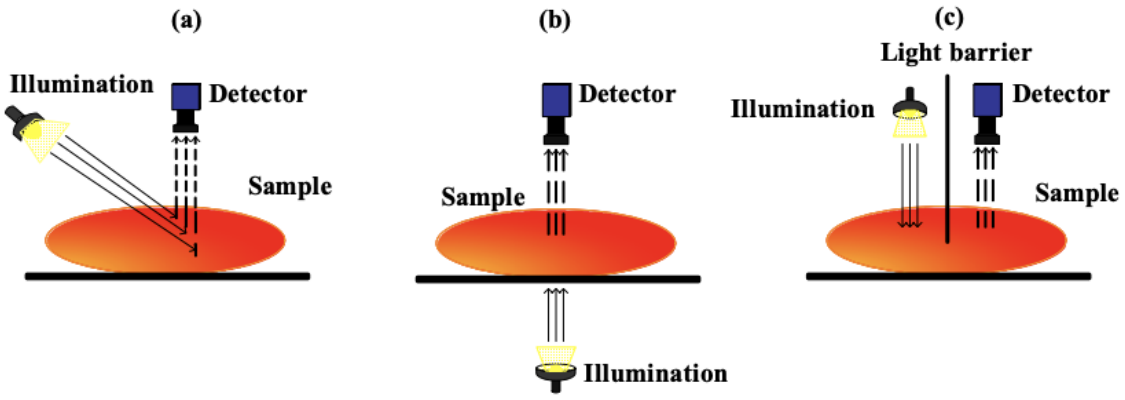

Fig. 8. Modes of data collection in NIRS system. (a) Reflectance mode, (b) Transmittance mode, and (c) Interactance mode (Qu et al., 2015).

In recent years, the last two decades or so, NIRS has become a spectroscopic tool of choice for many across the sciences. This is because the instrument is chemical-free, cost-effective, environmentally friendly, safe and easy to use, non-invasive, non-destructive and suitable for *in situ* analysis. NIR spectroscopy can be carried out in non-contact mode or using an optical fibre, making it much easier to study and analyze aqueous solutions (Ozaki, 2012). However, as with all characterisation techniques, there are certain limitations associated with NIRS. For one, analysis and interpretation of large data sets can be extremely difficult (due to wavelength-dependent scattering effects, instrumental noise, ambient effects, and other sources of variability), which can contribute to less robust and reliable results. In this case, chemometrics (a combination of statistical and mathematical sciences) can be employed to complement the NIRS and help resolve issues associated with the interpretation of the NIR data (Nobari Moghaddam et al., 2022; Qu et al., 2015; Teixeira Dos Santos et al., 2013).

According to the flowchart (**Fig. 7**), chemometrics is mainly used during three phases of the NIRS data processing flow: pre-processing of data, classification or regression model building, and model validation. A variety of spectral pretreatments are necessary when dealing with NIRS data, since there is plenty of noise and redundant information, which give rise to noise and baseline fluctuations (Ozaki, 2012; Qu et al., 2015). Thus, by employing appropriate chemometric algorithms, the pre-processed data could be employed to develop qualitative and/ or quantitative models. Of course, the choice of the applied chemometric techniques depends heavily on the nature of the dataset. Accordingly, multivariate statistical analysis is used for extracting useful information from NIR spectra. This analysis helps solve

the complex interactions between components and considers their collective effects on the matrices and scrutinizes the sample holistically (Kowalski, 1984).

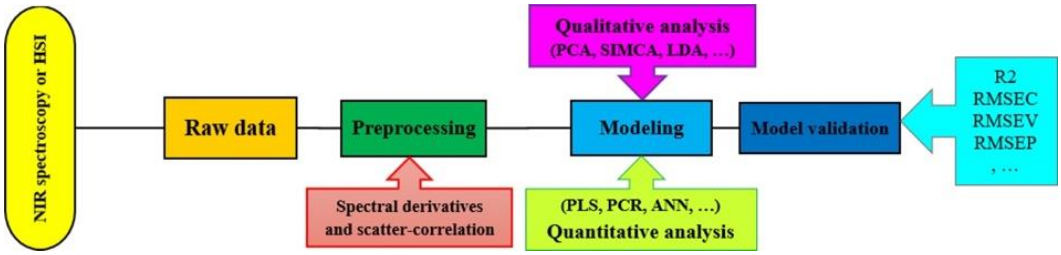

Fig. 7. Work flow of the chemometrics analysis (Nobari Moghaddam et al., 2022)

In recent years, the use of NIRS in combination with chemometrics for the detection of food fraud and for food authentication purposes has been employed. The growth of chemometrics methods combined with technological advances in NIR spectroscopic instrumentation have increased the value of this technology (Nobari Moghaddam et al., 2022). The application of NIR spectroscopy is far-reaching and has been used to probe many foods including, but not limited to: dairy products (Dvorak et al., 2016; Hsieh et al., 2011; Ottavian et al., 2012), oils (Li et al., 2020; Luna et al., 2013; Mendes et al., 2015), meat (Alamprese et al., 2013; Morsy & Sun, 2013; Prieto et al., 2009), fish and fishery products (Currò et al., 2022; Fasolato et al., 2012; Varrà et al., 2022), honey (Bisutti et al., 2019) and wine (Cozzolino et al., 2006; Hencz et al., 2022; Liu et al., 2006). The above-mentioned studies highlighted the potential of NIR spectroscopy as rapid and at-line detection method for non-destructive estimation of several chemical properties useful to classify the samples according to the different experimental conditions under investigation.

Recently, considerable effort has been made to miniaturize spectroscopic devices such that they be portable (Beć et al., 2021). These new developments in spectrometer design have partly been driven by the advances in microelectromechanical systems (MEMS) production (Sorak et al., 2012). Portable NIR spectrometers offer several advantages for non-destructive, *in situ* analysis. Such advantages include; small size, low cost, robustness, simplicity of analysis, sample user interface, portability, and ergonomic design (Teixeira Dos Santos et al., 2013). With that said, several issues associated with the miniaturization of the spectrometers have become apparent. Most noticeable among them are the narrower spectral regions and/or lower spectral resolution with which the portable devices operate (Beć et al., 2020).

NIRS is promising in food safety assessments, so more research is needed to investigate its full power and limitations, especially when coupled with different modeling

techniques as a way of improving its accuracy and robustness. In the chapters that follow (**Chapters 3, 4, 5**, respectively) the reliability of using bench-top and portable NIR in the detection of pyrrolizidine alkaloids in bee pollen, the assessment of chicken breast shelf-life and for the classification of eggs from quail fed with silkworm meal is tested combined with different multivariate approaches.

1.5 Chemometrics applications

Data analysis has become a fundamental task in analytical chemistry due to the vast amount of information that can be generated by modern analytical instruments. Therefore it is necessary to apply multivariate statistical procedures to efficiently extract the maximum amount of meaningful information from the large datasets that are gathered and to distinguish significant trends in the data (Berrueta et al., 2007; Bevilacqua et al., 2017). Specifically and in relation to this thesis, chemometric techniques can be used to extract meaningful information about food authenticity from large datasets gathered using the various spectroscopic techniques discussed herein.

1.5.1 Procedure flow

In **Fig. 8**, a typical procedure flow highlighting the core components of a well-designed study is shown. After the hypothesis has been formed, the design of experiment (DoE) is determined (step 1), whereby the choice of what kind of samples will be collected and how those samples will be reliably handled and measured is made. After the sampling and the samples preparation (step 2) the data is then analysed according to the strategy outlined (step 3) and pre-processed to extract information from the raw instrumental data and remove random or systematic sources of variation in the data set (Nunes et al., 2015) (step 4). In fact, many analytical signals are associated with useless noise or redundant information and data pre-treatment (selection of a limited number of informative predictors or data compression) is often necessary to filter the useful information and help generate useful models (Oliveri & Downey, 2012). After data pre-processing, statistical analysis of the data has to be performed to elucidate any trends that exist (step 5). Finally, the results have to be interpreted (step 6).

Chemometrics play a critical role in this process flow since getting meaningful results requires not only meaningful data but also meaningful analysis (Kjeldahl & Bro, 2010). In chemometrics, chemical compounds are not generally identified – instead, their spectral

patterns and intensities are recorded and used to identify spectral features that distinguish sample classes (Trygg et al., 2007). Various statistical analysis methods are grouped under the well-established term 'chemometrics'. Typically, unsupervised methods are used during feature identification, to find affiliations and classifications groups, assuming no preliminary information about the samples (Creydt & Fischer, 2018). In contrast, supervised methods are generated based on preliminary information about the samples. Many different algorithms can be applied to multivariate data sets, some of which are summarized in **Fig. 8**.

1.5.2 Unsupervised and preliminary approach (graphical approach to the dataset)

Classical unsupervised techniques are very useful for the initial interrogation of data (Bevilacqua et al., 2017). Such techniques are examples of exploratory data analysis (EDA) and are used to gain deeper insight into high-volume complex data such as a large NIR datasets (Beć & Huck, 2019). One such example is principal component analysis (PCA) which is especially useful for the analysis of multidimensional data that have some degree of correlation (Zhao & Maclean, 2000). The technique involves the reduction of the data dimensionality, allowing visualization while retaining much of the information in the original dataset. PCA transforms the original measured variables into uncorrelated variables called *principal components* and is frequently used in exploratory data analysis to determine whether there are trends in the dataset. With that said, PCA is not always appropriate. For instance, when data are from designed experiments, PCA has limited capacity in extracting the information related to the different factors in the design (Bevilacqua et al., 2017).
Other unsupervised pattern recognition techniques such as cluster analysis (CA), can be used for preliminary evaluation of the information in the data matrices (Lavine, 2006). In CA, samples are grouped by similarities without taking into account the class information. Clusters refer to sets of observations which are more similar to each other than they are to the remaining objects. CA is based on the premise that this similarity is inversely related to the distance between samples (Kaufman & Rousseeuw, 1990). The most used type of CA is the hierarchical approach (HCA) (Nunes et al., 2015).

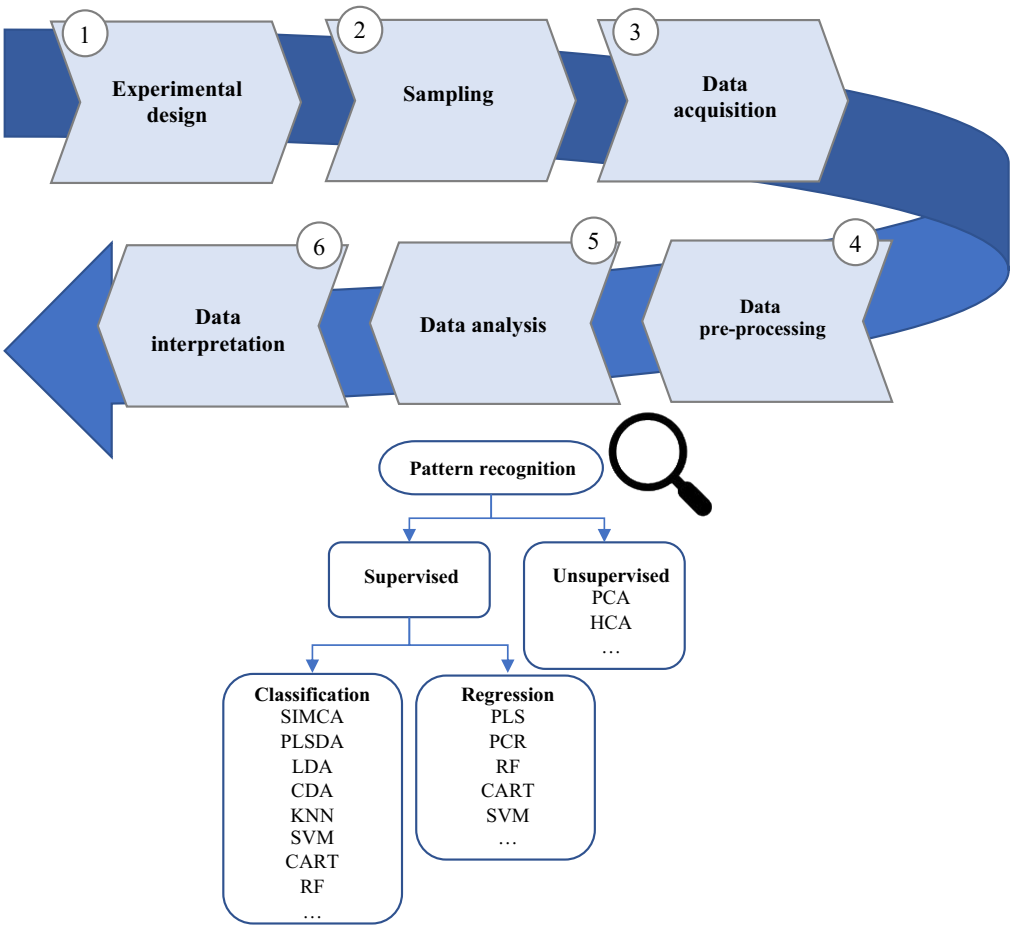

Fig. 8. Flowchart of a typical food study with the main related topics and the commonly used pattern recognition methods. Modified from Bevilacqua et al. (2017) and Jiménez-Carvelo et al. (2019).

1.5.3 Supervised approach

Supervised classification involves predicting interesting characteristics about the samples using the data together with some additional information (Bevilacqua et al., 2017). Supervised pattern recognition techniques use the class membership of the samples in order to classify new unknown samples in one of the known classes (Vandeginste et al., 1998). Classifying a sample involves predicting one or more of its properties based on the information collected during the characterization of the sample. The term class or category refers to a collection of objects sharing similar characteristics. It is imperative to highlight that the definition of these characteristics is problem-dependent. The same set of samples can be grouped in different ways, depending on the problem and the statistical models to be used. Supervised methods of analysis are divided into two groups: (i) classification methods and (ii) regression methods (**Fig. 8**). Classification techniques are used for the separation,

sorting and grouping of samples with regard to a specific sample property whereas regression analysis groups the methods used for the prediction/quantification of chemical content (predictive models) (Beć & Huck, 2019). Given the chemometric applications used in the following chapters, supervised classification models rather than regression methods will be further discussed. Classification methods play an essential role in food quality assessment and are often used to solve various kinds of authentication issues (Bevilacqua et al., 2013) and are conventionally divided into discriminant analysis methods and class modelling methods depending on how the model is built.

Linear discriminant analysis (LDA) is based on the determination of linear discriminant functions, which maximize the ratio of inter-class variance and minimize the ratio of intra-class variance (Berrueta et al., 2007). With LDA, the number of variables should not exceed the number of samples (Bevilacqua et al., 2013; Medina et al., 2019), however this can easily be solved by employing PCA or feature selection procedures. The canonical discriminant analysis (CDA) is a synonym of LDA, and the name points out that the linear discriminant model can be expressed directly in terms of the coordinates of samples along the direction(s) of maximum class separation (the canonical variates) (Cruz-Castillo et al., 1994), instead of the original variables. CDA is used in **Chapter 3** & **4** which follow as a discriminating method for the purpose of the designed experiments.

Partial least squares discriminant analysis (PLS-DA) method involves performing a multivariate regression and assigning a numeric value to each sample, followed by classification into specific classes (Brereton & Lloyd, 2014). Despite their differences, many authors (Barker & Rayens, 2003; Indahl et al., 2007; Nørgaard et al., 2006) have shown that PLS-DA and LDA/CDA are perfectly equivalent. Variable importance in projection (VIP) method is often used for identifying significant variables in complex datasets from the PLS-DA model by calculating the VIP score for each variable. It also removes non-important variables with VIP score below a threshold (default = 1) (Medina et al., 2019).VIP method is implemented in **Chapter 3** & **4** to highlight the most influential absorbance wavelengths from the PLSDA model. LDA and PLS-DA have been widely used in food research in order to obtain classification models, the most often used discriminant approaches in food fingerprinting (Medina et al., 2019; Nunes et al., 2015).

The nearest method (KNN) is a distance based non-parametric procedure that is based on the determination of the distances between an unknown object and the objects of the training set. The smallest distance is selected for the assignment of the class membership.

This method is relatively simple to implement and is especially useful when there are few samples.

Soft independent modelling of class analogies (SIMCA) is a supervised classification technique that uses samples with known origin (training samples) to create a classification rule which allows the classification of new samples (test samples) with unknown origin (Mees et al., 2018). The SIMCA method has garnered much attention from those who are interested in solving food authentication problems in areas such as food chemistry. In such applications, a training set represents authentic samples, the properties of which are compared to those of a suspect sample (Pomerantsev & Rodionova, 2020).

In recent years, the application of new pattern recognition tools is becoming popular in the area of food science, due to their potential ability to solve complex problems related to food authenticity. To date, support vector machine (SVM), classification and regression tree (CART) and random forest (RF) are the most widely used since they can be used in both classification and calibration models. Their application is widespread in areas such as metabolomics and is growing in the area of food quality and authenticity (Jiménez-Carvelo et al., 2019). RF, a relatively new pattern recognition method (Breiman, 2001), is based on a strategy named "ensemble learning" whereby many classifiers are generated and their results are aggregated. It is very suitable for unstable models and for class imbalance problems (Liu et al., 2013). In **Chapter 4 & 5**, RF is used as a feature selection tool for selecting the most informative NIR wavelengths and to improve the classification performance.

Support vector machine (SVM) is a supervised learning technique, based on the statistical learning theory (Cortes & Vapnik, 1995; Xu et al., 2006). SVM is applicable to both classification and regression problems. This method can circumvent the issue of having non-evident separation between the regions of the different classes of the samples. However, development of the model is often quite difficult, and a lot of informatics resources are necessary (Jiménez-Carvelo et al., 2019). In **Chapter 5**, SVM, KNN and PLS-DA supervised recognition algorithms were performed on NIR informative wavelengths in order to exploit the spectroscopic information for pursuing classification purposes.

1.5.4 Validation procedure

Prediction models are only useful if appropriate criteria are defined and applied to measure the performance of the model (Varmuza & Filzmoser, 2016). To investigate the prediction performance of a model, a validation procedure can be conducted during supervised pattern

recognition procedures no matter which algorithm is applied. That strategy consists of the following methodological steps (Berrueta et al., 2007; Riedl et al., 2015) common for both, classification and regression models:

(1) Selection of a training, and a test set. These sets consist of objects of known class for which variables are measured. The training set is used for the optimization of parameters of each multivariate technique. Exploratory data analysis (EDA) and unsupervised pattern recognition are commonly used to simplify and gain better understanding of datasets. As is often the case, the great challenge is to remove the noise while retaining the meaningful information (Siebert, 2001).

(2) Variable selection. Variables that contain information pertaining to the targeted classification are kept, whereas the variables contributing to noise and/or with no discriminating power are eliminated. Datasets with excessive numbers of variables can give rise to some complications. Firstly, from a technical perspective, too many variables can cause the algorithms to run unnecessarily slow; secondly, the predictive performances of the algorithms can decrease, especially in the case of spectroscopy analyses where the wavelength measurements are highly correlated to each other (Bisutti et al., 2019). A strategy against the so-called minimal-optimal problem is to use a small (possibly minimal) feature set that avoids the use of irrelevant variables (Nilsson et al., 2007). Herein, both a RF feature selection (**Chapter 4 & 5)** procedure based on the Boruta algorithm (Kursa & Rudnicki, 2010) and a Stepwise feature selection (**Chapter 3, 4 & 6**) based on the analysis of variance (ANOVA) were used to select the most informative wavelengths and to remove unrelated and noisy data.

(3) Construction of a model using the training set. A mathematical model is derived using a certain number of variables measured on the samples (the training set) and their known categories.

(4) Validation of the model using an independent set of samples. This is done to evaluate the reliability of the classification achieved (Brereton, 2003; Vandeginste et al., 1998). Model validation process is essential since it demonstrates that the models obtained by the supervised pattern recognition techniques are sufficient to perform classification of unknown samples. At best, there are enough available samples to create separate (independent) training and test sets, with each set containing class-representative samples. This validation procedure is known as external validation (**Chapter 5**) whereby the test set is completely independent from the model building process. However, in food analysis, this ideal situation is rarely the case. In this situation, cross-validation methods (**Chapter 3**) are commonly

employed whereby, the prediction ability of the model is determined by developing a model using part of the dataset (training or learning set) and applying it to another part of dataset (test set) to validate it.

1.5.5 Data fusion

Data fusion is a very useful tool that can be used in parallel with the other aforementioned chemometric methods. It can be used in an integrated way, to make good use of the abundance of data that often is analysed in food omics studies (Bevilacqua et al., 2017). The use of data fusion is expected to increase the global classification/prediction ability, decrease the uncertainty of results and enable better outlier detection (Borràs et al., 2015).

Statistical data fusion achieves a global view of the system being investigated by simultaneously focusing on the analysis of multiple sets of data. Low-level data fusion is when individual data matrices from different experiments are treated as a single "super-matrix" to be processed by a multivariate technique of choice to extract the information about both experiments; mid-level data fusion involves the integration of the data at the level of features which are extracted from each different data block and is generally preferred, over low-level, when the goal is to predict rather than interpret. Both strategies are applicable to exploratory and predictive analysis. Further data fusion of the latter is possible, which occurs at the level of the predictions and is known as high level fusion (Bevilacqua et al., 2017). The use of data fusion approaches coupled with chemometric classification techniques has mostly been reported for the authentication of the food matrices (Biancolillo et al., 2014; Borràs et al., 2015; Riuzzi et al., 2021). In **Chapter 6** low-level data fusion was performed to improve the discriminating capacity of the model applied.

1.6 References

Akhtar, M. T., Samar, M., Shami, A. A., Mumtaz, M. W., Mukhtar, H., Tahir, A., Shahzad-Ul-hussan, S., Chaudhary, S. U., & Kaka, U. (2021). H-NMR-based metabolomics: An integrated approach for the detection of the adulteration in chicken, chevon, beef and donkey meat. *Molecules*, *26*(15), 4643. https://doi.org/10.3390/molecules26154643

Alamprese, C., Casale, M., Sinelli, N., Lanteri, S., & Casiraghi, E. (2013). Detection of minced beef adulteration with turkey meat by UV-vis, NIR and MIR spectroscopy. *LWT*, *53*(1), 225–232. https://doi.org/10.1016/j.lwt.2013.01.027

Amargianitaki, M., & Spyros, A. (2017). NMR-based metabolomics in wine quality control and authentication. *Chemical and Biological Technologies in Agriculture*, *4*(1), 9. https://doi.org/10.1186/s40538-017-0092-x

Azeredo, R. B. V., Colnago, L. A., Souza, A. A., & Engelsberg, M. (2003). Continuous wave free precession: Practical analytical tool for low-resolution nuclear magnetic resonance measurements. *Analytica Chimica Acta*, *478*(2), 313–320. https://doi.org/10.1016/S0003-2670(02)01514-3

Ballin, N. Z., & Laursen, K. H. (2019). To target or not to target? Definitions and nomenclature for targeted versus non-targeted analytical food authentication. *Trends in Food Science and Technology*, *86*, 537–543. https://doi.org/10.1016/j.tifs.2018.09.025

Barker, M., & Rayens, W. (2003). Partial least squares for discrimination. *Journal of Chemometrics*, *17*(3), 166–173. https://doi.org/10.1002/cem.785

Beć, K. B., Grabska, J., & Huck, C. W. (2020). Near-infrared spectroscopy in bio-applications. *Molecules*, *25*(12), 2948. https://doi.org/10.3390/molecules25122948

Beć, K. B., Grabska, J., & Huck, C. W. (2021). Principles and Applications of Miniaturized Near-Infrared (NIR) Spectrometers. *Chemistry - A European Journal*, *27*(5), 1514–1532. https://doi.org/10.1002/chem.202002838

Beć, K. B., & Huck, C. W. (2019). Breakthrough potential in near-infrared spectroscopy: Spectra simulation. A review of recent developments. *Frontiers in Chemistry*, *7*(48). https://doi.org/10.3389/fchem.2019.00048

Berrueta, L. A., Alonso-Salces, R. M., & Héberger, K. (2007). Supervised pattern recognition in food analysis. *Journal of Chromatography A*, *1158*(1–2), 196–214.

https://doi.org/10.1016/j.chroma.2007.05.024

Bertram, H. C., & Ersen, H. J. (2004). Applications of NMR in Meat Science. In *Annual Reports on NMR Spectroscopy* (Vol. 53, pp. 157–202). Elsevier. https://doi.org/10.1016/S0066-4103(04)53003-X

Bevilacqua, M., Bro, R., Marini, F., Rinnan, Å., Rasmussen, M. A., & Skov, T. (2017). Recent chemometrics advances for foodomics. *TrAC - Trends in Analytical Chemistry*, *96*, 42–51. https://doi.org/10.1016/j.trac.2017.08.011

Bevilacqua, M., Bucci, R., Magrì, A. D., Magrì, A. L., Nescatelli, R., & Marini, F. (2013). Classification and Class-Modelling. In *Data Handling in Science and Technology* (Vol. 28, pp. 171–233). Elsevier. https://doi.org/10.1016/B978-0-444-59528-7.00005-3

Biancolillo, A., Bucci, R., Magrì, A. L., Magrì, A. D., & Marini, F. (2014). Data-fusion for multiplatform characterization of an italian craft beer aimed at its authentication. *Analytica Chimica Acta*, *820*, 23–31. https://doi.org/10.1016/j.aca.2014.02.024

Bisutti, V., Merlanti, R., Serva, L., Lucatello, L., Mirisola, M., Balzan, S., Tenti, S., Fontana, F., Trevisan, G., Montanucci, L., Contiero, B., Segato, S., & Capolongo, F. (2019). Multivariate and machine learning approaches for honey botanical origin authentication using near infrared spectroscopy. *Journal of Near Infrared Spectroscopy*, *27*(1), 65–74. https://doi.org/10.1177/0967033518824765

Borràs, E., Ferré, J., Boqué, R., Mestres, M., Aceña, L., & Busto, O. (2015). Data fusion methodologies for food and beverage authentication and quality assessment - A review. *Analytica Chimica Acta*, *891*, 1–14. https://doi.org/10.1016/j.aca.2015.04.042

Breiman, L. (2001). Random forests. *Machine Learning*, *45*(1), 5–32. https://doi.org/10.1023/A:1010933404324

Brereton, R. G. (2003). Model Validation. In *Chemometrics: Data Analysis for the Laboratory and Chemical Plant* (pp. 1313–1323). John Wiley & Sons, Ltd. https://doi.org/10.1002/0470863242

Brereton, R. G., & Lloyd, G. R. (2014). Partial least squares discriminant analysis: Taking the magic away. *Journal of Chemometrics*, *28*(4), 213–225. https://doi.org/10.1002/cem.2609

Cagliani, L. R., Scano, P., & Consonni, R. (2017). NMR-based metabolomics: Quality and authenticity of plant-based foods. In *Modern Magnetic Resonance* (pp. 1–20). Springer.

https://doi.org/10.1007/978-3-319-28388-3_1

Cattaneo, T. M. P., & Stellari, A. (2019). Review: NIR spectroscopy as a suitable tool for the investigation of the horticultural field. *Agronomy*, *9*(9), 503. https://doi.org/10.3390/agronomy9090503

Cavanna, D., Righetti, L., Elliott, C., & Suman, M. (2018). The scientific challenges in moving from targeted to non-targeted mass spectrometric methods for food fraud analysis: A proposed validation workflow to bring about a harmonized approach. *Trends in Food Science and Technology*, *80*, 223–241. https://doi.org/10.1016/j.tifs.2018.08.007

Choudhary, A., Gupta, N., Hameed, F., & Choton, S. (2020). An overview of food adulteration: Concept, sources, impact, challenges and detection. *International Journal of Chemical Studies*, *8*(1), 2564–2573. https://doi.org/10.22271/chemi.2020.v8.i1am.8655

Cifuentes, A. (2009). Food analysis and foodomics. *Journal of Chromatography A*, *1216*(43), 7109. https://doi.org/10.1016/j.chroma.2009.09.018

Cifuentes, A. (2012). Food Analysis: Present, Future, and Foodomics. *ISRN Analytical Chemistry*, *2012*, 1–16. https://doi.org/10.5402/2012/801607

Consonni, R., & Cagliani, L. R. (2008). Ripening and geographical characterization of Parmigiano Reggiano cheese by 1H NMR spectroscopy. *Talanta*, *76*(1), 200–205. https://doi.org/10.1016/j.talanta.2008.02.022

Consonni, R., & Cagliani, L. R. (2019). The potentiality of NMR-based metabolomics in food science and food authentication assessment. *Magnetic Resonance in Chemistry*, *57*(9), 558–578. https://doi.org/10.1002/mrc.4807

Consonni, R., & Cagliani, L. R. (2022). Quality assessment of traditional food by NMR analysis. *Food Control*, *142*, 109226. https://doi.org/10.1016/J.FOODCONT.2022.109226

Consonni, R., Polla, D., & Cagliani, L. R. (2018). Organic and conventional coffee differentiation by NMR spectroscopy. *Food Control*, *94*, 284–288. https://doi.org/10.1016/j.foodcont.2018.07.013

Cortes, C., & Vapnik, V. (1995). Support-Vector Networks. *Machine Learning*, *20*(3), 273–297. https://doi.org/10.1023/A:1022627411411

Cozzolino, D. (2012). Recent trends on the use of infrared spectroscopy to trace and authenticate natural and agricultural food products. *Applied Spectroscopy Reviews*, *47*(7), 518–530. https://doi.org/10.1080/05704928.2012.667858

Cozzolino, D. (2022). Advantages, Opportunities, and Challenges of Vibrational Spectroscopy as Tool to Monitor Sustainable Food Systems. *Food Analytical Methods*, *15*(5), 1390–1396. https://doi.org/10.1007/s12161-021-02207-w

Cozzolino, D., Dambergs, R. G., Janik, L., Cynkar, W. U., & Gishen, M. (2006). Analysis of grapes and wine by near infrared spectroscopy. *Journal of Near Infrared Spectroscopy*, *14*(5), 279–289. https://doi.org/10.1255/jnirs.679

Creydt, M., & Fischer, M. (2018). Omics approaches for food authentication. *Electrophoresis*, *39*(13), 1569–1581. https://doi.org/10.1002/elps.201800004

Cruz-Castillo, J. G., Ganeshanandam, S., MacKay, B. R., Lawes, G. S., Lawoko, C. R. O., & Woolley, D. J. (1994). Applications of canonical discriminant analysis in horticultural research. *HortScience*, *29*(10), 1115–1119. https://doi.org/10.21273/hortsci.29.10.1115

Cubero-Leon, E., De Rudder, O., & Maquet, A. (2018). Metabolomics for organic food authentication: Results from a long-term field study in carrots. *Food Chemistry*, *239*, 760–770. https://doi.org/10.1016/j.foodchem.2017.06.161

Currò, S., Fasolato, L., Serva, L., Boffo, L., Ferlito, J. C., Novelli, E., & Balzan, S. (2022). Use of a portable near-infrared tool for rapid on-site inspection of freezing and hydrogen peroxide treatment of cuttlefish (Sepia officinalis). *Food Control*, *132*, 108524. https://doi.org/10.1016/j.foodcont.2021.108524

Daglia, M., Antiochia, R., Sobolev, A. P., & Mannina, L. (2014). Untargeted and targeted methodologies in the study of tea (Camellia sinensis L.). *Food Research International*, *63*, 275–289. https://doi.org/10.1016/j.foodres.2014.03.070

Dais, P., & Hatzakis, E. (2013). Quality assessment and authentication of virgin olive oil by NMR spectroscopy: A critical review. *Analytica Chimica Acta*, *765*, 1–27. https://doi.org/10.1016/J.ACA.2012.12.003

Danezis, G. P., Tsagkaris, A. S., Brusic, V., & Georgiou, C. A. (2016a). Food authentication: state of the art and prospects. *Current Opinion in Food Science*, *10*, 22–31. https://doi.org/10.1016/j.cofs.2016.07.003

Danezis, G. P., Tsagkaris, A. S., Camin, F., Brusic, V., & Georgiou, C. A. (2016b). Food authentication: Techniques, trends & emerging approaches. *TrAC - Trends in Analytical Chemistry*, *85*, 123–132. https://doi.org/10.1016/j.trac.2016.02.026

De Araújo Gomes, A., Azcarate, S. M., Diniz, P. H. G. D., de Sousa Fernandes, D. D., & Veras, G. (2022). Variable selection in the chemometric treatment of food data: A tutorial review. *Food Chemistry*, *370*, 131072. https://doi.org/10.1016/j.foodchem.2021.131072

De Marchi, M., Penasa, M., Zidi, A., & Manuelian, C. L. (2018). Invited review: Use of infrared technologies for the assessment of dairy products—Applications and perspectives. *Journal of Dairy Science*, *101*(12), 10589–10604. https://doi.org/10.3168/jds.2018-15202

Donarski, J., Camin, F., Fauhl-Hassek, C., Posey, R., & Sudnik, M. (2019). Sampling guidelines for building and curating food authenticity databases. *Trends in Food Science and Technology*, *90*, 187–193. https://doi.org/10.1016/j.tifs.2019.02.019

Dvorak, L., Mlcek, J., & Sustova, K. (2016). Comparison of FT-NIR spectroscopy and ELISA for detection of adulteration of goat cheeses with cow's milk. *Journal of AOAC International*, *99*(1), 180–186. https://doi.org/10.5740/jaoacint.15-0190

Erikson, U., Standal, I. B., Aursand, I. G., Veliyulin, E., & Aursand, M. (2012). Use of NMR in fish processing optimization: A review of recent progress. *Magnetic Resonance in Chemistry*, *50*(7), 471–480. https://doi.org/10.1002/mrc.3825

Esteve Agelet, L. (2011). Single seed discriminative applications using near infrared technologies [Iowa State University]. In *ProQuest Dissertations and Theses*. https://doi.org/https://doi.org/10.31274/etd-180810-1160

Farag, M. A., Labib, R. M., Noleto, C., Porzel, A., & Wessjohann, L. A. (2018). NMR approach for the authentication of 10 cinnamon spice accessions analyzed via chemometric tools. *LWT*, *90*, 491–498. https://doi.org/10.1016/j.lwt.2017.12.069

Fasolato, L., Balzan, S., Riovanto, R., Berzaghi, P., Mirisola, M., Ferlito, J. C., Serva, L., Benozzo, F., Passera, R., Tepedino, V., & Novelli, E. (2012). Comparison of visible and near-infrared reflectance spectroscopy to authenticate fresh and frozen-thawed swordfish (xiphias gladius L). *Journal of Aquatic Food Product Technology*, *21*(5), 493–507. https://doi.org/10.1080/10498850.2011.615103

Fotakis, C., & Zervou, M. (2016). NMR metabolic fingerprinting and chemometrics driven authentication of Greek grape marc spirits. *Food Chemistry*, *196*, 760–768. https://doi.org/10.1016/j.foodchem.2015.10.002

Galvin-King, P., Haughey, S. A., & Elliott, C. T. (2018). Herb and spice fraud; the drivers, challenges and detection. *Food Control*, *88*, 85–97. https://doi.org/10.1016/j.foodcont.2017.12.031

Grunert, K. G. (2005). Food quality and safety: Consumer perception and demand. *European Review of Agricultural Economics*, *32*(3), 369–391. https://doi.org/10.1093/eurrag/jbi011

Hatzakis, E. (2019). Nuclear Magnetic Resonance (NMR) Spectroscopy in Food Science: A Comprehensive Review. *Comprehensive Reviews in Food Science and Food Safety*, *18*(1), 189–220. https://doi.org/10.1111/1541-4337.12408

Hencz, A., Nguyen, L. L. P., Baranyai, L., & Albanese, D. (2022). Assessment of Wine Adulteration Using Near Infrared Spectroscopy and Laser Backscattering Imaging. *Processes*, *10*(1), 95. https://doi.org/10.3390/pr10010095

Hsieh, C. L., Hung, C. Y., & Kuo, C. Y. (2011). Quantization of adulteration ratio of raw cow milk by Least Squares Support Vector Machines (LS-SVM) and visible/near infrared spectroscopy. In L. Iliadis & C. Jayne (Eds.), *Engineering Applications of Neural Networks. EANN AIAI 2011 2011. IFIP Advances in Information and Communication Technology* (Vol. 363, pp. 130–139). Springer Berlin Heidelberg. https://doi.org/10.1007/978-3-642-23957-1_15

Indahl, U. G., Martens, H., & Næs, T. (2007). From dummy regression to prior probabilities in PLS-DA. *Journal of Chemometrics*, *21*(12), 529–536. https://doi.org/10.1002/cem.1061

Jiménez-Carvelo, A. M., González-Casado, A., Bagur-González, M. G., & Cuadros-Rodríguez, L. (2019). Alternative data mining/machine learning methods for the analytical evaluation of food quality and authenticity – A review. *Food Research International*, *122*, 25–39. https://doi.org/10.1016/j.foodres.2019.03.063

Kartheek, M., Anton Smith, A., Kottai Muthu, A., & Manavalan, R. (2011). Determination of adulterants in food: A review. *Journal of Chemical and Pharmaceutical Research*, *3*(2), 629–636.

Kaufman, L., & Rousseeuw, P. J. (1990). Finding Groups in Data: An Introduction to Cluster Analysis. In *Wiley Series in Probability and Statistics* (Vol. 66). John Wiley & Sons, Inc. https://doi.org/10.1002/9780470316801

Kaufmann, A., Butcher, P., Maden, K., Walker, S., & Widmer, M. (2015). Reliability of veterinary drug residue confirmation: High resolution mass spectrometry versus tandem mass spectrometry. *Analytica Chimica Acta*, *856*, 54–67. https://doi.org/10.1016/j.aca.2014.11.034

Kjeldahl, K., & Bro, R. (2010). Some common misunderstandings in chemometrics. *Journal of Chemometrics*, *24*(7–8), 558–564. https://doi.org/10.1002/cem.1346

Klein, M. S., Buttchereit, N., Miemczyk, S. P., Immervoll, A. K., Louis, C., Wiedemann, S., Junge, W., Thaller, G., Oefner, P. J., & Gronwald, W. (2012). NMR metabolomic analysis of dairy cows reveals milk glycerophosphocholine to phosphocholine ratio as prognostic biomarker for risk of ketosis. *Journal of Proteome Research*, *11*(2), 1373–1381. https://doi.org/10.1021/pr201017n

Kowalski, B. R. (1984). Chemometrics: Mathematics and Statistics in Chemistry. In *NATO Science Series C*. Springer Science+Business Media Dordrecht. https://doi.org/https://doi.org/10.1007/ 978-94-017-1026-8

Kritikou, A. S., Aalizadeh, R., Damalas, D. E., Barla, I. V., Baessmann, C., & Thomaidis, N. S. (2022). MALDI-TOF-MS integrated workflow for food authenticity investigations: An untargeted protein-based approach for rapid detection of PDO feta cheese adulteration. *Food Chemistry*, *370*, 131057. https://doi.org/10.1016/j.foodchem.2021.131057

Kuballa, T., Hausler, T., Okaru, A. O., Neufeld, M., Abuga, K. O., Kibwage, I. O., Rehm, J., Luy, B., Walch, S. G., & Lachenmeier, D. W. (2018). Detection of counterfeit brand spirits using 1H NMR fingerprints in comparison to sensory analysis. *Food Chemistry*, *245*, 112–118. https://doi.org/10.1016/j.foodchem.2017.10.065

Kursa, M. B., & Rudnicki, W. R. (2010). Feature selection with the boruta package. *Journal of Statistical Software*, *36*(11), 1–13. https://doi.org/10.18637/jss.v036.i11

Lavine, B. K. (2006). Pattern Recognition. *Critical Reviews in Analytical Chemistry*, *36*(3–4), 153–161. https://doi.org/10.1080/10408340600969411

Li, X., Zhang, L., Zhang, Y., Wang, D., Wang, X., Yu, L., Zhang, W., & Li, P. (2020).

Review of NIR spectroscopy methods for nondestructive quality analysis of oilseeds and edible oils. *Trends in Food Science and Technology*, *101*, 172–181. https://doi.org/10.1016/j.tifs.2020.05.002

Lineback, D. R., Pirlet, A., Van Der Kamp, J. W., & Wood, R. (2009). Globalization, food safety issues & role of international standards. *Quality Assurance and Safety of Crops and Foods*, *1*(1), 23–27. https://doi.org/10.1111/j.1757-837X.2009.00005.x

Liu, L., Cozzolino, D., Cynkar, W. U., Gishen, M., & Colby, C. B. (2006). Geographic classification of Spanish and Australian tempranillo red wines by visible and near-infrared spectroscopy combined with multivariate Analysis. *Journal of Agricultural and Food Chemistry*, *54*(18), 6754–6759. https://doi.org/10.1021/jf061528b

Liu, M., Wang, M., Wang, J., & Li, D. (2013). Comparison of random forest, support vector machine and back propagation neural network for electronic tongue data classification: Application to the recognition of orange beverage and Chinese vinegar. *Sensors and Actuators, B: Chemical*, *177*, 970–980. https://doi.org/10.1016/j.snb.2012.11.071

Lohumi, S., Lee, S., Lee, H., & Cho, B. K. (2015). A review of vibrational spectroscopic techniques for the detection of food authenticity and adulteration. *Trends in Food Science and Technology*, *46*(1), 85–98. https://doi.org/10.1016/j.tifs.2015.08.003

Luna, A. S., Da Silva, A. P., Pinho, J. S. A., Ferré, J., & Boqué, R. (2013). Rapid characterization of transgenic and non-transgenic soybean oils by chemometric methods using NIR spectroscopy. *Spectrochimica Acta - Part A: Molecular and Biomolecular Spectroscopy*, *100*, 115–119. https://doi.org/10.1016/j.saa.2012.02.085

Luykx, D. M. A. M., & van Ruth, S. M. (2008). An overview of analytical methods for determining the geographical origin of food products. *Food Chemistry*, *107*(2), 897–911. https://doi.org/10.1016/J.FOODCHEM.2007.09.038

Masetti, O., Sorbo, A., & Nisini, L. (2021). Nmr tracing of food geographical origin: The impact of seasonality, cultivar and production year on data analysis. *Separations*, *8*(12), 230. https://doi.org/10.3390/separations8120230

McVey, C., McGrath, T. F., Haughey, S. A., & Elliott, C. T. (2021). A rapid food chain approach for authenticity screening: The development, validation and transferability of a chemometric model using two handheld near infrared spectroscopy (NIRS) devices. *Talanta*, *222*, 121533. https://doi.org/10.1016/j.talanta.2020.121533

Medina, S., Perestrelo, R., Silva, P., Pereira, J. A. M., & Câmara, J. S. (2019). Current trends and recent advances on food authenticity technologies and chemometric approaches. *Trends in Food Science and Technology*, *85*, 163–176. https://doi.org/10.1016/j.tifs.2019.01.017

Mees, C., Souard, F., Delporte, C., Deconinck, E., Stoffelen, P., Stévigny, C., Kauffmann, J. M., & De Braekeleer, K. (2018). Identification of coffee leaves using FT-NIR spectroscopy and SIMCA. *Talanta*, *177*, 4–11. https://doi.org/10.1016/j.talanta.2017.09.056

Mendes, T. O., da Rocha, R. A., Porto, B. L. S., de Oliveira, M. A. L., dos Anjos, V. de C., & Bell, M. J. V. (2015). Quantification of Extra-virgin Olive Oil Adulteration with Soybean Oil: a Comparative Study of NIR, MIR, and Raman Spectroscopy Associated with Chemometric Approaches. *Food Analytical Methods*, *8*(9), 2339–2346. https://doi.org/10.1007/s12161-015-0121-y

Minoja, A. P., & Napoli, C. (2014). NMR screening in the quality control of food and nutraceuticals. *Food Research International*, *63*, 126–131. https://doi.org/10.1016/j.foodres.2014.04.056

Monakhova, Y. B., Kuballa, T., & Lachenmeier, D. W. (2012). Rapid Quantification of Ethyl Carbamate in Spirits Using NMR Spectroscopy and Chemometrics. *ISRN Analytical Chemistry*, *2012*, 1–5. https://doi.org/10.5402/2012/989174

Morsy, N., & Sun, D. W. (2013). Robust linear and non-linear models of NIR spectroscopy for detection and quantification of adulterants in fresh and frozen-thawed minced beef. *Meat Science*, *93*(2), 292–302. https://doi.org/10.1016/j.meatsci.2012.09.005

Nicolaï, B. M., Beullens, K., Bobelyn, E., Peirs, A., Saeys, W., Theron, K. I., & Lammertyn, J. (2007). Nondestructive measurement of fruit and vegetable quality by means of NIR spectroscopy: A review. *Postharvest Biology and Technology*, *46*(2), 99–118. https://doi.org/10.1016/j.postharvbio.2007.06.024

Nie, J., Li, Y., Xing, J., Chao, J., Qin, X., & Li, Z. (2019). Comparison of two types of vinegar with different aging times by NMR-based metabolomic approach. *Journal of Food Biochemistry*, *43*(5), e12835. https://doi.org/10.1111/jfbc.12835

Niero, G., Meoni, G., Tenori, L., Luchinat, C., Visentin, G., Callegaro, S., Visentin, E., Cassandro, M., De Marchi, M., & Penasa, M. (2022). Grazing affects metabolic pattern of individual cow milk. *Journal of Dairy Science*, *105*(12), 9702–9712.

https://doi.org/10.3168/jds.2022-22072

Nilsson, R., Peña, J. M., Björkegren, J., & Tegnér, J. (2007). Consistent feature selection for pattern recognition in polynomial time. *Journal of Machine Learning Research*, *8*, 589–612.

Nobari Moghaddam, H., Tamiji, Z., Akbari Lakeh, M., Khoshayand, M. R., & Haji Mahmoodi, M. (2022). Multivariate analysis of food fraud: A review of NIR based instruments in tandem with chemometrics. *Journal of Food Composition and Analysis*, *107*, 104343. https://doi.org/10.1016/j.jfca.2021.104343

Nørgaard, L., Bro, R., Westad, F., & Engelsen, S. B. (2006). A modification of canonical variates analysis to handle highly collinear multivariate data. *Journal of Chemometrics*, *20*(8–10), 425–435. https://doi.org/10.1002/cem.1017

Nunes, C. A., Alvarenga, V. O., de Souza Sant'Ana, A., Santos, J. S., & Granato, D. (2015). The use of statistical software in food science and technology: Advantages, limitations and misuses. *Food Research International*, *75*, 270–280. https://doi.org/10.1016/j.foodres.2015.06.011

Olawode, E. O., Tandlich, R., & Cambray, G. (2018). 1H-NMR profiling and chemometric analysis of selected honeys from South Africa, Zambia, and Slovakia. *Molecules*, *23*(3), 578. https://doi.org/10.3390/molecules23030578

Oliveri, P., & Downey, G. (2012). Multivariate class modeling for the verification of food-authenticity claims. *TrAC - Trends in Analytical Chemistry*, *35*, 74–86. https://doi.org/10.1016/j.trac.2012.02.005

Osborne, B. G. (2000). Near-Infrared Spectroscopy in Food Analysis. *Encyclopedia of Analytical Chemistry*, 1–14. https://doi.org/10.1002/9780470027318.a1018

Ottavian, M., Facco, P., Barolo, M., Berzaghi, P., Segato, S., Novelli, E., & Balzan, S. (2012). Near-infrared spectroscopy to assist authentication and labeling of Asiago d'allevo cheese. *Journal of Food Engineering*, *113*(2), 289–298. https://doi.org/10.1016/j.jfoodeng.2012.05.037

Ozaki, Y. (2012). Near-infrared spectroscopy-its versatility in analytical chemistry. *Analytical Sciences*, *28*(6), 545–563. https://doi.org/10.2116/analsci.28.545

Ozaki, Y. (2021). Infrared Spectroscopy—Mid-infrared, Near-infrared, and Far-infrared/Terahertz Spectroscopy. *Analytical Sciences*, *37*(9), 1193–1212.

https://doi.org/10.2116/analsci.20R008

Petrescu, D. C., Vermeir, I., & Petrescu-Mag, R. M. (2020). Consumer understanding of food quality, healthiness, and environmental impact: A cross-national perspective. *International Journal of Environmental Research and Public Health*, *17*(1), 169. https://doi.org/10.3390/ijerph17010169

Pomerantsev, A. L., & Rodionova, O. Y. (2020). Popular decision rules in SIMCA: Critical review. *Journal of Chemometrics*, *34*(8), e3250. https://doi.org/10.1002/cem.3250

Prieto, N., Roehe, R., Lavín, P., Batten, G., & Andrés, S. (2009). Application of near infrared reflectance spectroscopy to predict meat and meat products quality: A review. *Meat Science*, *83*(2), 175–186. https://doi.org/10.1016/j.meatsci.2009.04.016

Qu, J. H., Liu, D., Cheng, J. H., Sun, D. W., Ma, J., Pu, H., & Zeng, X. A. (2015). Applications of Near-infrared Spectroscopy in Food Safety Evaluation and Control: A Review of Recent Research Advances. *Critical Reviews in Food Science and Nutrition*, *55*(13), 1939–1954. https://doi.org/10.1080/10408398.2013.871693

Reg. (EU) 2017/625 of the European Parliament and of the Council on official controls and other official activities performed to ensure the application of food and feed law, rules on animal health and welfare, plant health and plant protection products, (2017). http://data.europa.eu/eli/reg/2017/625/oj

Riedl, J., Esslinger, S., & Fauhl-Hassek, C. (2015). Review of validation and reporting of non-targeted fingerprinting approaches for food authentication. *Analytica Chimica Acta*, *885*, 17–32. https://doi.org/10.1016/j.aca.2015.06.003

Riuzzi, G., Tata, A., Massaro, A., Bisutti, V., Lanza, I., Contiero, B., Bragolusi, M., Miano, B., Negro, A., Gottardo, F., Piro, R., & Segato, S. (2021). Authentication of forage-based milk by mid-level data fusion of (+/−) DART-HRMS signatures. *International Dairy Journal*, *112*, 104859. https://doi.org/10.1016/j.idairyj.2020.104859

Robson, K., Dean, M., Haughey, S., & Elliott, C. (2021). A comprehensive review of food fraud terminologies and food fraud mitigation guides. *Food Control*, *120*, 107516. https://doi.org/10.1016/j.foodcont.2020.107516

Rusilowicz, M., O'Keefe, S., Wilson, J., & Charlton, A. (2014). Chemometrics Applied to NMR Analysis. In *Encyclopedia of Analytical Chemistry* (pp. 1–32). John Wiley & Sons, Ltd. https://doi.org/10.1002/9780470027318.a9300

Saadat, S., Pandya, H., Dey, A., & Rawtani, D. (2022). Food forensics: Techniques for authenticity determination of food products. *Forensic Science International*, *333*, 111243. https://doi.org/10.1016/j.forsciint.2022.111243

Scano, P., Cusano, E., Caboni, P., & Consonni, R. (2019). NMR metabolite profiles of dairy: A review. *International Dairy Journal*, *90*, 56–67. https://doi.org/10.1016/J.IDAIRYJ.2018.11.004

Segato, S., Caligiani, A., Contiero, B., Galaverna, G., Bisutti, V., & Cozzi, G. (2019). 1H NMR metabolic profile to discriminate pasture based alpine asiago PDO cheeses. *Animals*, *9*(10), 722. https://doi.org/10.3390/ani9100722

Selamat, J., Rozani, N. A. A., & Murugesu, S. (2021). Application of the metabolomics approach in food authentication. *Molecules*, *26*(24), 7565. https://doi.org/10.3390/molecules26247565

Shumilina, E., Slizyte, R., Mozuraityte, R., Dykyy, A., Stein, T. A., & Dikiy, A. (2016). Quality changes of salmon by-products during storage: Assessment and quantification by NMR. *Food Chemistry*, *211*, 803–811. https://doi.org/10.1016/j.foodchem.2016.05.088

Siebert, K. J. (2001). Chemometrics in brewing - A review. *Journal of the American Society of Brewing Chemists*, *59*(4), 147–156. https://doi.org/10.1094/asbcj-59-0147

Sorak, D., Herberholz, L., Iwascek, S., Altinpinar, S., Pfeifer, F., & Siesler, H. W. (2012). New developments and applications of handheld raman, mid-infrared, and near-infrared spectrometers. *Applied Spectroscopy Reviews*, *47*(2), 83–115. https://doi.org/10.1080/05704928.2011.625748

Sun, D. W. (2009). *Infrared Spectroscopy for Food Quality Analysis and Control* (1st ed.). Elsevier Science Publishing Co Inc. https://doi.org/10.1016/B978-0-12-374136-3.X0001-6

Sundekilde, U. K., Poulsen, N. A., Larsen, L. B., & Bertram, H. C. (2013). Nuclear magnetic resonance metabonomics reveals strong association between milk metabolites and somatic cell count in bovine milk. *Journal of Dairy Science*, *96*(1), 290–299. https://doi.org/10.3168/jds.2012-5819

Tang, F., Vasas, M., Hatzakis, E., & Spyros, A. (2019). Magnetic resonance applications in food analysis. In *Annual Reports on NMR Spectroscopy* (Vol. 98, pp. 239–306).

https://doi.org/10.1016/bs.arnmr.2019.04.005

Teixeira Dos Santos, C. A., Lopo, M., Páscoa, R. N. M. J., & Lopes, J. A. (2013). A review on the applications of portable near-infrared spectrometers in the agro-food industry. *Applied Spectroscopy*, *67*(11), 1215–1233. https://doi.org/10.1366/13-07228

Tibola, C. S., da Silva, S. A., Dossa, A. A., & Patrício, D. I. (2018). Economically Motivated Food Fraud and Adulteration in Brazil: Incidents and Alternatives to Minimize Occurrence. *Journal of Food Science*, *83*(8), 2028–2038. https://doi.org/10.1111/1750-3841.14279

Tomassini, A., Curone, G., Solè, M., Capuani, G., Sciubba, F., Conta, G., Miccheli, A., & Vigo, D. (2019). NMR-based metabolomics to evaluate the milk composition from Friesian and autochthonous cows of Northern Italy at different lactation times. *Natural Product Research*, *33*(8), 1085–1091. https://doi.org/10.1080/14786419.2018.1462183

Trygg, J., Holmes, E., & Lundstedt, T. (2007). Chemometrics in metabonomics. *Journal of Proteome Research*, *6*(2), 469–479. https://doi.org/10.1021/pr060594q

Tumanov, A. A. (1984). Biological methods of analysis. *Trends in Analytical Chemistry*, *3*(3), 67–71. https://doi.org/10.1016/0165-9936(84)87065-X

Tümsavaş, Z., Tekin, Y., & Mouazen, A. M. (2013). Effect of moisture content on the prediction of cation exchange capacity using visible and near infrared spectroscopy. *Journal of Food, Agriculture and Environment*, *11*(1), 760–764.

U.S. Food & Drug Administration. (n.d.). *Economically Motivated Adulteration (Food Fraud)*. Retrieved October 10, 2022, from https://www.fda.gov/food/compliance-enforcement-food/economically-motivated-adulteration-food-fraud

Valand, R., Tanna, S., Lawson, G., & Bengtström, L. (2020). A review of Fourier Transform Infrared (FTIR) spectroscopy used in food adulteration and authenticity investigations. *Food Additives and Contaminants - Part A Chemistry, Analysis, Control, Exposure and Risk Assessment*, *37*(1), 19–38. https://doi.org/10.1080/19440049.2019.1675909

Vandeginste, B. G. M., Massart, D. L., Buydens, L. M. C., de Jong, S., Lewi, P. J., & Verbeke, J. S. (1998). Handbook of Chemometrics and Qualimetrics, Part B. In *Data Handling in Science and Technology* (1st ed., Vol. 20B). Elsevier Science Publishing Co Inc.

Varmuza, K., & Filzmoser, P. (2016). *Introduction to Multivariate Statistical Analysis in*

Chemometrics (1st ed.). CRC Press. https://doi.org/10.1201/9781420059496

Varrà, M. O., Ghidini, S., Fabrile, M. P., Ianieri, A., & Zanardi, E. (2022). Country of origin label monitoring of musky and common octopuses (Eledone spp. and Octopus vulgaris) by means of a portable near-infrared spectroscopic device. *Food Control*, *138*, 109052. https://doi.org/10.1016/J.FOODCONT.2022.109052

Viskić, M., Bandić, L. M., Korenika, A. M. J., & Jeromel, A. (2021). NMR in the service of wine differentiation. *Foods*, *10*(1), 120. https://doi.org/10.3390/foods10010120

Wang, X., Wang, J., Kamal, G. M., Jiang, B., Sun, P., Zhang, X., & Liu, M. (2016). Characterization and Comparison of Commercial Chinese Cereal and European Grape Vinegars Using 1H NMR Spectroscopy Combined with Multivariate Analysis. *Chinese Journal of Chemistry*, *34*(11), 1183–1193. https://doi.org/10.1002/cjoc.201600365

Xu, Y., Zomer, S., & Brereton, R. G. (2006). Support vector machines: A recent method for classification in chemometrics. *Critical Reviews in Analytical Chemistry*, *36*(3–4), 177–188. https://doi.org/10.1080/10408340600969486

Zanardi, E., Caligiani, A., Palla, L., Mariani, M., Ghidini, S., Di Ciccio, P. A., Palla, G., & Ianieri, A. (2015). Metabolic profiling by 1H NMR of ground beef irradiated at different irradiation doses. *Meat Science*, *103*, 83–89. https://doi.org/10.1016/j.meatsci.2015.01.005

Zhang, Y., Jiang, H., & Wang, W. (2019). Feasibility of the detection of carrageenan adulteration in chicken meat using visible/near-infrared (Vis/NIR) hyperspectral imaging. *Applied Sciences (Switzerland)*, *9*(18), 3926. https://doi.org/10.3390/app9183926

Zhao, G., & Maclean, A. L. (2000). A comparison of canonical discriminant analysis and principal component analysis for spectral transformation. *Photogrammetric Engineering and Remote Sensing*, *66*(7), 841–847.

Zheng, X., Li, Y., Wei, W., & Peng, Y. (2019). Detection of adulteration with duck meat in minced lamb meat by using visible near-infrared hyperspectral imaging. *Meat Science*, *149*, 55–62. https://doi.org/10.1016/j.meatsci.2018.11.005

CHAPTER 2

Aim of the study

The main objective of this doctoral thesis is to evaluate NIR and NMR spectroscopic techniques in combination with pattern recognition tools as chemometric approaches for assessing authenticity of food products from animal origin through analytical methods based on safety inspection and/or quality traits assessment.

- Presence of pyrrolizidine alkaloids (PAs) and their N-oxides (PANOs) in bee pollen have been reported to cause toxicity in humans. Since consumption of bee pollen as a food supplement has increased recently, there is need for rapid detection of these natural toxins in food; a challenge that could be met by NIR spectroscopy. Two NIR spectroscopic devices (portable and benchtop) were used to discriminate levels of PAs and PANOs in bee pollen and their capacities to do so were evaluated (**Chapter 3**).
- Fresh chicken meat is highly perishable, leading to a fast loss of freshness during storage. Due to its relatively short shelf life, a rapid, cost-effective and non-destructive quality control system to assess meat freshness is needed. The capacities of two NIR spectroscopic devices (portable and benchtop) to analyse chicken meat freshness are explored in discriminating among four refrigeration time (2, 6, 10 and 14 days post mortem) coupled with multivariate classifier models (**Chapter 4**).
- Insects represent an alternative to conventional protein and lipid feedstuffs for monogastric animals, providing strategic solutions to address some environmental and ethical concerns. Therefore, the need for rapid and reliable analytical methods for evaluating product quality, preferably exploiting real-time methods arises. For these reasons, capabilities of a VIS/NIR and two NIR instruments (portable and bench-top) to discriminate among table eggs from quails fed with different inclusion levels of silkworm pupa meal is evaluated throughout four supervised pattern recognition models. An in-depth interpretation of the most predictive VIS/NIR and NIR features selected by a random forest (RF) algorithm was another challenge of the experimental trial (**Chapter 5**).
- Forage may affect the environmental sustainability of a given dairy chain, the quality of milk and its suitability for high-value dairy products. To better understand the influence of the dietary forage proportion, especially in the case of intensive dairy systems, NMR

metabolomic and FAs profiles of milk are gathered and analysed giving better understanding of the relationship between feeding system and the wide pool of biomarkers useful to authenticate the milk dairy chain (**Chapter 6**).

CHAPTER 3

Discriminant Analysis of Pyrrolizidine Alkaloid Contamination in Bee Pollen Based on Near-Infrared Data from Lab-Stationary and Portable Spectrometers

---

Luciana De Jesus Inacio[1], Ilaria Lanza[2], Roberta Merlanti[1], Barbara Contiero[2], Lorena Lucatello[1], Lorenzo Serva[2], Vittoria Bisutti[2], Massimo Mirisola[2], Sandro Tenti[2], Severino Segato[2], Francesca Capolongo[1].

[1]Department of Comparative Biomedicine and Food Science, University of Padova, 35020 Legnaro, PD, Italy

[2]Department of Animal Medicine, Production and Health, University of Padova, 35020 Legnaro, PD, Italy

European Food Research and Technology (2020) 246:2471–2483

European Food Research and Technology (2020) 246:2471–2483
https://doi.org/10.1007/s00217-020-03590-0

ORIGINAL PAPER

Discriminant analysis of pyrrolizidine alkaloid contamination in bee pollen based on near-infrared data from lab-stationary and portable spectrometers

Luciana De Jesus Inacio[1] · Ilaria Lanza[2] · Roberta Merlanti[1] · Barbara Contiero[2] · Lorena Lucatello[1] · Lorenzo Serva[2] · Vittoria Bisutti[2] · Massimo Mirisola[2] · Sandro Tenti[2] · Severino Segato[2] · Francesca Capolongo[1]

Received: 23 June 2020 / Revised: 6 August 2020 / Accepted: 10 August 2020 / Published online: 29 August 2020

Abstract
Bee pollen may be contaminated with pyrrolizidine alkaloids (PAs) and their *N*-oxides (PANOs), which are mainly detected by liquid chromatography coupled to tandem mass spectrometry (LC–MS/MS), even though the use of fast near-infrared (NIR) spectroscopy is an ongoing alternative. Therefore, the main challenge of this study was to assess the feasibility of both a lab-stationary (Foss) and a portable (Polispec) NIR spectrometer in 60 dehydrated bee pollen samples. After an ANOVA-feature selection of the most informative NIR spectral data, canonical discriminant analysis (CDA) was performed to distinguish three quantitative PA/PANO classes (µg/kg): < LOQ (0.4), low; 0.4–400, moderate; > 400, high. According to the LC–MS/MS analysis, 77% of the samples were contaminated with PAs/PANOs and the sum content of the 17 target analytes was higher than 400 µg/kg in 28% of the samples. CDA was carried out on a pool of 18 (Foss) and 22 (Polispec) selected spectral variables and allowed accurate classification of samples from the low class as confirmed by the high values of Matthews correlation coefficient (≥ 0.91) for both NIR spectrometers. Leave-one-out cross-validation highlighted precise recognition of samples characterised by a high PA/PANO content with a low misclassification rate (0.02) as false negatives. The most informative wavelengths were within the < 1000, 1000–1660 and > 2400 nm regions for Foss and > 1500 nm for Polispec that could be associated with cyclic amines, and epoxide chemical structures of PAs/PANOs. In sum, both lab-stationary and portable NIR systems are reliable and fast techniques for detecting PA/PANO contamination in bee pollen.

Keywords Pyrrolizidine alkaloids · Bee pollen · LC–MS/MS · NIR spectroscopy · Canonical discriminant analysis

Introduction

Bee pollen is a mixture of flower pollen, nectar and bee saliva. This beehive product is rich in essential nutrients and biologically active substances, such as phenolic compounds that can exhibit antioxidant, anti-inflammatory and anti-microbial activity. Thus, the consumption of bee pollen as a food supplement and a health product has increased in recent years [1]. However, depending on the geographical and botanical origin, bee pollen might be potential hazard for human intake due to the presence of natural toxins like pyrrolizidine alkaloids (PAs) and their *N*-oxides (PANOs) [2].

PAs/PANOs are secondary metabolites produced by plants as a chemical defence against herbivorous insects. They are predominant in all genera of the Boraginaceae family, in the Senecioneae and Eupatorieae tribes (Asteraceae), but they are also present in the genus *Crotalaria* (Fabaceae) [3]. PAs/PANOs have been reported to cause toxicity in many animal species, including humans. Experimental data obtained from in vitro and in vivo studies suggest that chronic exposure to PAs/PANOs may lead to hepatotoxicity, genotoxicity, carcinogenicity and pulmonary lesions [4, 5]. However, the toxicity of PAs/PANOs is dependent on their chemical structure [6]. Only those compounds that contain a double bond at the 1,2-position of the necine base can be transformed into highly reactive pyrroles in the liver. Furthermore, PAs/PANOs can be classified according to their

✉ Roberta Merlanti
roberta.merlanti@unipd.it

[1] Department of Comparative Biomedicine and Food Science, University of Padova, 35020 Legnaro, PD, Italy

[2] Department of Animal Medicine, Production and Health, University of Padova, 35020 Legnaro, PD, Italy

esterification level as cyclic diesters, open-chain diesters and monoesters, which are in decreasing order of toxicity [4–6]. Based on botanical origin and chemical structure, PAs/PANOs can be classified into different groups, such as lycopsamine, senecionine and heliotrine types [3]. The lycopsamine-type PAs/PANOs consist of monoesters (e.g., lycopsamine and its *N*-oxide, indicine *N*-oxide, intermedine) and open-chain diesters (e.g., echimidine and its *N*-oxide) produced by plants from the Boraginaceae and tribe Eupatorieae. The senecionine-type compounds are cyclic diesters (e.g., jacobine, retrorsine, senecionine, seneciphylline and their *N*-oxides, and senkirkine), particularly found in plants from the tribe Senecioneae, while the heliotrine-type PAs/PANOs are monoesters (e.g., heliotrine and its *N*-oxide) that occur in the genus *Heliotropium* (Boraginaceae) [3].

Although PAs/PANOs can cause toxic effects, it has not yet been possible to establish a limit in food and feed due to analytical uncertainties [7]. In addition, there is a lack of toxicological data relating to the PAs/PANOs found most frequently in food [8]. Some authorities, such as the European Food Safety Authority (EFSA), have performed independent risk assessments by applying the margin of exposure (MOE) approach, based on the benchmark dose lower confidence limit for a 10% excess cancer risk ($BMDL_{10}$) derived from animal studies. In this approach, an MOE value of at least 10,000 is of low concern for carcinogenic effects [3]. In 2011, the EFSA proposed an orientation value of 0.007 µg/kg body weight (b.w) for the sum content of PAs/PANOs, based on a $BMDL_{10}$ of 70 µg/kg b.w/day of lasiocarpine in male rats, and an MOE value of 10,000 [3, 9, 10]. In 2017, the EFSA updated its risk characterisation using the MOE approach and a new $BMDL_{10}$ of 237 µg/kg b.w, derived from the incidence of liver haemangiosarcoma in female rats exposed to riddelliine [8]. Thus, an orientation value of 0.024 µg/kg b.w/day for the sum of PAs/PANOs could be considered of low concern for public health [11]. Regarding non-carcinogenic risks, with PA/PANO concentrations lower than 0.1 µg/kg b.w/day, these kinds of effect are not expected to occur [10]. This orientation value was obtained from a No Observed Adverse Effect Level (NOAEL) for riddelliine in rats of 10 µg/kg b.w/day, divided by an uncertainty factor of 100 [10]. Based on data published by EFSA [12], possible limits for PAs/PANOs in those foods that most contribute to human exposure through the diet are currently being discussed at European Union level [13]. Maximum PA/PANO levels of 400 and 500 µg/kg have been proposed for pollen products [14, 15]. Nevertheless, given that intake of even low PA/PANO amounts could increase the risk to health, especially if consumed frequently, the recommendation is still that the intake of these natural toxins should be minimised to the lowest level possible [16]. For this reason, the EFSA recommends the development of more sensitive methods to detect PAs/PANOs in food [8].

The main methods for analysis of PAs/PANOs are based on liquid chromatography coupled to tandem mass spectrometry (LC–MS/MS), which is highly sensitive, specific and reliable [17–19] but also time-consuming and expensive. Therefore, there is a need to develop fast, non-destructive, cost-effective and multi-modality analytical methods that support at-line control of natural toxins throughout the supply chain. Near-infrared (NIR) spectroscopy is a powerful technology that has been already proposed in food-contaminant monitoring related to human health concern [20]. Hence, there is an ongoing increase in the application of NIR to detect mycotoxins [21, 22], allergens [23] and gluten [24] in food products, even at low levels (µg/kg). However, to the best of our knowledge, NIR spectroscopy applications for the detection of PAs/PANOs in bee pollen or analogous food supplements have not yet been performed. So far, only Carvalho et al. have reported the potential of NIR to predict the PA/PANO content in fresh and dried leaves of three *Senecio* species [25]. Furthermore, there is a lack of literature on the feasibility of applying miniaturised and portable spectroscopic devices, which could further raise the rapidity of measurement as well as avoiding the transportation of samples to the laboratory [26, 27].

In this context, this study first aimed to evaluate the distribution of PAs in bee pollen through univariate analysis across a classification criterion based on 400 µg/kg that could be considered a potential threshold of compliance in line with the future policy of food safety authorities. Regardless of the compliance limit, there is a need for rapid detection of these natural toxins in food, a challenge that could be reliably met by NIR spectroscopy technique. Thus, the main goal of this trial was to assess the feasibility of two NIR systems by means of a statistical modelling approach based on targeted canonical discriminant analysis (CDA). To achieve these aims, 60 bee pollen samples were analysed by a validated LC–MS/MS method, suitable for detecting and quantifying 17 PAs/PANOs suggested by EFSA to be monitored in food.

Materials and methods

Sampling and experimental design

Sixty dehydrated bee pollen samples were purchased from stores and online shops from different countries (39 from Italy, 17 from EU countries, 4 from non-EU countries). Based on standard guidelines and literature data, the samples were supposed to have a moisture level lower than 6% [28, 29]; therefore, they were kept in a dark, cool and dry place until analysis by LC–MS/MS and NIR spectroscopy. Approximately 50 g of each bee pollen sample was ground and homogenised by a GRINDOMIX GM 200 mill (Retsch,

Italia, Torre Boldone, Italy) at 6000 rpm for 15 s. The NIR spectral data collection and LC–MS/MS analysis were carried out on ground bee pollen.

LC–MS/MS analysis

Standards, solvents and reagents

Analytical standards were obtained from different suppliers as follows: echimidine (purity 97%), echimidine *N*-oxide (purity 97%), heliotrine (purity 91%), heliotrine *N*-oxide (purity 91%), lycopsamine (purity 80%) and lycopsamine *N*-oxide (purity 80%) from PhytoLab GmbH & Co. KG (Vestenbergsgreuth, Germany); senecionine (purity 99%), senecionine *N*-oxide (purity 99%), seneciphylline (purity 94%) and seneciphylline *N*-oxide (purity 94%) from Carl Roth & Co. KG (Karlsruhe, Germany); indicine-*N*-oxide (purity 99%), intermedine (purity 99%), jacobine (purity 98%), jacobine *N*-oxide (purity 98%), retrorsine (purity 90%), retrorsine *N*-oxide (purity 96.0%) and senkirkine (purity 98%) from Phytoplan (Heidelberg, Germany); caffeine (purity 98%), used as an internal standard, was from Sigma-Aldrich (Steinheim, Germany).

Methanol (LC–MS grade) and sulphuric acid (98% purity, analytical grade) were from Carlo Erba reagents (Milan, Italy). Ammonia (28% purity, analytical grade) was from VWR Chemicals. Formic acid (98% purity, LC–MS grade) was from Sigma-Aldrich. Ultra-pure water was obtained from a water purification system (Purelab Classic, ELGA Lab Water, High Wycombe, UK).

Sample preparation and LC–MS/MS analysis

Sample preparation, PA/PANO extraction from bee pollen samples and LC–MS/MS analysis were performed as described by De Jesus Inacio et al. [30]. The validated LC–MS/MS method used in this work is suitable for detecting and quantifying 17 PAs/PANOs in bee pollen. Detailed information on the analytical parameters (specificity, linearity, apparent recovery, precision, absolute recovery and matrix effect) evaluated in the LC–MS/MS method validation for target PAs/PANOs were reported in De Jesus Inacio et al. [30].

Briefly, the PAs/PANOs were extracted from 2.5 g of ground bee pollen samples using 15 mL of 0.05 M sulphuric acid solution. After 10 min of shaking, 10 mL of *n*-hexane was added and the samples were shaken for another 10 min and centrifuged at 3000*g* for 10 min. The organic phase was discarded and the aqueous extracts were then applied onto strong cation polymeric solid phase cartridges (Bond Elut Plexa PCX, 200 mg/6 mL, Agilent), previously conditioned with 6 mL methanol and 6 mL 0.1% formic acid in water. After loading, the cartridges were washed with 3 mL methanol and then eluted with 6 mL of 5% ammonia in methanol. The eluates were dried under an air stream at 50 °C, re-suspended with 1 mL of caffeine (internal standard, 500 ng/mL) in 0.1% formic acid in methanol and 0.5% formic acid in water (20:80, v/v) and filtered with a syringe filter consisting of a 0.22-µm regenerated cellulose (RC) membrane [31]. The PA/PANO extracts were analysed using a high-performance liquid chromatography system consisting of an Accela 600 HPLC pump equipped with a CTC automatic injector (Thermo Fischer Scientific, San Jose, CA, USA) and coupled to an LTQ XL ion trap mass spectrometer (Thermo Fischer Scientific, San Jose, CA, USA) with a heated electrospray ionisation (HESI-II) probe. Five microliters of extract samples was loaded onto the analytical column (Hypersil GOLD 100 × 2.1 mm, 1.9 µm, Thermo Fisher Scientific, San Jose, CA, USA), and the PA/PANO separation was performed in a gradient of solvent A (water with 0.1% formic acid) and B (methanol with 0.1% formic acid) at a flow rate of 200 µL/min as follows: isocratic condition from 0 to 4 min (90% A and 10% B); from 10 to 15% (B) in 0.5 min; 15% (B) from 4.5 to 9 min; from 15 to 40% (B) in 5 min; from 40 to 80% (B) in 1 min; 80% (B) for 1.5 min; from 80 to 10% (B) in 0.5 min; from 17 to 20 min 10% (B) to re-equilibrate the column.

The 17 PAs/PANOs were detected by the MS with the ESI source operating in positive-ion mode. The optimised operational LC–ESI(+)–MS/MS and detection conditions used for all the PAs/PANOs were as follows: sheath gas flow, 35 arbitrary units; auxiliary gas flow, six arbitrary units; ion spray voltage, 3.5 kV; capillary temperature, 350 °C; capillary voltage, 11 V; and tube lens, 60 V. The MS/MS conditions (collision energy, precursor and product ions) and the retention times obtained for each analyte were reported in Inacio et al. [30].

The limit of quantification (LOQ) of each PA/PANO was set at 0.4 µg/kg which is the lowest calibrator concentration on the calibration curve that could be quantified with a precision within 20%, and trueness between 80 and 120% as reported by the European Commission Decision 2002/657/EC [30].

The concentration of individual PAs/PANOs was calculated based on calibration curves prepared with a pool of blank bee pollen spiked with the 17 PAs/PANOs prior to the extraction to obtain the final concentration in the range 0.4–100 µg/kg.

NIR analysis

All bee pollen samples were analysed in triplicate using both a FOSS DS-2500 scanning monochromator (FOSS NIRSystem, Hillerød, Denmark) and portable NIR apparatus (PoliSPEC^{NIR}, ITPhotonics, Breganze, Italy). In the case of the lab-stationary system (referred to as Foss), scans

were recorded in reflectance mode (850–2500 nm at 0.5-nm intervals) using a slurry cup with a quartz window (12.6 cm^2 area) in 30 g aliquots. With regard to the portable system (referred to as Polispec), scans were also performed in reflectance mode (902–1670 nm at 2-nm intervals) using a quartz cylinder (9.1 cm^2 area) in 5 g aliquots. Spectral data were recorded as absorbance (A) calculated as $\log(1/R)$, where R represents reflectance, using WinISI4 software V4.10.0.15326 (FOSS Analytical A/S, Hillerød, Denmark) for Foss and using poliDATA (ITPhotonics, Breganze, Italy) for Polispec. For both systems, to carry out the statistical analysis, spectra were exported to an Excel (Microsoft Office®, USA) spreadsheet and averaged before further chemometric modelling.

Data and statistical analysis

The 60 bee pollen samples analysed were grouped into three quantitative (µg/kg) classes according to the sum of the 17 PAs/PANOs: < LOQ (0.4), low; 0.4–400, moderate; and > 400, high. As the PA/PANO data were not normally distributed, a Kruskal–Wallis test was carried out to analyse the effect of the distribution of these alkaloids within the three quantitative classes (XLSTAT, Addinsoft, release 2019, NY, USA). To evaluate the classifying effect, a multiple pairwise comparison was conducted using the Steel–Dwass–Critchlow–Fligner procedure (based on the averaged rank).

The variable importance in projection (VIP) indices were calculated using the relevance of predictors according to the threshold criterion of 'greater than one' of the PLS-DA algorithm [32], by means of MATLAB R2017a software V9.2.0.538062 (The MathWorks Inc., Natick, MA, USA) and PLS Toolbox (PLS Toolbox V5.8.2.1, Eigenvector Research Inc., Manson, WA, USA).

To discriminate the PA/PANO classes, a supervised CDA was also adopted for each NIR spectrometer (SAS 9.4 software, SAS Institute Inc., Cary, NC, USA). The first step was processing of the Foss dataset to reduce the number of wavelengths. For this purpose, the absorbance (A) was averaged every 8-nm interval, and the mean value was assigned to the intermediate wavelength (i.e., λ_{854} is equal to the average of A from 850 to 858 nm, λ_{2494} is equal to the average of A from 2492 to 2500 nm). The second step was a stepwise feature selection based on analysis of variance (ANOVA) to select those significant ($p < 0.05$) spectral variables related to the PA/PANO classes. CDA was performed on the selected spectral variables (PROC CANDISC of SAS), to explain the total variance of the model in two main canonical functions (CAN 1 and CAN 2). The degree of dissimilarity among the three quantitative PA/PANO classes was measured by squared Mahalanobis distances (D^2-Mahalanobis).

The reliability of the CDA model was assessed by a confusion matrix obtained by means of a cross-validation based on the leave-one-out criterion (PROC DISCRIM of SAS). As suggested by Bisutti et al. [33], the reliability of the related confusion matrix was evaluated by a set of statistical metrics: accuracy, precision, sensitivity, specificity and Matthews correlation coefficient (MCC).

Results and discussion

LC–MS/MS analysis and distribution of PAs/PANOs in bee pollen

LC–MS/MS analysis of the 60 dehydrated bee pollen samples was performed according to a validated method published in a previous study [30].

PAs/PANOs were found in 46 (77%) of the 60 bee pollen samples and the sum amounts of the detected compounds were noticeably distinct (from 2 to 3356 µg/kg); a detailed framework of the descriptive statistics is reported in Table 1. In 17 (37%) of the contaminated samples, the sum of PA/PANO concentration was over the value of 400 µg/kg, which has been considered as threshold for further analyses performed in this study. Lycopsamine-type PAs/PANOs were found in the majority (85%) of the contaminated bee pollen samples, followed by senecionine-type (48%) and heliotrine-type PAs/PANOs (11%) that were rarely found. Figure 1 summarises the descriptive statistics of the main individual and total PAs/PANOs within the three quantitative classes through univariate non-parametric analysis. There was a predominance of echimidine, echimidine *N*-oxide and lycopsamine. The most noticeable feature is that there is high variability in the distribution of the PA/PANO concentration within the high class, while it is negligible for the moderate class. This is especially observed for lycopsamine (Fig. 1a), senecionine and seneciphylline *N*-oxides (Fig. 1b), while for echimidine and echimidine *N*-oxide (Fig. 1a), the range of variability is much lower and the distribution of samples is quite close to the median value.

The results of this trial are in agreement with those published by Mulder et al. [17] and Picron et al. [18] who also reported a similar pattern for PAs/PANOs in bee pollen, with echimidine and its *N*-oxide as the main contributors to the sum content of these natural toxins. Even though the LC–MS/MS methods used by these authors cover a higher number of analytes (28–30), most of the additional compounds, including lasiocarpine and its *N*-oxide, have not been detected or they were found at trace levels and therefore, such compounds do not contribute remarkably to sum of PA/PANO concentration. Furthermore, the PA/PANO composition identified in the bee pollen samples, is also in agreement with that

Table 1 Descriptive statistics of the 17 pyrrolizidine alkaloids (PAs) and PA *N*-oxides (PANOs) and ΣPAs/PANOs (µg/kg) monitored in bee pollen

Analytes	Range	Mean (± sd)	Percentiles			nd
			10th	50th	90th	(n)
Echimidine	0–2128	124 (332)	0	0	316	33
Echimidine *N*-oxide	0–2078	96 (310)	0	0	254	32
Jacobine	–	–	–	–	–	60
Jacobine *N*-oxide	–	–	–	–	–	60
Indicine *N*-oxide	0–318	20 (58)	0	0	47	32
Intermidine	0–246	10 (34)	0	0	34	32
Lycopsamine	0–418	30 (77)	0	1	115	27
Lycopsamine *N*-oxide	0–368	23 (61)	0	0	92	30
Retrorsine	0–109	2 (14)	0	0	3	52
Retrorsine *N*-oxide	0–953	17 (123)	0	0	0	57
Senkirkine	–	–	–	–	–	60
Senecionine	0–64	6 (16)	0	0	22	47
Senecionine *N*-oxide	0 – 297	19 (59)	0	0	74	44
Seneciphylline	0–173	8 (27)	0	0	24	45
Seneciphylline *N*-oxide	0–679	24 (104)	0	0	30	49
Heliotrine	0–2	0 (0)	0	0	0	57
Heliotrine *N*-oxide	0–11	0 (2)	0	0	0	55
ΣPAs/PANOs	0–3356	382 (736)	0	32	1081	14

nd number (*n*) of samples where the analytes were not detected; *sd* standard deviation

reported for honeys from Europe [18, 34]. In addition, the data from this work underline the high variability of the presence of PAs/PANOs in bee pollen, as observed for lycopsamine (Fig. 1a) and senecionine *N*-oxide (Fig. 1b). This phenomenon is probably due to the fact that bees collect pollen from both plants that do not synthesise these toxins and PA-producing plants [18]. Indeed, both the PA/PANO concentration and composition depend on the botanical taxon, geographical origin [35] and developmental stage of the plants. Moreover, synthesis of PAs/PANOs by plants is influenced by many other agronomic and environmental factors such as soil fertility, water availability and climate conditions [36–38]. Since most bee pollen samples analysed were from Italy and other European countries, possible sources of the lycopsamine-type PAs/PANOs could be plants from the genus *Echium* (e.g., *E. vulgare*), which is known to produce high levels of echimidine and its *N*-oxide, and *Borago officinalis* and *Eupatorium cannabinum* that synthesise lycopsamine, lycopsamine *N*-oxide and their isomers. *Echium* and *Borago* species are abundant in the Mediterranean region [39, 40], while *Eupatorium cannabinum* is diffuse in Europe [40]. Regarding senecionine-type PAs/PANOs, their origin could be *Senecio* species, which are widely distributed in Europe and grow everywhere [25, 39]. Although these plants are abundant, if other more attractive pollen sources are available, bees may prefer them [40], and this could also explain the high variability of the PA/PANO concentration and frequency in bee pollen.

NIR spectral data and discriminant analysis of PAs/PANOs

The development of a rapid spectroscopic method in the detection of PAs/PANOs in food supplements was the main challenge of this trial. For food safety purposes, this challenge was to verify if NIR combined with a statistical modelling approach could be a feasible technique to discriminate bee pollen samples grouped into three classes according to their PA/PANO content.

NIR spectra

The NIR spectral data were recorded for ground bee pollen because the grinding process tends to improve the discriminative performance. As reported by Pasikitan et al. [41], NIR analysis is sensitive to the particle size and homogeneity of the matrix, both of which can affect the spectra and, consequently, the predictive performance. Thus, to guarantee a satisfactory precision in discriminative analyses, a grinding step is useful to obtain a more homogeneous matrix and reduce the light scattering effects that result in spectral noise. In the previous study of De Jesus

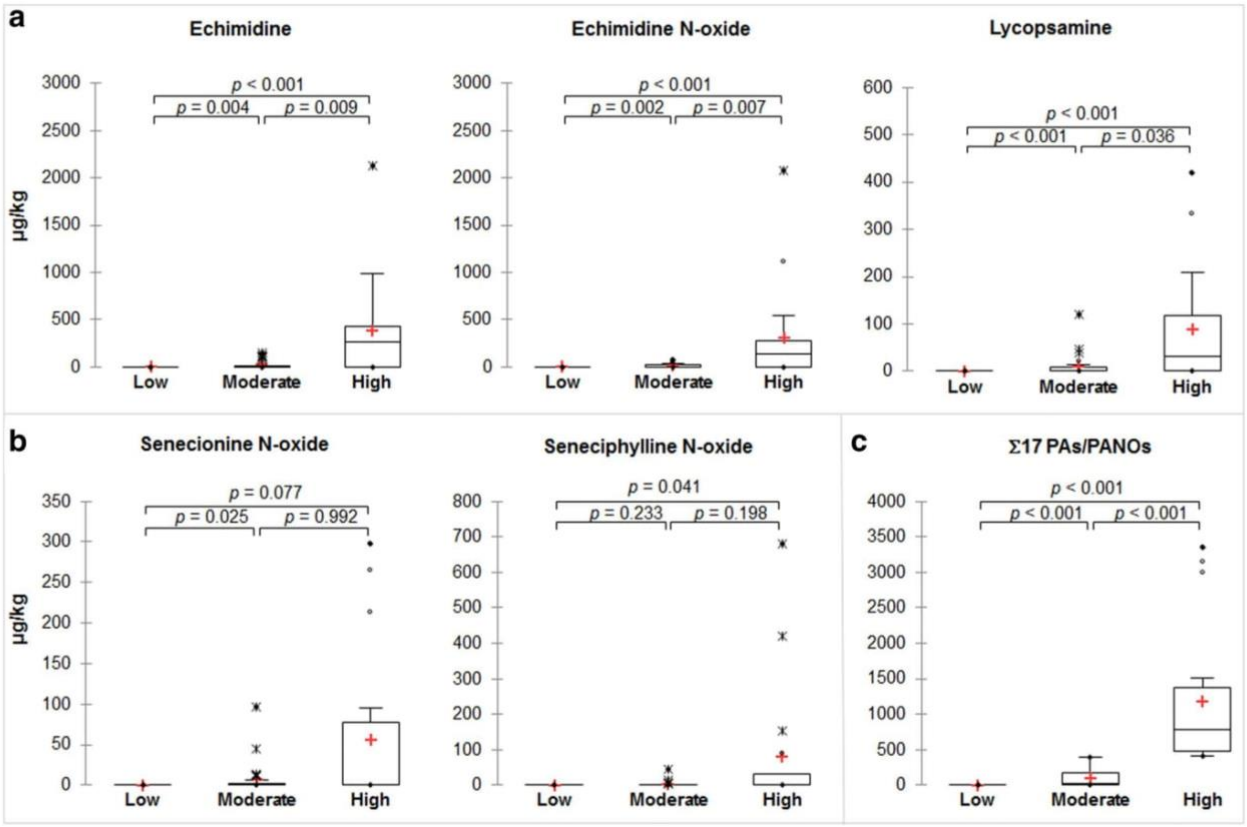

Fig. 1 Box–whisker plots of lycopsamine-type (**a**) and senecionine-type compounds (**b**) and total PAs/PANOs (**c**) according to the three quantitative (µg/kg) PA/PANO classes (<LOQ (0.4), low; 0.4–400, moderate; and>400, high). The box plots represent the following descriptive statistics: median (bar in box), mean (+, red cross), 25–75% quartile (bottom and top end of the box), minimum and maximum values (whiskers) except for outliers (°circles, distance to box 1.5–3.0 times interquartile range) and extreme values (*asterisks, distance to box>3 times interquartile range). The significance (*p* values on the top) of the multiple comparisons among the three PA/PANO classes was determined by Kruskal–Wallis non-parametric test

Inacio et al. [30], which tested the capability of a visible spectrophotometer to predict the presence of PAs/PANOs in bee pollen, the highest correlation between PA/PANO amount and the spatial colour coordinate named lightness was observed in ground samples.

Figure 2 evidences the averaged NIR spectra of the three quantitative PA/PANO classes. For both NIR systems, in the first part of the spectrum region (< 1450 nm), there was overlapping of the absorbance (*A*) among the three classes, while the absorbance of the low class was noticeably separated from the other two classes at higher wavelengths (> 1500 nm). In the study of González-Martín et al. [42], which applied NIR spectroscopy to assess bee pollen quality parameters, the spectra seemed to be comparable to those of the Foss system, with a meaningful absorbance peak around 1950 nm and a subsequent increasing trend up to 2500 nm. Costa et al. [43] reported a similar absorbance profile, although they analysed samples with a Fourier transform (FT)-NIR system. With regard to the portable system, it was not possible to confirm the absorbance pattern with data from the literature. The main outcomes of this alternative NIR instrument are an increasing absorbance from 1450 nm and *A* values about half of the Foss ones.

The VIP scores chart obtained for each NIR spectrometer is shown in Fig. 3. The VIP pathway was characterised by intense peaks (VIP scores > 1) in the < 1000, 1000–1660 and > 2400 nm regions for Foss and only > 1500 nm for Polispec. The explicative VIP predictors showed an overlap between low and moderate classes throughout almost all the spectral range of the Foss system, meaning that the informative bands correlated with the smallest or medium PA/PANO content involved similar dominant wavelength regions. In contrast, the Foss-VIP pattern of the high class was almost distinguished from the other ones, and its explicative predictors (VIP scores > 1) belonged to the 900–1350-nm region.

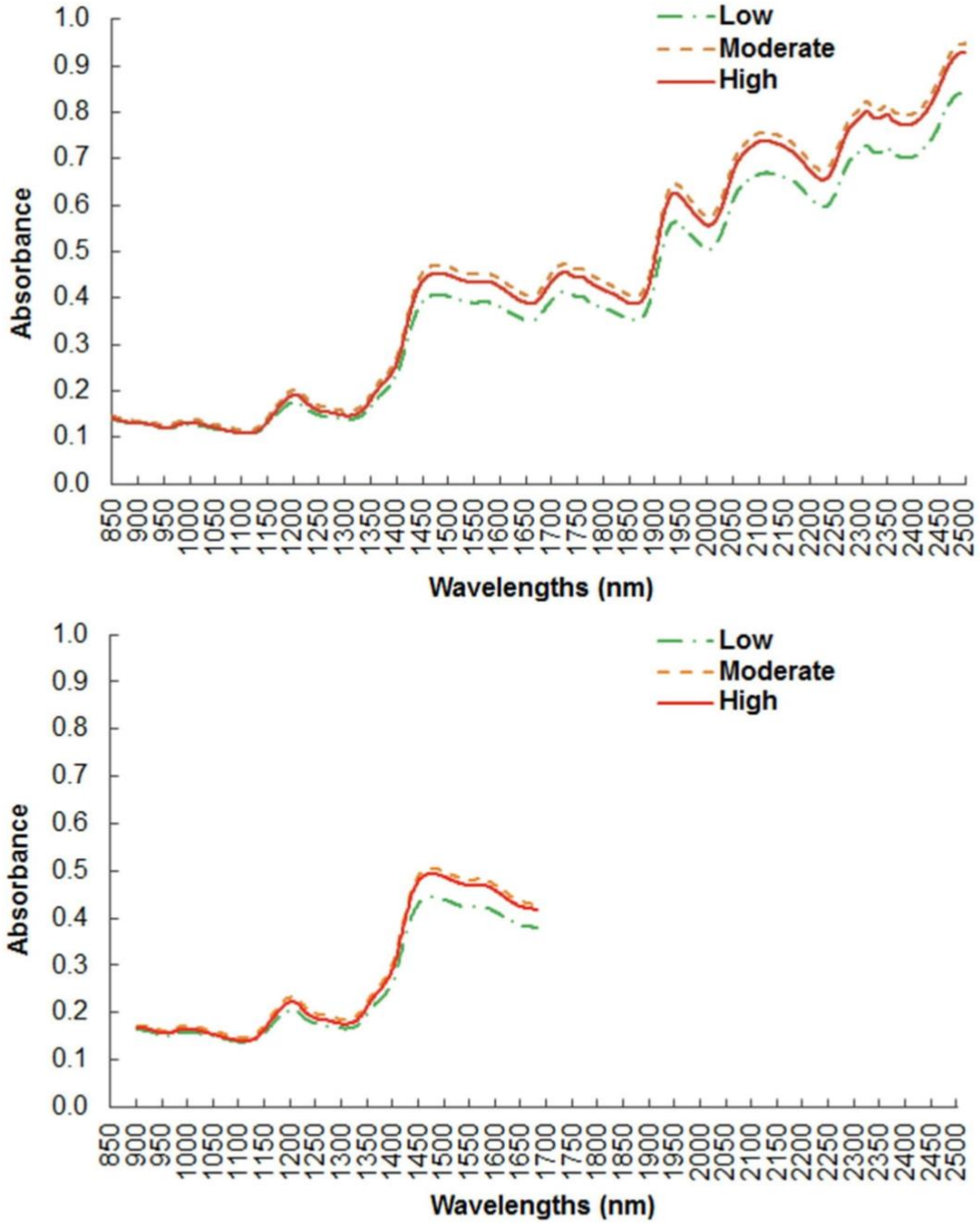

Fig. 2 Absorbance spectra for the three quantitative classes of pyrrolizidine alkaloids (PAs) and their *N*-oxides (PANOs) in bee pollen, based on lab-stationary (Foss, upper panel) and portable (Polispec, lower panel) near-infrared (NIR) systems. Quantitative (µg/kg) PA/PANO classes: < LOQ (0.4), low; 0.4–400, moderate; > 400, high

However, in the last part of the spectrum (> 2400 nm) there was a similar trend among the three classes. In the case of the portable NIR system, the VIP pathway was characterised by lower values (< 1.6) and slight differences among the PA/PANO groups. A potential relationship between VIP and PA/PANO detection could be due to a multiplicity of interferences that are discussed in the following section.

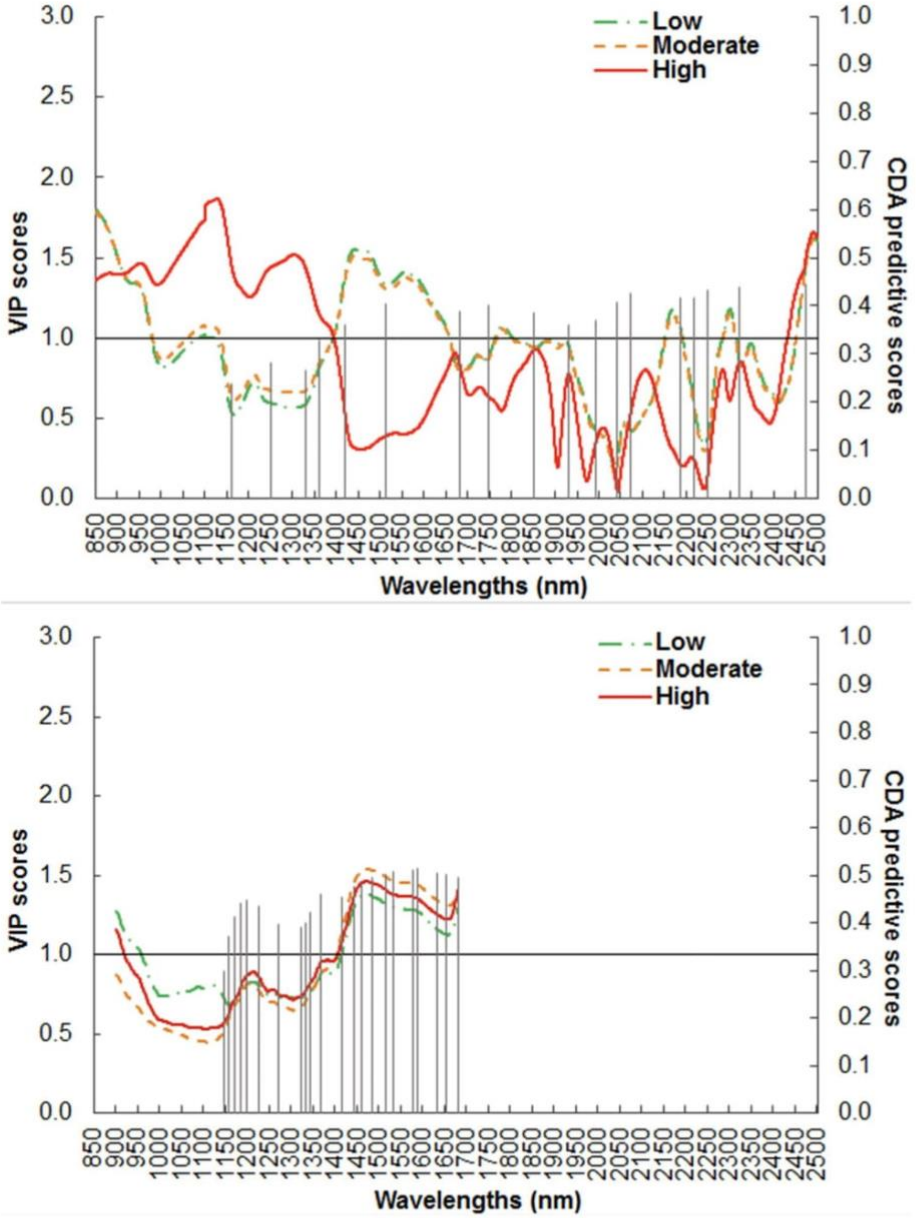

Fig. 3 Variable importance in projection (VIP) and predictive scores by partial least squares discriminant analysis (PLS-DA) and canonical discriminant analysis (CDA) models for the three quantitative classes of pyrrolizidine alkaloids (PAs) and their *N*-oxides (PANOs) in bee pollen, based on lab-stationary (Foss, upper panel) and portable (Polispec, lower panel) near-infrared (NIR) systems. VIP scores are presented as trends throughout the entire spectral range and the CDA selected predictive wavelengths as vertical bars according to the canonical structure correlation coefficient (CDA predictive scores). Quantitative (μg/kg) PA/PANO classes: < LOQ (0.4), low; 0.4–400, moderate; > 400, high

CDA based on NIR spectral data

The main purpose of this study was to apply a multivariate pattern recognition method to determine the functional relationship between spectral NIR data and the presence of PAs/PANOs in a set of bee pollen samples, simulating a rapid screening to enhance the safety of on-market operating conditions. Among the supervised discriminating methods, CDA has been already proposed as a statistical model able to classify a sub-population of samples within a specific genetic, geographical or chemical class (e.g., PA/PANO amount) according to the similarity of a huge set of chemometric variables such as the NIR spectra [30]. Despite being less frequently applied, the CDA algorithm allows a reduction of data redundancy, thus the discriminating power is preserved in the first canonical discriminant function [44]. Even though CDA seems to improve the classification accuracy when spatial separation of the experimental groups is achieved by the use of a large number of closed-spectral signatures, the use of a large dataset with too many highly correlated variables could be inappropriate for selecting the more informative wavelengths avoiding the irrelevant ones [32, 45]. Indeed, a data arrangement is required when a dataset has too many irrelevant variables, a high multicollinearity among instrumental signals and a number of predictors larger than

the sample size [46]. Therefore—in the case of the Foss system—before the stepwise selection, the dataset was restricted to 207 averaged spectral variables so that each one represents a 16 nm wavelength range (from λ_{854} to λ_{2494}). The portable NIR system presents a short window for spectral acquisition and a relatively longer measurement interval (2 nm); hence, there was no need to restrict the original dataset composed of 390 spectral variables.

For the lab-stationary NIR system (Foss), the stepwise procedure selected 18 significant averaged wavelengths: λ_{1162}, λ_{1250}, λ_{1330}, λ_{1362}, λ_{1418}, λ_{1514}, λ_{1682}, λ_{1746}, λ_{1850}, λ_{1930}, λ_{1994}, λ_{2042}, λ_{2074}, λ_{2186}, λ_{2218}, λ_{2250}, λ_{2322} and λ_{2474}. These spectral variables were used to perform the CDA algorithm that defined two significant functions, CAN1 and CAN2 (Wilks's $\lambda = 0.19$, approximate F value $= 2.85$, $df1 = 30$, $df2 = 80$, $p < 0.001$), which explained 78.9% and 21.1% of the total variability, respectively. Regarding the portable NIR system, 22 wavelengths were sorted as the most informative by the stepwise procedure: λ_{1146}, λ_{1158}, λ_{1172}, λ_{1186}, λ_{1200}, λ_{1226}, λ_{1270}, λ_{1324}, λ_{1332}, λ_{1344}, λ_{1368}, λ_{1416}, λ_{1442}, λ_{1460}, λ_{1484}, λ_{1514}, λ_{1534}, λ_{1576}, λ_{1588}, λ_{1632}, λ_{1652} and λ_{1680}. The CDA algorithm defined two canonical functions (CAN1 and CAN2) that showed a high discriminative power (Wilks's $\lambda = 0.25$, approximate F value $= 1.59$, $df1 = 44$, $df2 = 72$, $p = 0.039$), which accounted for 71.6% and 28.4% of the total variability, respectively. As shown in Fig. 4, for both NIR systems the CDA model highlighted the possibility of separating the 0.95 confidence circles for population centroids, especially the low class from the others. This discriminative capacity was confirmed by the significant D^2-Mahalanobis values, which were equal to 9.5 ($p < 0.001$) between low and moderate classes, and 16.1 ($p < 0.001$) between low and high classes for Foss, and 7.7 ($p = 0.023$) between low and moderate classes, and 9.9 ($p = 0.022$), between low and high classes for Polispec.

Furthermore, a confusion matrix obtained by leave-one-out cross-validation confirmed that the CDA classification functions allowed the correct assignment of each sample to its actual PA/PANO class based on the restricted pool of the selected NIR features (Table 2). Overall, both NIR spectrometers showed an accurate prediction of the absence of PAs/PANOs because of the high values of predictive parameters for the low class, as summarised by the MCC values of 0.96 and 0.91 for Foss and Polispec, respectively. Conversely, assessment of the high class by the NIR-based algorithm highlighted a decrease in discriminant performance that was more relevant for the portable apparatus (MCC of 0.73 versus 0.59), even though no sample was misclassified as low class (Table 2). Considering the hypothesis of rapid spectroscopy-based screening for the absence (low class) and presence of PAs/PANOs (fusion of moderate and high classes), both NIR systems showed a false negative misclassification rate equal to 0.02

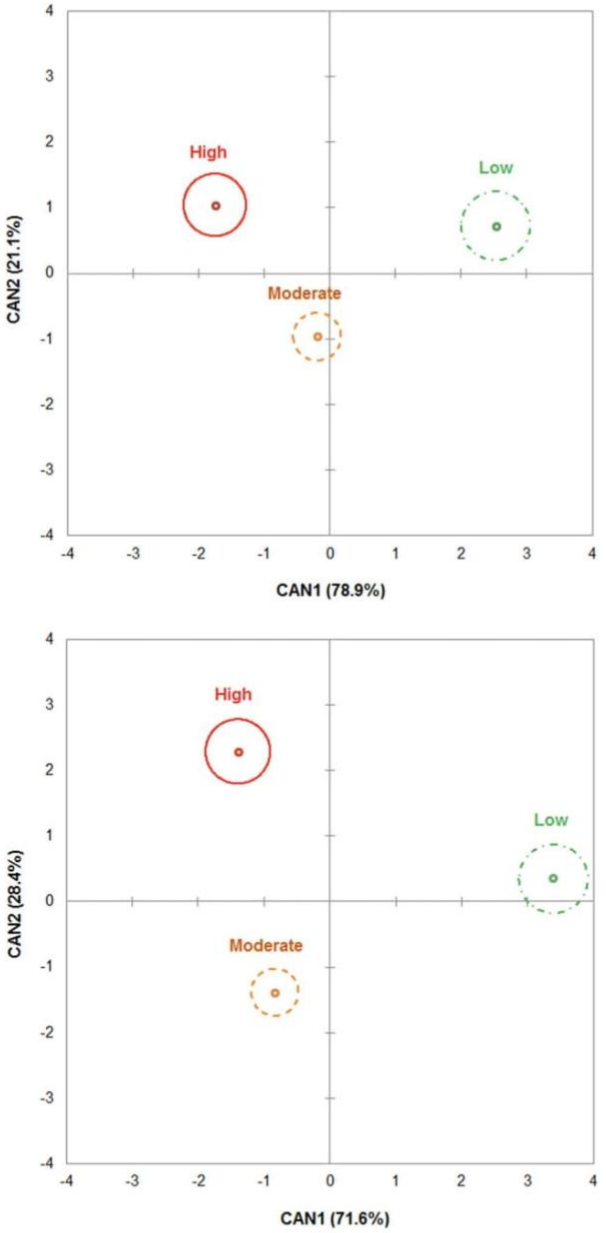

Fig. 4 Biplots of the 0.95 confidence circles around the centroids for the three quantitative classes of pyrrolizidine alkaloids (PAs) and their *N*-oxides (PANOs) in bee pollen, based on lab-stationary (Foss, upper panel) and portable (Polispec, lower panel) near-infrared (NIR) systems. Quantitative (μg/kg) PA/PANO classes: < LOQ (0.4), low; 0.4–400, moderate; and > 400, high

(1 out of 46), which refers to a sample from the moderate class that was recognised as from the low class. That value is lower than the 0.05 threshold for false negatives usually applied in toxicological screening tests [47]. For Polispec, there was also a false-positive misclassification rate of 0.07 (1 out of 14) related to wrong assignment of a

Table 2 Confusion matrix and descriptive statistics in cross-validation (leave-one-out criterion) for the three quantitative classes of pyrrolizidine alkaloids (PAs) and their *N*-oxides (PANOs) in ground bee pollen based on lab-stationary (Foss) and portable (Polispec) near-infrared (NIR) systems

	Foss				Polispec		
	Actual				Actual		
Predicted	Low	Moderate	High	**Predicted**	Low	Moderate	High
Low	**14**	1	0	Low	**13**	1	0
Moderate	0	**24**	3	Moderate	1	**22**	5
High	0	4	**14**	High	0	6	**12**
Total	14	29	17	**Total**	14	29	17
Sensitivity	1.00	0.83	0.82		0.93	0.76	0.71
Specificity	0.98	0.90	0.91		0.98	0.81	0.86
Accuracy	0.98	0.87	0.88		0.97	0.78	0.82
Precision	0.93	0.89	0.78		0.93	0.79	0.67
MCC	0.96	0.75	0.73		0.91	0.61	0.59

Quantitative (μg/kg) PA/PANO classes: < LOQ (0.4), low; 0.4–400, moderate; and > 400, high; bold values represent the samples classified correctly

MCC Matthews correlation coefficient

sample from the low class to the moderate class, but this represents only an additional charge because it implies further confirmatory analysis by LC–MS/MS, which is the analytical technique recommended by food safety authorities.

The outcomes of this study indicate the potential capability of NIR spectroscopy to perform reliable screening of bee pollen samples contaminated with PAs/PANOs. Indeed, these natural toxins significantly affected the spectral data, indicating that the NIR technology can be applied for a rapid evaluation of the presence of contaminants [48]. However, as underlined by the decrease in the sensitivity and specificity values (Table 2), the attempt to distinguish a moderate from a high level of PAs/PANOs seems to be partially predictable, probably due to the chemical structure and stereochemistry of these molecules, which influence their toxicity and physical–optical properties [49].

The slightly lower capability of the tested portable NIR instrument is in agreement with the literature. This phenomenon is probably due to worse optical properties and the negative interference of the field operative conditions compared to the lab-stationary apparatus [26, 50], even though its flexibility and the possibility of application at/in-line represent major advantages.

The CDA algorithm (by means of the canonical standardised coefficient) highlighted a relatively similar explicative power of all the predictors because their loading values (predictive scores) ranged from 0.30 to 0.50 and these selected wavelengths involved the spectral region > 1150 nm (Fig. 3). Among them, within the 1140–1370 nm region, λ_{1162}, λ_{1250}, λ_{1330} and λ_{1362} (Foss) and λ_{1146}, λ_{1158}, λ_{1172}, λ_{1200}, λ_{1226}, λ_{1270}, λ_{1324}, λ_{1332}, λ_{1344} and λ_{1368} (Polispec) could be related to C–H stretching second overtones [51]. The absorption bands λ_{1418} (Foss) and λ_{1416} (Polispec) can be related to O–H stretching first overtones of R–OH [52] that are present in the chemical structure of PAs/PANOs. The predictors λ_{1442} and λ_{1460} (Polispec) could be associated with the first overtones of cyclic amines [52], which compose the basic structure of all PAs/PANOs. In relation to these latter selected wavelengths, the 1400 nm has been already suggested as a shared region between tertiary-amines and *N*-oxides, where these molecules seemed to interact with electromagnetic radiation, resulting in vibrational spectroscopic signals [25]. Although the *N*-oxide spectrum is related to many wavelengths in the visible and infrared regions, the interpretation of the spectroscopic dynamic behaviour of the structure of PANOs is still lacking [53]. Another region that can also be affected by cyclic amines is within the 1900–2100 nm region [25], represented by λ_{1930}, λ_{1994}, λ_{2042} and λ_{2074} (Foss). The CDA feature stepwise procedure also sorted some informative wavelengths between 1500 and 1590 nm, including λ_{1514} (Foss) and λ_{1514}, λ_{1534}, λ_{1576} and λ_{1588} (Polispec). These wavelengths may be influenced by stretch overtones of O–H and combination bands of N–H with C=O, and C–N stretching of amine/amide structures [25]. The absorption peak at λ_{1850} (Foss) may be related to the second overtone of C=O stretching of carboxyl groups [52], which are also found in the PA/PANO chemical structure. Some of these alkaloids can also contain epoxide–amine structures that may influence the λ_{1632}, λ_{1652} (Polispec) and λ_{2218} (Foss) regions [25]. In the case of the Foss spectrometer, the selected wavelengths of λ_{2186}, λ_{2218}, λ_{2250}, λ_{2322} and λ_{2474} can be considered informative NIR variables because they correspond to combination bands of N–H from amines/amides and O–H from alcohols, and C–H and C–C stretching from –CH, $-CH_2$ and $-CH_3$ [43, 54].

Conclusions

The outcomes of this work highlighted that over 75% of the 60 bee pollen samples analysed were contaminated with PAs/PANOs, even though less than 30% might have a concentration higher than the threshold of 400 µg/kg used for the NIR analyses. However, a relevant variability was observed in the distribution of the 17 PAs/PANOs monitored, as confirmed by the relevant values of standard deviation within both moderate and high classes, which represent a classification method below or above the threshold of 400 µg/kg.

The presence of the PAs/PANOs in bee pollen significantly affected the NIR spectra, highlighted a rising level of absorbance as their concentration increased. This outcome suggests that their chemical structure interferes with the light scattering throughout many band regions. The application of CDA resulted in a modelling statistical approach that demonstrates the predictive capacity of NIR systems to distinguish among the three quantitative PA/PANO classes, especially for detection of those samples belonging to the low class, which corresponds to safe samples.

In summary, both NIR systems have the potential to be applied for rapid and reliable identification of contaminated bee pollens in large-scale screening in the food supply chain by also using an at-line operating system, however, the lab-stationary might be considered the more feasible NIR tool to achieve this purpose. PA/PANO detection could be strengthened by applying a chemometric approach based on a further informative dataset shared among the research community and food safety agencies.

Acknowledgements This work was funded by the University of Padova (CPDA 158894/15 project) and FONDAZIONE CARIVERONA (call 2016-SAFIL project).

Funding Open access funding provided by Università degli Studi di Padova within the CRUI-CARE Agreement.

Compliance with ethical standards

Conflict of interest The authors declare that they have no known competing financial interests or personal relationships that could have appeared to influence the work reported in this paper.

Compliance with ethics requirements This article does not contain any studies with human participants or animal performed by any of the authors.

References

1. Denisow B, Denisow-Pietrzyk M (2016) Biological and therapeutic properties of bee pollen: a review. J Sci Food Agric 96:4303–4309
2. Boppré M, Colegate SM, Edgar JA, Fischer OW (2008) Hepatotoxic pyrrolizidine alkaloids in pollen and drying-related implications for commercial processing of bee pollen. J Agric Food Chem 56:5662–5672. https://doi.org/10.1021/jf800568u
3. EFSA (2011) Scientific opinion on pyrrolizidine alkaloids in food and feed: EFSA panel on contaminants in the food chain (CONTAM). EFSA J 9:1–134. https://doi.org/10.2903/j.efsa.2011.2406
4. Fu PP, Xia Q, Lin G, Chou MW (2004) Pyrrolizidine alkaloids—genotoxicity, metabolism enzymes, metabolic activation, and mechanisms. Drug Metab Rev 36:1–55. https://doi.org/10.1081/DMR-120028426
5. Moreira R, Pereira DM, Valentão P, Andrade PB (2018) Pyrrolizidine alkaloids: chemistry, pharmacology, toxicology and food safety. Int J Mol Sci 19:1–22. https://doi.org/10.3390/ijms19061668
6. Merz KH, Schrenk D (2016) Interim relative potency factors for the toxicological risk assessment of pyrrolizidine alkaloids in food and herbal medicines. Toxicol Lett 263:44–57. https://doi.org/10.1016/j.toxlet.2016.05.002
7. Gottschalk C, Huckauf A, Dübecke A et al (2018) Uncertainties in the determination of pyrrolizidine alkaloid levels in naturally contaminated honeys and comparison of results obtained by different analytical approaches. Food Addit Contam Part A Chem Anal Control Expo Risk Assess 35:1366–1383. https://doi.org/10.1080/19440049.2018.1468929
8. EFSA (2017) Risks for human health related to the presence of pyrrolizidine alkaloids in honey, tea, herbal infusions and food supplements. EFSA J 15(7):1–34. https://doi.org/10.2903/j.efsa.2017.4908
9. BFR (Federal Institute for Risk Assessment)(2011) Chemical analysis and toxicity of pyrrolizidine alkaloids and assessment of the health risks posed bytheir occurrence in honey. BfR opinion No. 038/2011. Available online: https://www.bfr.bund.de/cm/349/chemical-analysis-and-toxicityof-pyrrolizidine-alkaloids-and-assessment-of-the-health-risks-posed-by-their-occurence-in-honey.pdf. Accessed 28 Apr 2020
10. Committee on toxicity of chemicals in food consumer products and the environment (2008) COT statement on pyrrolizidine alkaloids in food. cot.food.gov.uk/pdfs/cotstatementpa200806.pdf
11. Hurtado MC, Conchello Moreno MP, Daschner Á et al (2018) Informe del Comité Científico de la Agencia Española de Seguridad Alimentaria y Nutrición (AESAN) sobre el riesgo asociado a la presencia de alcaloides de la pirrolizidina en polen destinado al consumo humano. Rev del Com Científico la AESAN 28:127–140
12. EFSA (2016) Dietary exposure assessment to pyrrolizidine alkaloids in the European population. EFSA J. https://doi.org/10.2903/j.efsa.2016.4572
13. Agencia Española de Consumo SA y N (AECOSAN) (2019) Alcaloides De Pirrolizidina. https://www.aecosan.msssi.gob.es/AECOSAN/docs/documentos/seguridad_alimentaria/gestion_riesgos/PAs_ficha.pdf. Accessed 19 May 2020

14. AFEPADI (2019) Alcaloides de pirrolizidina. ¿Próxima limitación? In: Asoc. las Empres. Dietéticos y Complement. Aliment. https://www.afepadi.org/index.php/component/k2/item/442-alcaloides-de-pirrolizidina-proxima-limitacion. Accessed 10 Mar 2020
15. UK FSA (2019) June 2019 Stakeholder Update on Rapidly Developing Policy on food contaminants environmental and industrial contaminants. https://www.food.gov.uk/news-alerts/consultations/june-2019-stakeholder-update-on-rapidly-developing-policy-on-food-contaminants. Accessed 20 May 2020
16. BfR (Federal Institute for Risk Assessment) (2018) Updated risk evaluation of levels of 1, 2-unsaturated pyrrolizidine alkaloids (PA) in foods. BfR Opin 20:1–2. https://doi.org/10.17590/20180730-085425-0
17. Mulder PPJ, López P, Castelari M et al (2018) Occurrence of pyrrolizidine alkaloids in animal- and plant-derived food: results of a survey across Europe. Food Addit Contam Part A Chem Anal Control Expo Risk Assess 35:118–133. https://doi.org/10.1080/19440049.2017.1382726
18. Picron J, Herman M, Van Hoeck E, Goscinny S (2019) Monitoring of pyrrolizidine alkaloids in beehive products and derivatives on the Belgian market. Environ Sci Pollut Res. https://doi.org/10.1007/s11356-019-04499-2
19. Sixto A, Niell S, Heinzen H (2019) Straightforward determination of pyrrolizidine alkaloids in honey through simplified methanol extraction (QuPPE) and LC–MS/MS modes. ACS Omega 4:22632–22637. https://doi.org/10.1021/acsomega.9b03538
20. Alander JT, Bochko V, Martinkauppi B et al (2013) A review of optical nondestructive visual and near-infrared methods for food quality and safety. Int J Spectrosc. https://doi.org/10.1155/2013/341402
21. Hernández-Hierro JM, García-Villanova RJ, González-Martín I (2008) Potential of near infrared spectroscopy for the analysis of mycotoxins applied to naturally contaminated red paprika found in the Spanish market. Anal Chim Acta 622:189–194. https://doi.org/10.1016/j.aca.2008.05.049
22. De Girolamo A, von Holst C, Cortese M et al (2019) Rapid screening of ochratoxin A in wheat by infrared spectroscopy. Food Chem 282:95–100. https://doi.org/10.1016/j.foodchem.2019.01.008
23. Mishra P, Diezma B, Barreiro P (2015) NIR hyperspectral imaging for detection of nut contamination. New Food 18:30–33
24. Radman M, Jurina T, Benković M et al (2018) Application of NIR spectroscopy in gluten detection as a cross-contaminant in food. Croat J Food Technol Biotechnol Nutr 13:120–127. https://doi.org/10.31895/hcptbn.13.3-4.4
25. Carvalho S, Macel M, Schlerf M et al (2013) Changes in plant defense chemistry (pyrrolizidine alkaloids) revealed through high-resolution spectroscopy. ISPRS J Photogramm Remote Sens 80:51–60. https://doi.org/10.1016/j.isprsjprs.2013.03.004
26. Teixeira Dos Santos CA, Lopo M, Páscoa RNMJ, Lopes JA (2013) A review on the applications of portable near-infrared spectrometers in the agro-food industry. Appl Spectrosc 67:1215–1233. https://doi.org/10.1366/13-07228
27. Crocombe RA (2018) Portable spectroscopy. Appl Spectrosc 72:1701–1751. https://doi.org/10.1177/0003702818809719
28. Campos MGR, Bogdanov S, de Almeida-Muradian LB et al (2008) Pollen composition and standardisation of analytical methods. J Apic Res 47:154–161. https://doi.org/10.1080/00218839.2008.11101443
29. Anjos O, Santos AJA, Dias T, Estevinho LM (2017) Application of FTIR-ATR spectroscopy on the bee pollen characterization. J Apic Res 56:210–218. https://doi.org/10.1080/00218839.2017.1289657
30. De Jesus Inacio L, Merlanti R, Lucatello L et al (2020) Pyrrolizidine alkaloids in bee pollen identified by LC-MS/MS analysis and colour parameters using multivariate class modeling. Heliyon 6:e03593. https://doi.org/10.1016/j.heliyon.2020.e03593
31. Lucatello L, Merlanti R, Rossi A et al (2016) Evaluation of some pyrrolizidine alkaloids in honey samples from the Veneto Region (Italy) by LC–MS/MS. Food Anal Methods 9:1825–1836. https://doi.org/10.1007/s12161-015-0364-7
32. Segato S, Merlanti R, Bisutti V et al (2019) Multivariate and machine learning models to assess the heat effects on honey physicochemical, colour and NIR data. Eur Food Res Technol 245:2269–2278. https://doi.org/10.1007/s00217-019-03332-x
33. Bisutti V, Merlanti R, Serva L et al (2019) Multivariate and machine learning approaches for honey botanical origin authentication using near infrared spectroscopy. J Near Infrared Spectrosc 27:65–74. https://doi.org/10.1177/0967033518824765
34. Martinello M, Cristofoli C, Gallina A, Mutinelli F (2014) Easy and rapid method for the quantitative determination of pyrrolizidine alkaloids in honey by ultra performance liquid chromatography-mass spectrometry: an evaluation in commercial honey. Food Control 37:146–152. https://doi.org/10.1016/j.foodcont.2013.09.037
35. Kast C, Kilchenmann V, Reinhard H et al (2019) Pyrrolizidine alkaloids: the botanical origin of pollen collected during the flowering period of *Echium vulgare* and the stability of pyrrolizidine alkaloids in bee bread. Molecules. https://doi.org/10.3390/molecules24122214
36. Schramm S, Köhler N, Rozhon W (2019) Pyrrolizidine alkaloids: biosynthesis, biological activities and occurrence in crop plants. Molecules 24:498. https://doi.org/10.3390/molecules24030498
37. Stegemann T, Kruse LH, Brütt M, Ober D (2019) Specific distribution of pyrrolizidine alkaloids in floral parts of comfrey (*Symphytum officinale*) and its implications for flower ecology. J Chem Ecol 45:128–135. https://doi.org/10.1007/s10886-018-0990-9
38. Flade J, Beschow H, Wensch-Dorendorf M et al (2019) Occurrence of nine pyrrolizidine alkaloids in senecio vulgaris l. Depending on developmental stage and season. Plants 8:1–13. https://doi.org/10.3390/plants8030054
39. Stegelmeier B, Edgar J, Colegate S et al (1999) Pyrrolizidine alkaloid plants, metabolism and toxicity. J Nat Toxins 8:95–116. https://doi.org/10.1023/B:PHAM.0000016235.32639.23
40. Kast C, Kilchenmann V, Reinhard H et al (2018) Chemical fingerprinting identifies *Echium vulgare*, *Eupatorium cannabinum* and *Senecio* spp. as plant species mainly responsible for pyrrolizidine alkaloids in bee-collected pollen. Food Addit Contam Part A Chem Anal Control Expo Risk Assess 35:316–327. https://doi.org/10.1080/19440049.2017.1378443
41. Pasikatan MC, Steele JL, Spillman CK, Haque E (2001) Near infrared reflectance spectroscopy for online particle size analysis of powders and ground materials. J Near Infrared Spectrosc 9:153–164. https://doi.org/10.1255/jnirs.303
42. González-Martín I, Hernández-Hierro JM, Barros-Ferreiro N et al (2007) Use of NIRS technology with a remote reflectance fibre-optic probe for predicting major components in bee pollen. Talanta 72:998–1003. https://doi.org/10.1016/j.talanta.2006.12.039
43. Costa MCA, Morgano MA, Ferreira MMC, Milani RF (2017) Analysis of bee pollen constituents from different Brazilian regions: quantification by NIR spectroscopy and PLS regression. LWT Food Sci Technol 80:76–83. https://doi.org/10.1016/j.lwt.2017.02.003
44. Zhao G, Maclean AL (2000) A comparison of canonical discriminant analysis and principal component analysis for spectral transformation. Photogramm Eng Remote Sensing 66:841–847
45. Leardi R (2000) Application of genetic algorithm-PLS for feature selection in spectral data sets. J Chemom 14:643–655. https

://doi.org/10.1002/1099-128X(200009/12)14:5/6<643:AID-CEM621>3.0.CO;2-E
46. Akarachantachote N, Chadcham S, Saithanu K (2014) Cut-off threshold of variable importance in projection for variable selection. Int J Pure Appl Math 94:307–322. https://doi.org/10.12732/ijpam.v94i3.2
47. Oplatowska M, Elliott CT, Huet AC et al (2014) Development and validation of a rapid multiplex ELISA for pyrrolizidine alkaloids and their *N*-oxides in honey and feed rapid detection in food and feed. Anal Bioanal Chem 406:757–770. https://doi.org/10.1007/s00216-013-7488-7
48. Shen F, Wu Q, Shao X, Zhang Q (2018) Non-destructive and rapid evaluation of aflatoxins in brown rice by using near-infrared and mid-infrared spectroscopic techniques. J Food Sci Technol 55:1175–1184. https://doi.org/10.1007/s13197-018-3033-1
49. Villanueva-Cañongo C, Pérez-Hernández N, Hernández-Carlos B et al (2014) Complete 1H NMR assignments of pyrrolizidine alkaloids and a new eudesmanoid from *Senecio polypodioides*. Magn Reson Chem 52:251–257. https://doi.org/10.1002/mrc.4054
50. Marchesini G, Serva L, Garbin E et al (2017) Near-infrared calibration transfer for undried whole maize plant between laboratory and on-site spectrometers. Ital J Anim Sci. https://doi.org/10.1080/1828051X.2017.1345660
51. He J, Chen L, Chu B, Zhang C (2018) Determination of total polysaccharides and total flavonoids in *Chrysanthemum morifolium* using near-infrared hyperspectral imaging and multivariate analysis. Molecules 23:1–13. https://doi.org/10.3390/molecules23092395
52. Weyer LG (1985) Near-infrared spectroscopy of organic substances. Appl Spectrosc Rev 21:1–43. https://doi.org/10.1080/05704928508060427
53. Oliveira RP, Demuner AJ, Alvarenga ES et al (2017) Experimental and theoretical studies on the characterization of monocrotaline by infrared and Raman spectroscopies. J Mol Struct 1135:228–233. https://doi.org/10.1016/j.molstruc.2017.01.050
54. Márquez C, López MI, Ruisánchez I, Callao MP (2016) FT-Raman and NIR spectroscopy data fusion strategy for multivariate qualitative analysis of food fraud. Talanta 161:80–86. https://doi.org/10.1016/j.talanta.2016.08.003

CHAPTER 4

Assessment of Chicken Breast Shelf Life Based on Bench-Top and Portable Near-Infrared Spectroscopy Tools Coupled with Chemometrics

---

Ilaria Lanza[1], Daniele Conficoni[1], Stefania Balzan[2], Marco Cullere[1], LucaFasolato[2], LorenzoServa[1], ,BarbaraContiero[1], AngelaTrocino[2], Giorgio Marchesini[1], Gerolamo Xiccato[3], Enrico Novelli[2] , Severino Segato[1].

[1]Department of Animal Medicine, Productions and Health, University of Padova, 35020 Legnaro, PD, Italy.

[2]Department of Comparative Biomedicine and Food Science, University of Padova, 35020 Legnaro, PD, Italy

[3]Department of Agronomy, Food, Natural Resources, Animals and Environment, University of Padova, 35020 Legnaro, PD, Italy

Food Quality and Safety, 2021, 5, 1–11

OXFORD

Food Quality and Safety, 2021, 5, 1–11
doi:10.1093/fqsafe/fyaa032
Article

Article

Assessment of chicken breast shelf life based on bench-top and portable near-infrared spectroscopy tools coupled with chemometrics

Ilaria Lanza[1], Daniele Conficoni[1], Stefania Balzan[2], Marco Cullere[1], Luca Fasolato[2], Lorenzo Serva[1], Barbara Contiero[1], Angela Trocino[2], Giorgio Marchesini[1], Gerolamo Xiccato[3], Enrico Novelli[2] and Severino Segato[1]

[1]Department of Animal Medicine, Productions and Health, University of Padova, Legnaro, Italy; [2]Department of Comparative Biomedicine and Food Science, University of Padova, Legnaro, Italy and [3]Department of Agronomy, Food, Natural Resources, Animals and Environment, University of Padova, Legnaro, Italy

Correspondence to: Luca Fasolato, Department of Comparative Biomedicine and Food Science, University of Padova, 35020 Legnaro (PD), Italy. E-mail: luca.fasolato@unipd.it

Received 7 September 2020; Revised 12 November 2020; Editorial decision 15 November 2020.

Abstract

Objectives: Near-infrared (NIR) spectroscopy is a rapid technique able to assess meat quality even if its capability to determine the shelf life of chicken fresh cuts is still debated, especially for portable devices. The aim of the study was to compare bench-top and portable NIR instruments in discriminating between four chicken breast refrigeration times (RT), coupled with multivariate classifier models.

Materials and Methods: Ninety-six samples were analysed by both NIR tools at 2, 6, 10 and 14 days post mortem. NIR data were subsequently submitted to partial least squares discriminant analysis (PLS-DA) and canonical discriminant analysis (CDA). The latter was preceded by double feature selection based on Boruta and Stepwise procedures.

Results: PLS-DA sorted moderate separation of RT theses, while shelf life assessment was more accurate on application of Stepwise-CDA. Bench-top tool had better performance than portable one, probably because it captured more informative spectral data as shown by the variable importance in projection (VIP) and restricted pool of Stepwise-CDA predictive scores (SPS).

Conclusions: NIR tools coupled with a multivariate model provide deep insight into the physicochemical processes occurring during storage. Spectroscopy showed reliable effectiveness to recognise a 7-day shelf life threshold of breasts, suitable for routine at-line application for screening of meat quality.

Graphical Abstract

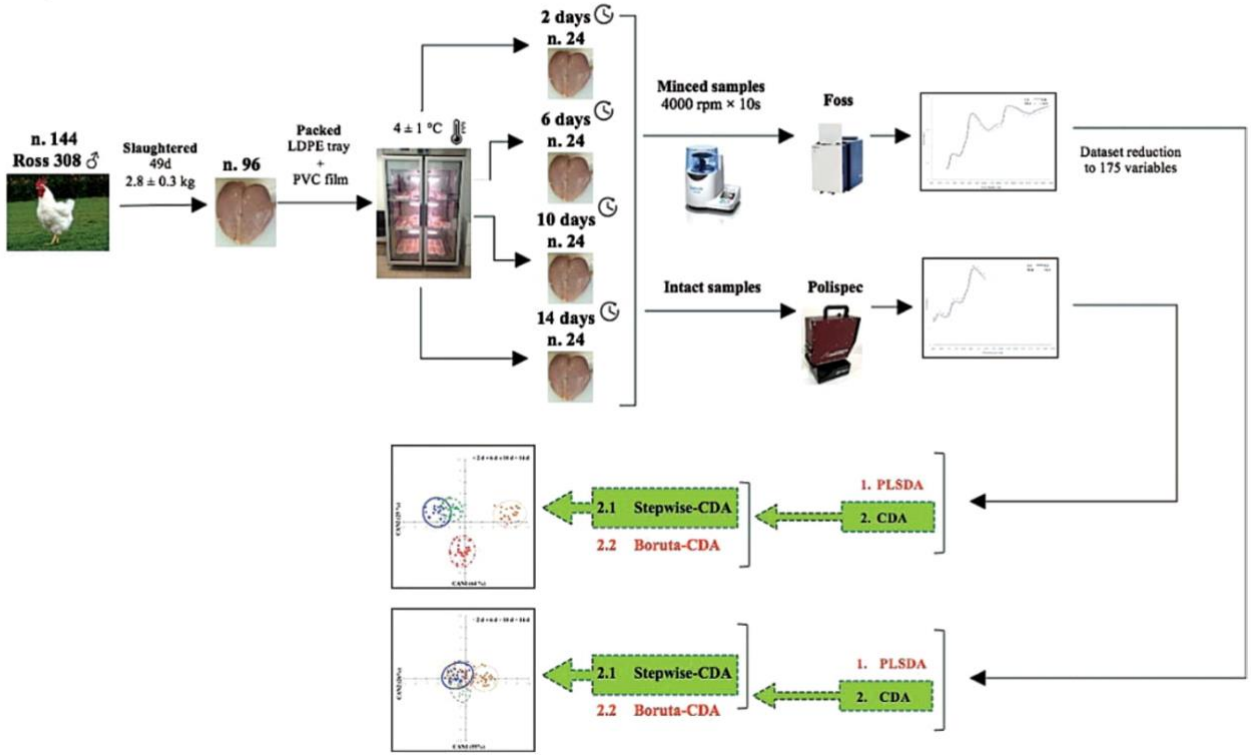

Key words: shelf life; chicken breast; Near-infrared (NIR) spectroscopy; bench-top NIR; portable NIR; canonical discriminant analysis.

Introduction

Globally, about 127 million tonnes of poultry meat is produced per year, making it the biggest meat sector worldwide (FAO, 2020a). The low price, valuable nutritional profile, mild sensory attributes, ease of cooking and cultural acceptability are all key factors pushing the market development of chicken meat (FAO, 2020b; Katiyo *et al.*, 2020). As for meat in general, the high nutrient and moisture content as well as the tendentially higher pH of fresh chicken meat make it highly perishable, leading to a fast loss of freshness during storage (Fernández-Pan *et al.*, 2014; Katiyo *et al.*, 2020). Inappropriate storage conditions (e.g. temperature variations, inadequate packaging and prolonged shelf life) can result in product discoloration, accumulation of off-flavours and off-odours, and alteration of sensory traits, ultimately making meat consumption unsuitable (Sivarajan *et al.*, 2017). Given poultry meat's relatively short shelf life (Fernández-Pan *et al.*, 2014), preservation of quality during refrigerated storage represents one of the main challenges for the poultry industry. Currently, meat ageing can be assessed by sensory, enzymatic, DNA-based, microbiological, bio-imaging and spectroscopic analytical approaches. However, non-spectroscopic methods are laborious, time-consuming and destructive and also require sophisticated laboratory procedures (Alamprese *et al.*, 2016; Falkovskaya *et al.*, 2019). Due to the dynamism of the meat industry, a cost-effective and non-destructive quality control system to assess meat freshness is therefore needed (Teixeira dos Santos *et al.*, 2013; Mendez *et al.*, 2019).

In this context, near-infrared (NIR) spectroscopy is a fast, eco-friendly, non-invasive and reliable technology for the analysis and authentication of a wide range of meat products (Morsy and Sun, 2013; Mendez *et al.*, 2019), for predicting chicken cut differentiation (Nolasco Perez *et al.*, 2018), identifying breed origin (Ding *et al.*, 1999), quality attributes (Barbin *et al.*, 2015) and spoilage (Alexandrakis *et al.*, 2012), and for the discrimination of fresh from frozen–thawed poultry meat (Atanassova *et al.*, 2018). NIR radiation ranges from 780 to 2500 nm on the electromagnetic spectrum. The interaction of this radiation with meat samples results in weak and broad absorption bands that must be analysed through multivariate analysis methods, coupled with spectral pre-processing techniques for clear data interpretation (Teixeira dos Santos *et al.*, 2013; Zareef *et al.*, 2020). Recently, considerable attention has been given to portable spectroscopic devices due to their valuable advantages compared to stationary ones. Portable spectrometers are lightweight and easy-to-use tools that allow direct, non-destructive and *in situ* sample measurement. Furthermore, they avoid laboratory transportation (time and cost saving), improve the efficiency of the testing process and provide the knowledge to make informed decisions on the spot (Teixeira dos Santos *et al.*, 2013; Crocombe, 2018).

Based on the above-mentioned premises, our aim was to evaluate the feasibility of using bench-top and portable NIR spectroscopy instruments for discriminating chicken breasts during a 14-day refrigeration period. The reliability of the portable NIR tool for a real time control of meat shelf life to make on-the-spot evaluations

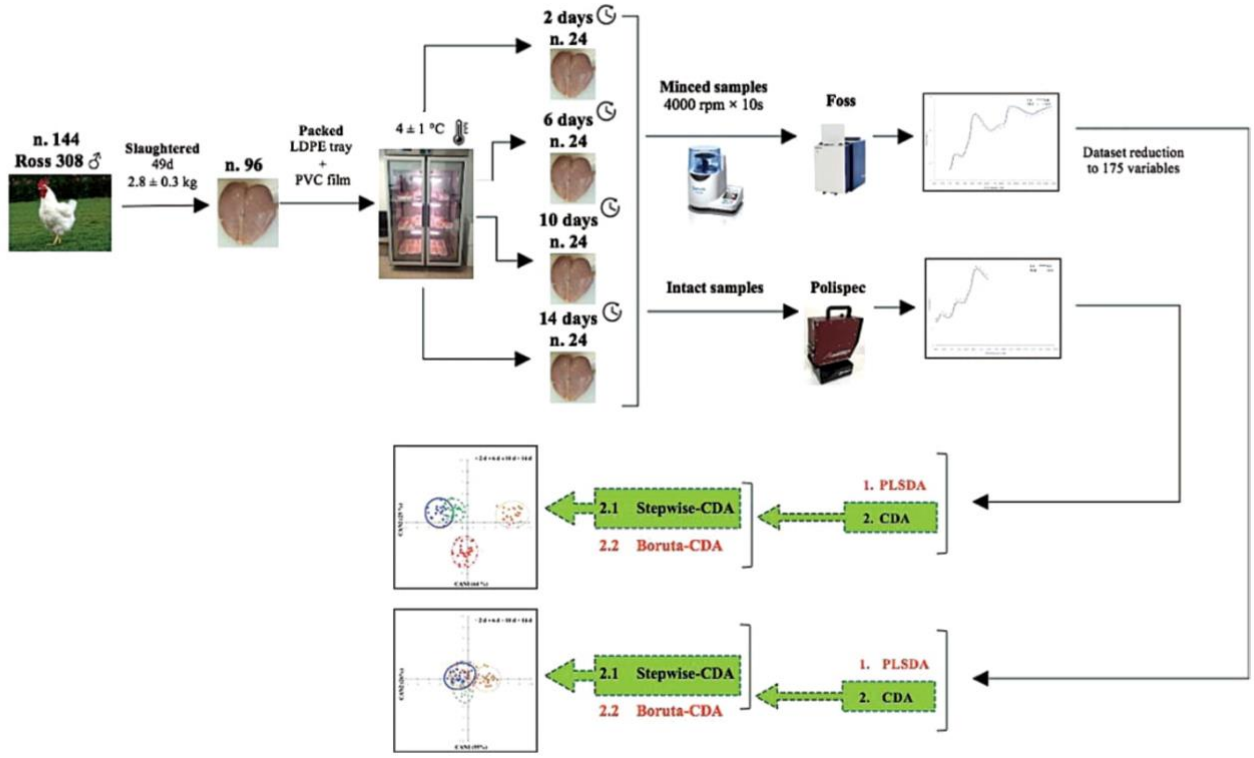

Figure 1. Flow chart of the experimental design: sampling, setting refrigeration time theses, acquiring NIR spectra and predicting discriminative modelling. LDPE, low-density polyethylene; PLSDA, partial least square-discriminant analysis; CDA, canonical discriminant analysis; NIR, near-infrared.

along supply chain, was compared to the well-known predictive performance of the bench-top instrument. An in-depth description of the interaction among electromagnetic radiation and alteration pathways aiming at obtaining detailed information about the physicochemical changes occurring during poultry meat shelf life. This comparative analysis of the spectroscopy behaviour was related to a restricted pool of informative NIR wavelengths selected by two multivariate discriminative models.

Materials and Methods

Experimental design and meat sampling

The study was conducted under ethical approval (project 17/2016; No 154392 of the 10 May 2016) of the Ethical Committee for Animal Experimentation of the University of Padova to perform experiments on animals. Moreover, all efforts were made to curtail the animal suffering throughout the trial.

A total of 96 male Ross 308 chickens were slaughtered (carcass weight: 2.8 ± 0.3 kg) in a commercial plant at 49 days old. After stunning, exsanguination, plucking and evisceration of birds, breast muscles were dissected (0.88 ± 0.09 kg as averaged weight), immediately (first experimental day) packed in low-density polyethylene trays wrapped in a 12 µm-thick PVC film (Weegal, KOEX 412, Gruppo Fabbri, Vignola, Modena, Italy) and stored in a refrigerated cabinet (Majolo® Plus 100 Seasoning Controller, Majolo, Cadoneghe, Padova, Italy). The storage was designed to simulate commercial refrigeration setting conditions: samples were exposed to a 36 W fluorescent lamp light for about 12 h daily (from 8 a.m. to 8 p.m.), and then in dark during night (from 8 p.m. to 8 a.m.), always keeping a temperature of 4 ± 1 °C.

As reported in Figure 1, to assess meat freshness during the shelf life by NIR spectroscopy, breasts were randomly grouped into four theses (n = 24) corresponding to the following refrigeration times (RT), as days *post mortem*: ≤2 (2 d), 3–6 (6 d), 7–10 (10 d) and 11–14 (14 d).

Chemical and sensorial analyses on breast samples

The breast samples were analyzed according to the set storage time (after 2, 6, 10 and 14 days post mortem) to measure their physicochemical and sensorial traits. The pH was recorded in triplicate with a portable pH-meter (KnickPortamess® 911, Berlin, Germany) equipped with a penetrating electrode (5 mm diameter conic tip, Crison 5232, Modena, Italy). Colour (averaged of 5 areas on the breast surface) was measured by a Konica Minolta CD-600 visible spectrophotometer (Konica Minolta Sensing, Inc., Osaka, Japan), applying CIE L*a*b* system (L*, lightness; a*, redness; b*, yellowness) with D65 as light source and 10° observed angle (Melro *et al.*, 2020). Drip loss was determined by weighing of 2.5 cm-slice cut from the surface of dorsal breast, which was packaged in polyethylene bags and kept overnight at 2 ± 1 °C. Drip loss (%) was calculated by the following equation: [(initial weight – final weight)/initial weight]. Sensory evaluation was conducted by a panel consisting of 10 trained students and researchers of the School of Agricultural Sciences and Veterinary Medicine of Padova University, and sensory traits (odour, texture and colour) were scored according to Raab *et al.* (2008) using a demerit 3-point scoring system (1 = not acceptable, 2 = acceptable, 3 = good quality). A synthetic sensory index (SI) was calculated as: [(2 × odour score + 2 × colour score + 1 × texture score)/5], with 1.8 score as the threshold to define spoiled samples (Raab *et al.*, 2008).

NIR spectroscopy analysis

As reported in Figure 1, after 2, 6, 10 and 14 days post mortem, chicken breast samples were analysed (at 18 ± 2 °C) within 45 ± 10 min using both a bench-top FOSS NIRSystems 5000 analyser (FOSS Analytical A/S, Hillerød, Denmark) and a portable Polispec NIR (PoliSPEC^{NIR}, ITPhotonics, Breganze, Italy).

For the lab-scale system (referred to as Foss) a right-side breast subsample (around 125 g) was minced at 4000 rpm for 10 s with a Grindomix GM200 knife mill (Retsch GmbH, Haan, Germany) and then poured and gently compressed into a small ring cup with a quartz window that allowed irradiation of an area of about 9.6 cm^2. Spectral data were recorded in duplicate by covering a range of 1100–2500 nm at 2 nm intervals. The instrument was equipped with a spinning module, and spectra were collected in reflectance mode, averaging 32 scans of the sample after 16 internal references.

For the portable system (referred to as Polispec), the raw left side of the breast (not minced) was submitted to NIR analysis through an embedded 3.2 cm^2 quartz cylinder probe for 10 s scanning time, thus covering around a 10 cm^2 meat surface; spectra were acquired in reflectance mode (900–1600 nm at 2 nm intervals), in duplicate. Each scan lasted 5 s (about 10 ms of integration time), covering about 10 cm^2 of the sample area.

For both NIR instruments, spectral data were recorded as absorbance (A) calculated as log(1/R), where R is the reflectance of the sample, by using WinISI 2 software V1.05 (Infrasoft International Inc., Port. Matilda, USA) and poliDATA (ITPhotonics, Breganze, Italy), for bench-top and portable instrument, respectively. Spectra were subsequently exported in .csv format for further chemometric analysis. Prior to statistical analysis, spectra of the two replicates were averaged. For both instruments, in order to reduce light scattering and to remove the baseline shift, smoothing, standard normal variate (SNV), first-order derivative and detrend transformations were applied (Bisutti *et al.*, 2019).

Statistical and chemometric analyses

Regarding meat quality variables, the assumption of normality was tested using the Shapiro-Wilk test (PROC UNIVARIATE). Then, instrumental colour, pH and drip loss data were submitted to a one-way ANOVA (PROC GLM) to test the effect of RT. The hypotheses of the linear model (normality, independence and homoscedasticity) were visually assessed on the residuals. Post hoc pairwise multiple comparisons among levels were conducted using Bonferroni correction. Orthogonal contrasts were performed to assess the linear and quadratic components of RT effect. Data not normally distributed (sensory traits) were analysed using a non-parametric Kruskal–Wallis test. Post-hoc multiple pairwise comparisons were conducted using the Steel–Dwass–Critchlow–Fligner procedure (based on the averaged ranks). The SAS software (release 9.4, SAS Institute Inc., Cary, USA) was used for all the above-mentioned analyses.

Then, partial least square-discriminant analysis (PLS-DA) and canonical discriminant analysis (CDA) statistical modelling approaches were applied on the NIR spectral variables of both spectrometers to discriminate among the 2 d, 6 d, 10 d and 14 d RT theses. The PLS-DA multivariate classifier model was performed using the PLS Toolbox (PLS Toolbox, V5.8.2.1, Eigenvector Research, Inc., Manson, WA, USA) of MATLAB software (v 9.2.0 538062; The MathWorks Inc., Natick, MA, USA). Smoothing, SNV, first-order derivative and detrend transformations gave better results for bench-top, while no pre-treatments were carried out for portable system. The reliability of PLS-DA was assessed by a cross-validation performing a venetian blind algorithm with 10 splits and one sample per split (Rubingh *et al.*, 2006). Furthermore, variable importance in projection (VIP), used to highlight the most influential absorbance wavelengths, was calculated using the relevance of predictors according to the PLS-DA threshold criterion of 'greater than one' (Ottavian *et al.*, 2015).

Despite CDA is reported as multivariate model able to improve the classification performance by using a high number of closed-spectral variables, a discriminative process based on a dataset of many highly correlated variables could not retain some informative wavelengths. Therefore, prior to application of supervised CDA, the bench-top dataset was arranged reducing averaged spectral variables to 175 (Akarachantachote *et al.*, 2014), each referring to an 8 nm interval range, so that the mean value was assigned by interpolating the R values to the intermediate wavelength (from λ_{1106}, equal to the average of R from 1102 to 1110 nm, to λ_{2490}, equal to the average of R from 2486 to 2494 nm). Double feature selection was carried out as the preliminary step of the CDA. The first (named Boruta) was based on the Boruta random forest feature selection (Kursa and Rudnicki, 2010), using an R software package (Comprehensive R Archive Network, R Development Core Team, 2010). The second (named Stepwise) was run within the forward Stepwise procedure (PROC STEPWISE) of SAS software. Both Boruta and Stepwise features were submitted to the last step of CDA (PROC CANDISC of SAS) to achieve the most discriminative analysis by maximising the distance among RT theses, and their degree of dissimilarity was measured by squared Mahalanobis distances (D^2-Mahalanobis). The outcomes of the CDA were plotted according to the main canonical functions CAN1 and CAN2 using XLSTAT software (release 2016, Addinsoft, New York, USA). The reliability of the CDA was assessed by a confusion matrix obtained by a cross-validation based on the leave-one-out criterion (PROC DISCRIM of SAS).

The metrics depicted in the confusion matrices used to assess the goodness of the classification performance of the PLS-DA and CDA models were the following descriptive statistics (Segato *et al.*, 2019): accuracy, sensitivity, specificity, precision and Matthews correlation coefficient (MCC).

Results and Discussion

Assurance of meat quality related to shelf life assessment has led to the design of models based on rapid and non-destructive high-throughput techniques. In this study, three targeted multivariate classifier models, PLS-DA, Boruta-CDA (random forest selection) and Stepwise-CDA (targeted selection), were built using the NIR spectral data from bench-top and portable NIR spectrometers. Their efficiency to predict chicken breast shelf life was evaluated according to four classes of freshness (days *post-mortem*): fresh (2 d), acceptable (6 d), spoiled (10 d) and rotten (14 d). Fresh and acceptable theses guarantee safety and maintain the overall quality attributes with respect to consumer preferences. During storage, shifts in biochemical pathways and spoiling microbial populations occur, leading to changes in meat appearance. Detrimental sensorial decay usually starts after a chilled storage period that coincides with a cut-off between the end of the acceptable and the beginning of the spoiled thesis. Since poultry meat is a highly perishable food, the predominant organisms and biochemical changes lead to intense proteolysis, amino acid degradation and lipid oxidation that at the end of storage (rotten thesis with more of 10 days of refrigerated storage) induce

the formation of by-products associated with the production of off-flavour and slime, thus prejudicing consumer acceptability (Gram *et al.*, 2002; Bruckner *et al.*, 2012).

Chemical and sensorial analyses

As reported in Table 1, RT significantly affected the physicochemical and sensorial traits of chicken breast samples. The pH values showed a linear increase ($P < 0.001$) after six days of refrigeration mainly due to the proliferation of spoilage microorganisms as reported by Sujiwo *et al.* (2018). Meat colour showed a significant change of L*: in detail, an initial decrease in lightness was observed after six days followed by a progressive increase in the latest conservation time (*P*-value of the quadratic component of variance < 0.001). This trend was related to changes in water retention ability and myofibrils structure along the storage period which affected the content of free water in meat. Moreover, during storage, a significant increase of drip losses was recorded which increased the lightness because water previously bound to myofibrils was released (Gratta *et al.*, 2019). The sensorial traits (odour, colour and texture) were associated to the highest level of freshness until six days of conservation, after which the SI (meat acceptability) decreased (Table 1). A detrimental effect of RT was observed for the rotten samples (thesis 14 d) that showed the lowest values of odour and colour contributing to an unacceptable (<1.8) SI (Raab *et al.*, 2008). The results of the sensorial evaluation defined a cut-off between 6 (fresh meat) and 10 (spoiled meat) days since at least 25% of 10 d-poultry breast samples had a SI value lower than 1.8 (Figure 2). The metabolism of spoilage bacteria leading to the formation of by-products associated with off-flavour and slime production, prejudicing acceptability in the rotten samples.

Shelf life assessment by PLS-DA

As reported in Table 2, the performance of the PLS-DA model in predicting the four chicken breast RT theses was moderately accurate, highlighting an overall better discriminative capacity for the bench-top instrument (MCC > 0.75) compared to portable (MCC > 0.35) one. The higher accuracy (>0.91) and precision (>0.83) values for the bench-top instrument are probably linked to the meat mincing pre-process. Muscle grinding tends to improve discriminative performance, reducing sample heterogeneity (i.e. texture, colour and proximate composition) and increasing the repeatability of NIR spectrum acquisition (Xu *et al.*, 2019). Moreover, analysis of intact muscles is susceptible to the effect of the high moisture content on the surface as well as fine subcutaneous fat, even if samples are well trimmed. The lower discriminative capability of the portable tool might be also explained by the size of the measuring head, the distinctive optical properties and the detector type, which must be resized in order to miniaturise the NIR device, resulting in a shorter spectral wavelength range (Teixeira dos Santos *et al.*, 2013).

Shelf life assessment by CDA

The main purpose of the research was to evaluate the feasibility of using NIR spectroscopy to predict chicken breast shelf life: for this purpose, further multivariate modelling was performed. CDA seemed to improve the spatial separation of the experimental groups, but could not work efficiently in the case of a large dataset with too many irrelevant and highly correlated variables obscuring the informative ones and worsening the discriminative performance (Leardi, 2000; Zhao and Maclean, 2000). Since the CDA algorithm allows a reduction of redundancy (Akarachantachote *et al.*, 2014), before the Stepwise selection, a spectral arrangement was carried out on the bench-top dataset, restricting it to 175 averaged spectral variables so that each one represented an 8 nm wavelength range (from λ_{1106} to λ_{2490}). Since the portable system was characterised by a shorter spectral acquisition time, there was no need to restrict the original dataset.

As described above, four CDAs were performed using two preliminary feature selections (Stepwise vs Boruta) for each instrument (bench-top vs portable). A summary of the predictive performance of this CDA set is reported in Table 3. Both NIR instruments had a lower value of Wilks' λ, a test statistic that is minimised within the procedure in order to obtain the widest spatial segregation of the experimental groups, when the algorithm was performed with the preliminary Stepwise criterion as feature selection. The better discriminative capacity of the preliminary Stepwise procedure was also assessed by higher D^2-Mahalanobis values than those observed for Boruta (Table 3).

Thus, we focus the discussion on the Stepwise forward CDA being the most accurate fitting model.

For the lab-scale NIR tool, the Stepwise procedure selected 32 significant averaged wavelengths (Table 3). These spectral variables were used to perform the CDA algorithm that defined two

Table 1. Effect of the refrigeration time (RT) on pH, colour (CIE L*a*b*), drip losses and sensorial attributes of chicken breasts

Quality traits	Refrigeration time (RT)				SEM	*P*-value		
	2 d	6 d	10 d	14 d		Global	Linear	Quadratic
pH	5.92^{c}	5.96^{c}	6.12^{b}	6.18^{a}	0.02	<0.001	<0.001	0.034
L* (lightness)	47.0^{ab}	45.7^{b}	45.7^{b}	48.1^{a}	0.6	0.014	0.249	0.003
a* (redness)	1.8^{ab}	2.2^{a}	1.8^{ab}	1.8^{b}	0.1	0.029	0.316	0.067
b* (yellowness)	10.6^{ab}	11.3^{a}	10.1^{b}	10.1^{b}	0.3	0.034	0.096	0.308
Drip losses (%)	3.0^{b}	3.8^{a}	3.4^{ab}	n. e.[1]	0.2	0.006	0.096	0.006
Sensorial analysis[2]								
Odour	3.0 (3.0-3.0)^{a}	3.0 (3.0-3.0)^{a}	2.5 (1.0–3.0)^{b}	1.0 (1.0–2.0)^{c}		<0.001		
Colour	3.0 (2.0–3.0)^{a}	3.0 (2.0–3.0)^{a}	2.0 (1.5–3.0)^{b}	1.5 (1.0–2.0)^{c}		<0.001		
Texture	3.0 (2.5–3.0)^{a}	3.0 (2.0–3.0)^{a}	2.0 (2.0–3.0)^{b}	2.0 (1.5–2.0)^{c}		<0.001		
SI[3]	3.0 (2.6–3.0)^{a}	3.0 (2.4–3.0)^{a}	2.3 (1.4–3.0)^{b}	1.5 (1.2–1.6)^{c}		<0.001		

SEM, standard error of the means. [1]Not estimated. [2]Results (medians and range) are reported as score units (1 means not acceptable; 2 means acceptable; 3 means good quality). [3]Sensory index calculated as: [(2 × odour score + 2 × colour score + 1 × texture score)/5]. [abc]Means with different superscript lowercase letter indicate significant differences between RT theses ($P < 0.05$). Refrigeration time theses (days *post-mortem*): ≤2 (2 d), 3–6 (6 d), 7–10 (10 d) and 11–14 (14 d).

significant functions, CAN1 and CAN2 (Wilks' λ = 0.001, approx. *F* value = 19.4, df1 = 96, df2 = 1833, $P < 0.001$) which explained 64.4 and 24.9% of the total variability, respectively. For the portable NIR instrument, 10 wavelengths were sorted as the most informative by the Stepwise procedure (Table 3). The CDA algorithm defined two canonical functions (CAN1 and CAN2) that showed a high discriminative power (Wilks' λ = 0.094, approx. *F* value = 9.9, df1 = 30, df2 = 241, $P < 0.001$), which accounted for 80.0 and 13.5% of the total variability, respectively. As shown in Figure 3A, for the bench-top system, the CDA model highlighted the possibility of satisfactory separation of the 0.95 confidence ellipses, even though there was a partial overlap between the two shorter shelf life theses. This discriminative capacity was confirmed by the significant D^2-Mahalanobis values, which ranged from 17.4 to 121.5 ($P < 0.001$). For the portable instrument (Figure 3B), there was a moderate spread of the 0.95 confidence ellipses across the two main canonical functions, with a partial overlap between the three shorter RT theses (2 d, 6 d, 10 d) as confirmed by the lower D^2-Mahalanobis values, which ranged from 2.8 to 20.6 ($P < 0.001$).

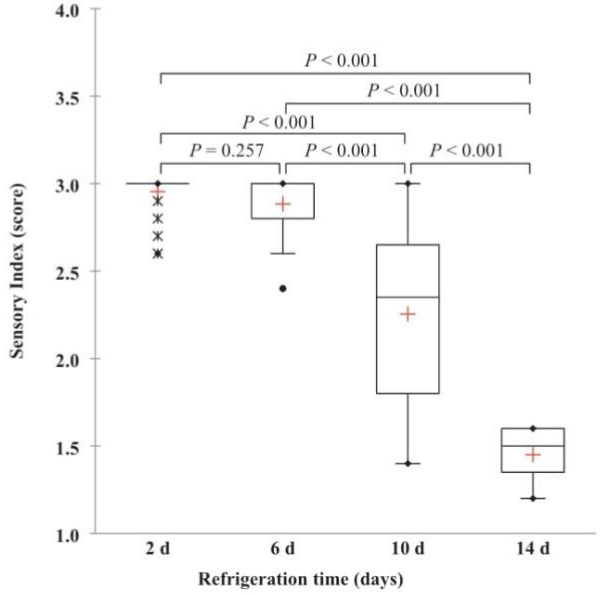

Figure 2. Box–whisker plot of sensory index (SI) across refrigeration time (RT) theses. The box plot represents the following descriptive statistics: median (bar in box), mean (+, red cross), 25–75% quartile (bottom and top end of the box), minimum and maximum values (whiskers) except for outliers (circles, distance to box 1.5–3.0 times interquartile range) and extreme values (* asterisks, distance to box > 3 times interquartile range). The significance (*P*-values on the top) of the pairwise multiple comparisons among the four RT theses was determined by Kruskal–Wallis non-parametric test (Steel–Dwass–Critchlow–Fligner correction). Refrigeration time theses (days *post-mortem*): ≤2 (2 d), 3–6 (6 d), 7–10 (10 d) and 11–14 (14 d).

The discriminating ability of the instruments was further investigated by means of a leave-one-out cross-validation to assess if the Stepwise-CDA classification functions allowed correct assignment of each chicken breast sample to its actual RT thesis (Table 4). The related confusion matrix shows how the bench-top is able to accurately distinguish all the theses (MCC > 0.94). Moreover, the bench-top instrument proves to be extremely reliable for discriminating fresh samples (2 d) compared to spoiled ones (10 d). There was a negligible misclassification of fresh samples, assigned to a class of lower freshness (6 d), which seemed to limit the monitoring effectiveness during the early stage of storage (fresh vs acceptable). However, there was no misclassification of samples with a shelf life longer than six days, thus ensuring meat safety. The portable instrument showed the lowest discriminatory capacity (MCC > 0.45) because it accurately recognised only the rotten class (MCC = 1.00), but showed a high level of misclassification between acceptable and spoiled samples (Table 4). However, it is noticeable that the discrimination performance seemed to be more reliable for fresh samples than for low-quality breast samples, and only one sample was misclassified as spoiled (MCC of 0.75). The CDA algorithm also confirmed the better discriminative capacity of bench-top with respect to portable instrument, which was previously explained in the PLS-DA paragraph.

NIR spectra, VIP and SPS and shelf life interpretation

Analysis of the discriminative models indicated a strong progressive separation during the shelf life of the refrigerated chicken breasts.

Table 2. Classification performance of PLS-DA (venetian blind cross-validation criterion) for the four chicken breast refrigeration time (RT) theses based on bench-top and portable NIR instruments

Predicted	Bench-top				Predicted	Portable			
	Actual					Actual			
	2 d	6 d	10 d	14 d		2 d	6 d	10 d	14 d
2 d	**19**	3	0	0	2 d	**16**	5	4	1
6 d	3	**19**	1	0	6 d	6	**13**	6	1
10 d	1	1	**22**	1	10 d	2	6	**11**	1
14 d	1	1	1	**23**	14 d	0	0	3	**21**
Total	24	24	24	24	**Total**	24	24	24	24
Sensitivity	0.79	0.79	0.92	0.96		0.67	0.54	0.43	0.88
Specificity	0.96	0.94	0.96	0.96		0.86	0.82	0.88	0.96
Accuracy	0.92	0.91	0.95	0.96		0.81	0.75	0.77	0.94
Precision	0.86	0.83	0.88	0.88		0.62	0.50	0.55	0.88
MCC	0.77	0.75	0.86	0.76		0.51	0.35	0.36	0.58

Refrigeration time theses (days *post-mortem*): ≤ 2 (2 d), 3–6 (6 d), 7–10 (10 d) and 11–14 (14 d). Bold values represent samples classified correctly. PLS-DA, partial least squares discriminant analysis; NIR, near-infrared; MCC, Matthews correlation coefficient.

Table 3. CDA statistics according to preliminary Stepwise and Boruta feature selection for discrimination of chicken breast refrigeration time by bench-top and portable NIR instruments

CDA statistics	Bench-top		Portable	
	Stepwise	Boruta	Stepwise	Boruta
Selected variables	32[a]	29[b]	10[c]	9[d]
Wilks' λ	0.001	0.010	0.094	0.169
CAN1 (%)	64.4	54.9	80.0	74.0
CAN2 (%)	24.9	26.2	13.5	15.7
D^2-Mahalanobis				
2 d vs 6 d	40.0	17.4	4.1	2.8
2 d vs 10 d	65.3	24.2	4.8	3.6
2 d vs 14 d	121.5	37.6	20.6	14.0

Wilks' λ and D^2-Mahalanobis always had a highly significant value ($P < 0.001$). CDA predictive scores (selected wavelengths, λ_{nm}):

[a] λ_{1174}, λ_{1206}, λ_{1302}, λ_{1406}, λ_{1430}, λ_{1454}, λ_{1470}, λ_{1478}, λ_{1518}, λ_{1870}, λ_{1886}, λ_{1894}, λ_{1902}, λ_{1974}, λ_{1982}, λ_{2006}, λ_{2086}, λ_{2110}, λ_{2206}, λ_{2222}, λ_{2230}, λ_{2334}, λ_{2358}, λ_{2366}, λ_{2374}, λ_{2390}, λ_{2398}, λ_{2422}, λ_{2430}, λ_{2438}, λ_{2462}, λ_{2490};

[b] λ_{1104}, λ_{1520}, λ_{1528}, λ_{1544}, λ_{1880}, λ_{1888}, λ_{1904}, λ_{1928}, λ_{1936}, λ_{1952}, λ_{2032}, λ_{2048}, λ_{2056}, λ_{2064}, λ_{2072}, λ_{2080}, λ_{2088}, λ_{2104}, λ_{2304}, λ_{2328}, λ_{2424}, λ_{2432}, λ_{2440}, λ_{2448}, λ_{2456}, λ_{2464}, λ_{2480}, λ_{2488}, λ_{2490};

[c] λ_{928}, λ_{1014}, λ_{1122}, λ_{1168}, λ_{1218}, λ_{1488}, λ_{1534}, λ_{1542}, λ_{1562}, λ_{1584};

[d] λ_{928}, λ_{1116}, λ_{1356}, λ_{1366}, λ_{1082}, λ_{1094}, λ_{1098}, λ_{1122}, λ_{1530}.

Refrigeration time theses (days post mortem): ≤2 (2 d), 3–6 (6 d), 7–10 (10 d) and 11–14 (14 d). CDA, canonical discriminant analysis; NIR, near-infrared; CAN1 and CAN2, two canonical functions.

Indeed, the overall results highlighted a moderate capacity of NIR spectroscopy to differentiate refrigerated poultry meat of the two shorter RT theses, probably due to mild biochemical and spoilage changes (Alexandrakis *et al.*, 2012). The findings for the chemometric models suggest that the effectiveness of NIR spectroscopy to correctly assess poultry meat shelf life seems to have a 6-day threshold for the bench-top tool, a cut-off that was delayed to around eight days for the portable one. These evidences are also supported by the results of SI that detected around 25% of spoiled samples within 10 d thesis (Figure 2). These performances are related to a simultaneous increase of many dominant NIR bands arising from the overall vibrations, overtones and combination bonds in functional groups such as –H, N–H, C–H and S–H (Liu *et al.*, 2001; Alamprese *et al.*, 2013; Barbin *et al.*, 2015). In this section, a deep biochemical interpretation of NIR wavelengths is carried out, evaluating the raw spectra, VIP indices and Stepwise-CDA predictive scores (SPS) patterns.

The raw spectra for experimental theses are reported in Figure 4, partitioned by the two NIR instruments. The distribution and magnitude of the main absorption bands observed in the present study agreed with those reported by Barbin *et al.* (2015) and Alexandrakis *et al.* (2012) referring to a wide region including the 900–2500 nm range of the applied instruments. Four high absorption bands are noticeable around 980, 1190, 1460 and 1930 nm, which are attributed to water absorption, protein changes and the effect of bacterial spoilage metabolites corresponding to O–H, C–H, NH_2 and $CONH_2$ stretching and bending, first, second and third overtones, and combination bands (Liu *et al.*, 2001; Alexandrakis *et al.*, 2012; Barbin *et al.*, 2015). The main difference between the two instruments was that the portable tool recorded high absorption values for the prolonged shelf life theses, whereas the bench-top instrument showed the opposite trend (Figure 4). The rotten thesis is the storage phase

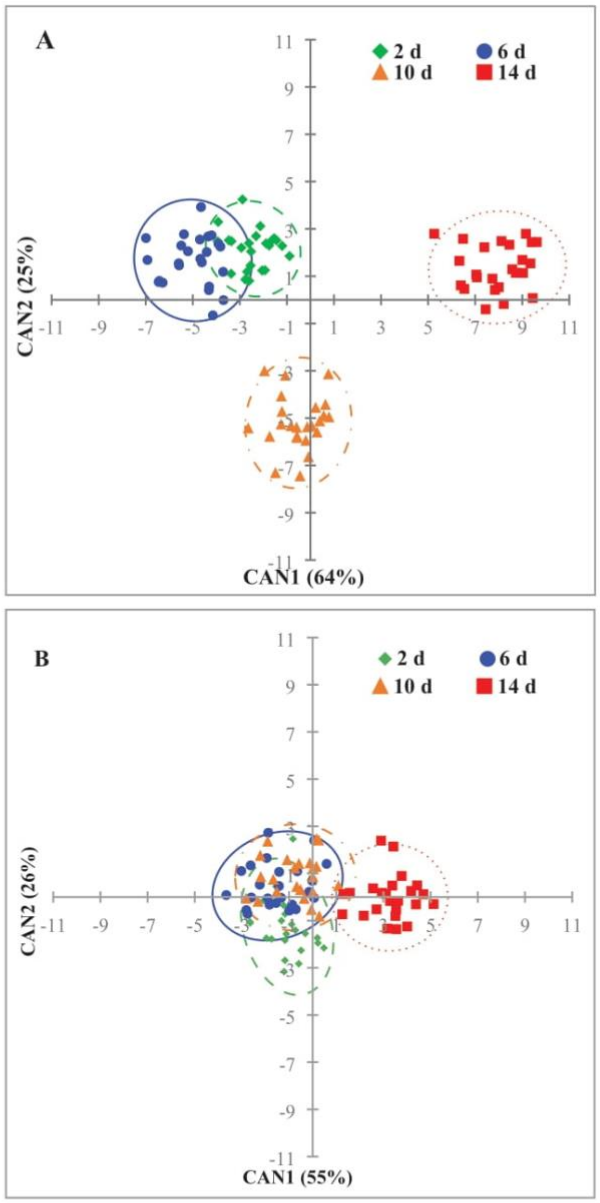

Figure 3. Stepwise-CDA scatterplots of the four chicken breast refrigeration time (RT) theses according to bench-top (**A**) and portable (**B**) NIR instruments; the 0.95 confidence ellipses are drawn around each centroid of groupings. RT theses (days *post-mortem*): ≤2 (2 d): green dotted line and diamonds; 3–6 (6 d): blue solid line and dots; 7–10 (10 d): orange dotted-pointed line and triangles; 11–14 (14 d): red pointed line and squares. CAN1 and CAN2, two canonical functions; CDA, canonical discriminant analysis; NIR, near-infrared.

with the highest muscle denaturation and intense proteolysis that increase the movement of water from intracellular into extracellular spaces (Bowker *et al.*, 2014). This means that a prolonged shelf life reduces the water holding capacity (WHC), increasing drip losses and NIR spectral absorbance, as in the case of portable tool, since free water is retained on the breast surface. The significant increase of L* values observed in the rotten theses was related to the release of exudates on breasts surface (Table 1). With regard to the bench-top instrument, mincing the samples promotes a partial loss of this water, with a probable subsequent reduction in absorption.

Table 4. Classification performance of Stepwise-CDA (leave-one-out cross-validation criterion) for the four chicken breast refrigeration time (RT) theses based on bench-top and portable NIR instruments

Predicted	Bench-top				Predicted	Portable			
	Actual					Actual			
	2 d	6 d	10 d	14 d		2 d	6 d	10 d	14 d
2 d	**22**	0	0	0	2 d	**20**	4	2	0
6 d	2	**24**	0	0	6 d	3	**13**	7	0
10 d	0	0	**24**	0	10 d	1	7	**15**	0
14 d	0	0	0	**24**	14 d	0	0	0	**24**
Total	24	24	24	24	**Total**	24	24	24	24
Sensitivity	0.92	1.00	1.00	1.00		0.83	0.54	0.61	1.00
Specificity	1.00	0.97	1.00	1.00		0.92	0.83	0.89	1.00
Accuracy	0.98	0.98	1.00	1.00		0.90	0.75	0.82	1.00
Precision	1.00	0.92	1.00	1.00		0.77	0.57	0.64	1.00
MCC	0.94	0.95	1.00	1.00		0.75	0.45	0.54	1.00

Refrigeration time theses (days post-mortem): ≤ 2(2 d), 3–6 (6 d), 7–10 (10 d) and 11–14 (14 d). Bold values represent samples classified correctly. CDA, canonical discriminant analysis; MCC, Matthews correlation coefficient.

An in-depth scrutiny of absorbance related to different chemical compounds could also help better understand meat behaviour during refrigeration. The VIP and SPS procedures captured a multitude of spectral information (Figure 5). The bench-top chilling preservation profile highlighted many significant VIP indices (>1.0), which represent the most relevant spectral features in the ranges 1100–1160, 1300–1350, 1380–1400 and 1850–1900 nm, and other additional features in the ranges 2050–2350 and over 2400 nm. Instead, the portable system refrigerated storage VIP pattern resulted in just three informative (>1.0) wavelengths belonging to the following spectral ranges: 1200–1250, 1350–1450 and over 1500 nm. With regard to SPS, these selected wavelengths belonged to four main spectral regions corresponding to 1200–1250, 1300–1500, 1900–2000 and over 2100 nm for bench-top system, and just two regions, 900–1200 and 1500–1580 nm, for portable one.

In general, the absorptions observed in the NIR region are overtones or combinations of the fundamental stretching bands which are usually due to C–H, N–H or O–H stretching mode (Cen and He, 2007). As confirmed by the physicochemical and sensorial analyses carried out as preliminary step (Table 1), *post-mortem* processes cause several biochemical changes including pH modification (i.e. early muscle acidification), alteration of cellular compartmentalisation, release of free catalytic iron, and myofibrillar contraction (Mir *et al.*, 2017). During meat storage, a shift in absorbance bands may be induced by changes that occur in proteins, due to the action of oxidising enzymes promoting the formation of protein carbonyls, and in lipids, due to the evolution of oxidative reactions, resulting in the formation and release of secondary products including lipid alcohols, ketones, epoxides, aldehydes and hydrocarbons (Estévez, 2011) that affected odour acceptability (Table 1). Overall, physicochemical modifications of meat structure induce a decrease in WHC, a change in surface colour and the development of microbial spoilage (Mir *et al.*, 2017). We have attempted to explain the significance of VIP and SPS in terms of the relationship between these muscle chemical changes and NIR spectral patterns, for both bench-top and portable, during 14 days of chicken breast storage.

Compared to the portable one, the bench-top instrument provides a wide range of spectral information suitable for the in-depth interpretation of biochemical and spoilage phenomena causing meat deterioration (Figure 5A). Thus, we focus the following discussion on the bench-top tool, even though the few VIPs for the portable one, found around 1190, 1370, 1400, 1440 and 1600 nm, are involved in the same biochemical processes described below. The 1100–1400 nm region is mainly characterised by the second overtones of C–H stretching and vibration modes associated with carbonyl formation (Alamprese *et al.*, 2016), which is an irreversible and non-enzymatic process involving the formation of carbonyl moieties and further aldehydes and ketones by the oxidation of many amino acids (Estévez, 2011). Probably, these chemical pathways related to carbonylation are recognised by NIR spectroscopy because they affect the vibration of functional groups. Several VIPs were observed at wavelengths related to water interactions through hydrogen bonds and other meat components (Nolasco Perez *et al.*, 2018). A few broad and high VIP scores are noticeable around the region of the first overtone of water, especially the wavelengths around 1384–1388 nm that could be assigned to H_2O–OH-bonded water molecules, while around 1410 nm the VIPs are mainly related to free water molecular species (Tsenkova *et al.*, 2015). Indeed, the 1400–1600 nm region basically includes the first overtones of the O–H/N–H stretching modes of self-associated and water-bonded OH/NH groups of N-compounds in meat (Liu *et al.*, 2001). Once again, changes in this spectral region could be linked to protein denaturation, proteolysis and WHC reduction. Thus, the physical relationship between water molecular species and protein and lipid C–H/N–H seem to be the major contributors to sample shelf life differentiation. In this study, additional weak sharp spectral markers were found at 1700 and 1732 nm, corresponding to the first overtones of C–H stretching modes, which might be linked to a change in lipid deterioration (Ding *et al.*, 1999; Peng and Wang, 2015). The NIR spectra of chicken meat showed a prominent VIP in the absorbance region 1850–1910 nm, specific to O–H functional groups, H_2O overtones and vibration of O–H bonds (1920 nm) (Alamprese *et al.*, 2016; Ghidini *et al.*, 2019). Specific carbonyl and N–H asymmetric stretching has been reported in this region, probably due to amides and amines, major N-catabolites arising from the late proteolytic process (Alamprese *et al.*, 2016). A strong relationship between informative bands and both amides and amines has already been reported by the authors in Alexandrakis *et al.* (2012), as a consequence of prolonged storage associated with ammonia and volatile amines from free amino acids and peptides related to autolytic and microbial enzyme activity (Alexandrakis *et al.*, 2012). The second overtone of carbonyl groups related to peptides, aldehydes and ketones has been already selected at 1900–1960 nm, even though

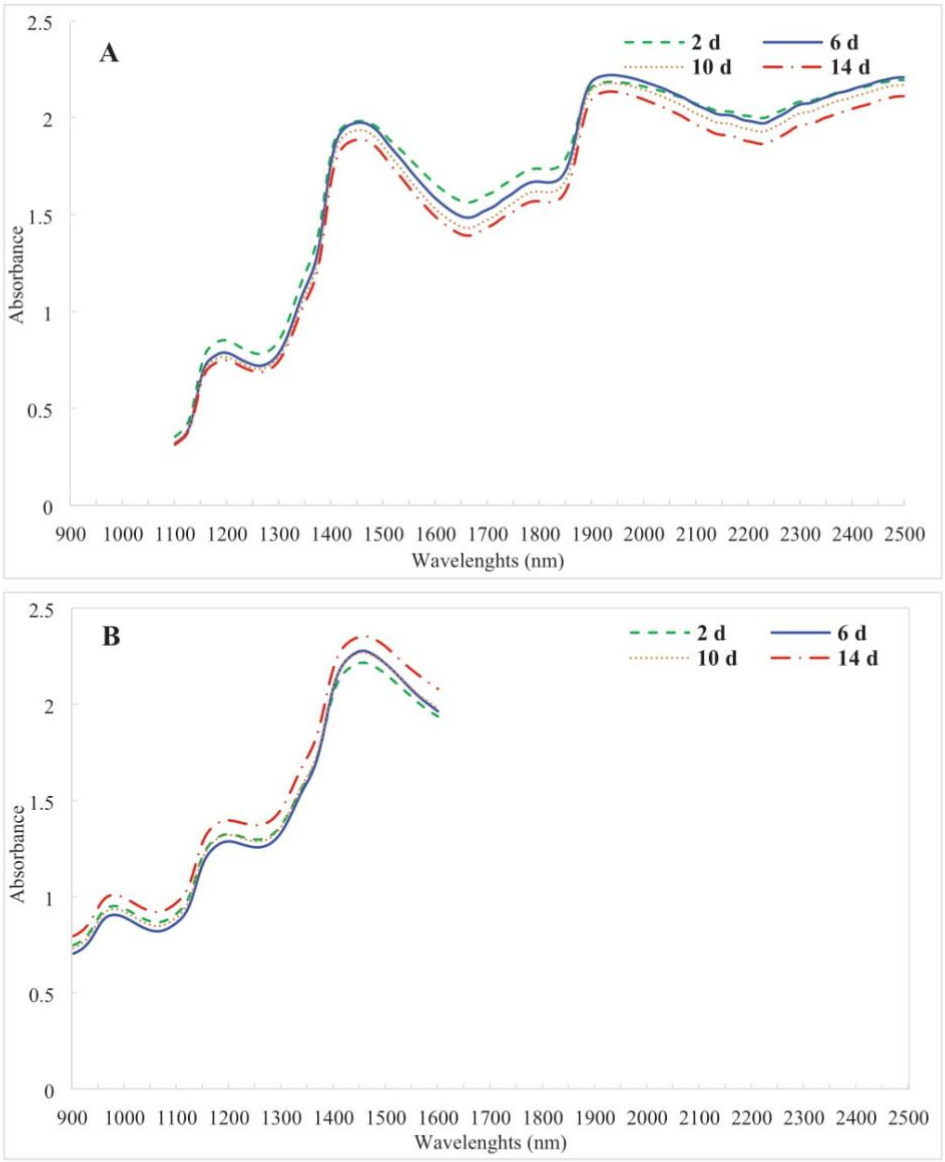

Figure 4. Average spectra of the four refrigeration time (RT) theses related to bench-top (**A**) and portable (**B**) NIR instruments. Refrigeration time theses (days *post-mortem*): ≤2 (2 d), 3–6 (6 d), 7–10 (10 d) and 11–14 (14 d). NIR, near-infrared.

these wavelengths are overlap with the water band at 1940 nm (Jha, 2010). The 2040–2350 nm region might be associated with myoglobin N–H bonds (Burns and Ciurczak, 2008) and related to C–H combination tones (2340 nm) of unsaturated fatty acids (Cozzolino *et al.*, 2002; Peng and Wang, 2015).

Interpretation of the SPS feature variables was similar to that for VIP indices previously mentioned. These were partly overlapping or closer to the VIPs previously described. However, around 1000, 1500, 2000 and 2400 nm, in particular in λ_{1014}, λ_{1488} (for portable instrument), λ_{1174}, λ_{1206}, λ_{1430}, λ_{1454}, λ_{1470}, λ_{1478}, λ_{1518}, λ_{1974}, λ_{1982}, λ_{2006}, λ_{2358}, λ_{2366}, λ_{2374}, λ_{2390} and λ_{2398} (for bench-top instrument), the SPS are distant from the VIP peaks, but identify themselves in wavelengths that express those biochemical processes already described.

The findings of this study suggested that the VIPs pattern and SPS could be useful markers of meat deterioration related to proteolysis (1100–1400 and 1850–1920 nm) and amino acids oxidation (1400–1600 nm), lipid oxidation (1700–1740 nm) and decrease in WHC (1380–1410 nm). Moreover, we advise the use of the selected spectral ranges described above, as a NIR benchmark for a rapid assessment of spoilage threshold of chicken breasts.

Conclusions

Overall results of the present experiment highlighted that NIR technology could be considered a potential safety and quality labelling tool to prevent deceptive practices related to meat freshness, both for food industry and consumer protection. The combination of NIR technology with discriminating chemometric approaches potentially allowed a reliable assessment of chicken breasts shelf life, with a refrigeration cut-off of a week. Based on a multivariate model, a selection of NIR features were suitable for the interpretation of the main physicochemical changes during poultry meat storage.

Based on actual findings, the bench-top tool seemed to be more effective for predicting chicken breast shelf life than the portable

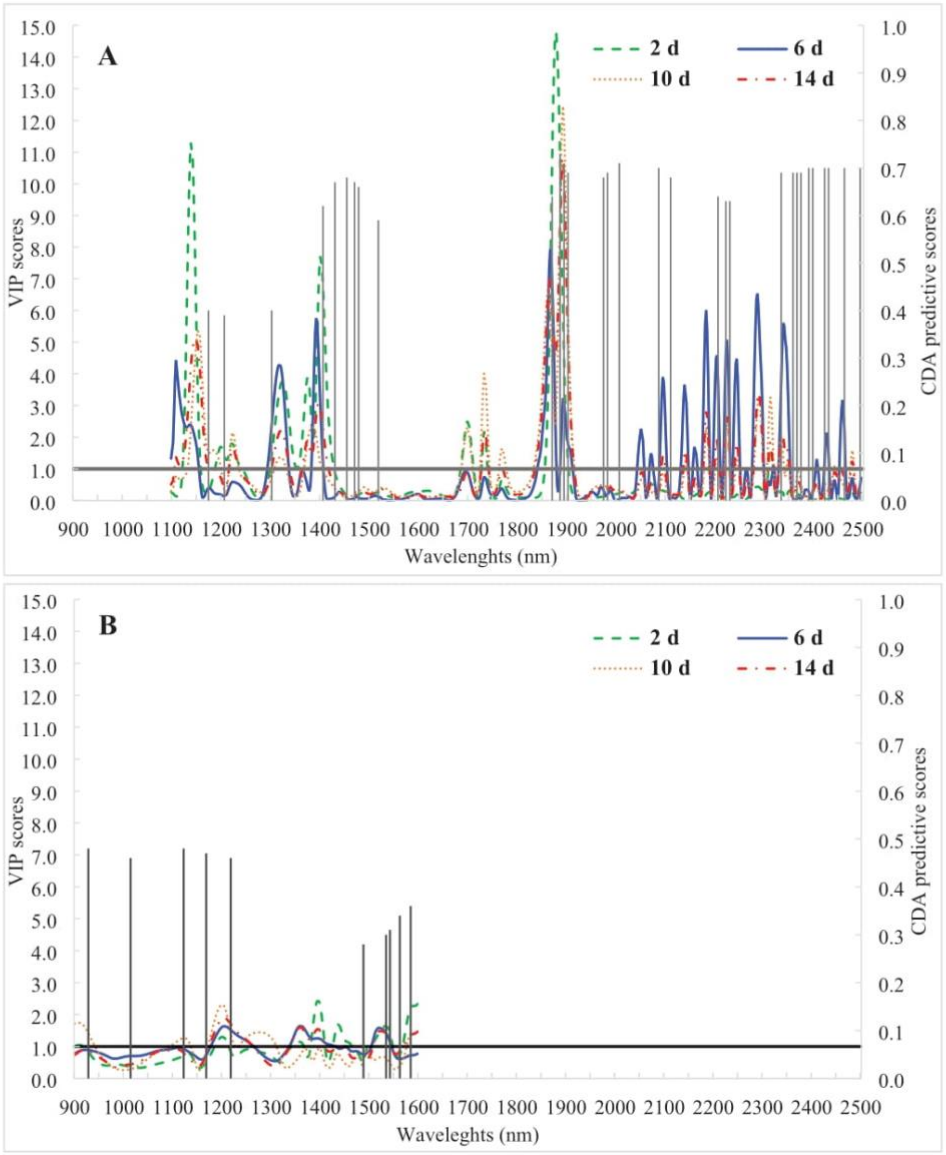

Figure 5. VIP index scores obtained by PLS-DA algorithm and CDA predictive scores (SPS) sorted by the Stepwise feature selection procedure according to the four refrigeration time (RT) theses related to bench-top (**A**) and portable (**B**) NIR instruments. Refrigeration time theses (days *post-mortem*): ≤2 (**2 d**), 3–6 (**6 d**), 7–10 (**10 d**) and 11–14 (**14 d**). VIP, variable importance in projection; PLS-DA, partial least squares discriminant analysis; CDA, canonical discriminant analysis; NIR, near-infrared.

one, probably due to better optical properties and the longer spectral range. Considering an operative scenario, the challenge of portable NIR instruments could be its suitability for rapid at-line screening of poultry meat along the supply chain in a real enterprise environment. Meanwhile, the application of the bench-top NIR might be proposed as spectroscopy gold standard for evaluating the shelf life of fresh cuts. Perhaps it could be useful for minced meat quality control and meat preparation at the slaughterhouse and in cutting plants. Further experimental trials are needed to improve the accuracy and reliability of the portable spectrometer in detecting biochemical meat changes.

Author Contributions

Ilaria Lanza: Data curation, interpreted the results and wrote the manuscript. Daniele Conficoni, Marco Cullere, Angela Trocino, Gerolamo Xiccato: Writing the manuscript. Stefania Balzan, Luca Fasolato, Enrico Novelli, Severino Segato: Conceptualization, planned the experiment, carried out the experiments, interpreted the results and wrote the manuscript. Lorenzo Serva, Barbara Contiero: Data Curation, statistical analyses, interpreted the results. Enrico Novelli, Severino Segato: Funding acquisition.

Funding

This works was supported by FONDAZIONE CARIVERONA (projects Tre Poli 4 and 6, call 2012 and 2016); University of Padova (2019 SID assignment), Italy.

Conflict of Interest

The authors declare no conflict of interest.

References

Akarachantachote, N., Chadcham, S., Saithanu, K. (2014). Cutoff threshold of variable importance in projection for variable selection. *International Journal of Pure and Applied Mathematics*, 94: 307–322.

Alamprese, C., Casale, M., Sinelli, N., *et al.* (2013). Detection of minced beef adulteration with turkey meat by UV-vis, NIR and MIR spectroscopy. *LWT - Food Science and Technology*, 53: 225–232.

Alamprese, C., Amigo, J. M., Casiraghi, E., *et al.* (2016). Identification and quantification of turkey meat adulteration in fresh, frozen-thawed and cooked minced beef by FT-NIR spectroscopy and chemometrics. *Meat Science*, 121: 175–181.

Alexandrakis, D., Downey, G., Scannell, A. G. M. (2012). Rapid non-destructive detection of spoilage of intact chicken breast muscle using near-infrared and Fourier transform mid-infrared spectroscopy and multivariate statistics. *Food and Bioprocess Technology*, 5: 338–347.

Atanassova, S., Stoyanchev, T., Yorgov, D., *et al.* (2018). Differentiation of fresh and frozen-thawed poultry breast meat by near infrared spectroscopy. *Bulgarian Journal of Agricultural Science*, 24: 162–168.

Barbin, D. F., Kaminishikawahara, C. M., Soares, A. L., *et al.* (2015). Prediction of chicken quality attributes by near infrared spectroscopy. *Food Chemistry*, 168: 554–560.

Bisutti, V., Merlanti, R., Serva, L., *et al.* (2019). Multivariate and machine learning approaches for honey botanical origin authentication using near infrared spectroscopy. *Journal of Near Infrared Spectroscopy*, 27: 65–74.

Bowker, B., Hawkins, S., Zhuang, H. (2014). Measurement of water-holding capacity in raw and freeze-dried broiler breast meat with visible and near-infrared spectroscopy. *Poultry Science*, 93(7): 1834–1841.

Bruckner, S., Albrecht, A., Petersen, B., *et al.* (2012). Characterization and comparison of spoilage processes in fresh pork and poultry. *Journal of Food Quality*, 35: 372–382.

Burns, D. A., Ciurczak, E. W. (2007). Handbook of near-infrared analysis. Taylor & Francis Group, Boca Raton, FL, pp. 521–527.

Cen, H. Y., He, Y. (2007). Theory and application of near infrared reflectance spectroscopy in determination of food quality. *Trends in Food Science and Technology*, 18: 72–83.

Cozzolino, D., De Mattos, D., Vaz Martins, D. (2002). Visible/near infrared reflectance spectroscopy for predicting composition and tracing system of production of beef muscle. *Animal Science*, 74: 477–484.

Crocombe, R. A. (2018). Portable spectroscopy. *Applied Spectroscopy*, 72(12): 1701–1751.

Ding, H. B., Xu, R. J., Chan, D. K. O. (1999). Identification of broiler chicken meat using a visible / near-infrared spectroscopic technique. *Journal of the Science of Food and Agriculture*, 79: 1382–1388.

Estévez, M. (2011). Protein carbonyls in meat systems: a review. *Meat Science*, 89: 259–279.

Falkovskaya, A., Herrero-Langreo, A., Gowen, A. (2019). Comparison of Vis-Nir (400–1,000 Nm) and Nir (978–1,678 Nm) hyperspectral imaging for discrimination between fresh and previously frozen poultry. 2019 10th Workshop on Hyperspectral Imaging and Signal Processing: Evolution in Remote Sensing (WHISPERS). 24-26 September 2019, IEEE, Amsterdam, Netherlands, pp. 1–5.

FAO (The Food and Agriculture Organization). (2020a). FAOSTAT [Online]. http://www.fao.org/faostat/en/#home. Accessed on June 10, 2020.

FAO (The Food and Agriculture Organization). (2020b). Gateway to Poultry Production and Products [Online]. http://www.fao.org/poultry-production-products/en/. Access on June 10, 2020.

Fernández-Pan, I., Carrión-Granda, X., Maté, J. I. (2014). Antimicrobial efficiency of edible coatings on the preservation of chicken breast fillets. *Food Control*, 36: 69–75.

Ghidini, S., Varrà, M. O., Zanardi, E. (2019). Approaching authenticity issues in fish and seafood products by qualitative spectroscopy and chemometrics. *Molecules*, 24: 1812.

Gram, L., Ravn, L., Rasch, M., *et al.* (2002). Food spoilage–interactions between food spoilage bacteria. *International Journal of Food Microbiology,* 78(1–2): 79–97.

Gratta, F., Fasolato, L., Birolo, M., *et al.* (2019). Effect of breast myopathies on quality and microbial shelf life of broiler meat. *Poultry Science*, 98(6): 2641–2651.

Jha, S. N. (2010). Near infrared spectroscopy. In: Nondestructive evaluation of food quality: theory and practice. Springer Science & Business Media, Berlin, Germany.

Katiyo, W., de Kock, H. L., Coorey, R., *et al.* (2020). Sensory implications of chicken meat spoilage in relation to microbial and physicochemical characteristics during refrigerated storage. *LWT - Food Science and Technology*, 128: 109468.

Kursa, M. B., Rudnicki, W. R. (2010). Feature selection with the boruta package. *Journal of Statistical Software*, 36: 1–13.

Leardi, R. (2000). Application of genetic algorithm-PLS for feature selection in spectral data sets. *Journal of Chemometrics*, 14: 643–655.

Liu, Y., Chen, Y. R., Ozaki, Y. R. (2001). Two-dimensional visible / near-infrared correlation spectroscopy study of thermal treatment of chicken meats. *Meat Science*, 54: 1458–1470.

Melro, E., Antunes, F., Cruz, I. *et al.* (2020). Morphological, textural and physico-chemical characterization of processed meat products during their shelf life. *Food Structure*, 26: 100164.

Mendez, J., Mendoza, L., Cruz-Tirado, J. P., *et al.* (2019). Trends in application of NIR and hyperspectral imaging for food authentication. *Scientia Agropecuaria*, 10: 143–161.

Mir, N. A., Rafiq, A., Kumar, F., *et al.* (2017). Determinants of broiler chicken meat quality and factors affecting them: a review. *Journal of Food Science and Technology*, 54(10): 2997–3009.

Morsy, N., Sun, D. W. (2013). Robust linear and non-linear models of NIR spectroscopy for detection and quantification of adulterants in fresh and frozen-thawed minced beef. *Meat Science*, 93(2): 292–302.

Nolasco Perez, I. M., Badaró, A. T., Barbon, S. Jr, *et al.* (2018). Classification of chicken parts using a portable near-infrared (NIR) spectrophotometer and machine learning. *Applied Spectroscopy*, 72(12): 1774–1780.

Ottavian, M., Franceschin, E., Signorin, E., *et al.* (2015). Application of near infrared reflectance spectroscopy (NIRS) on faecal samples from lactating dairy cows to assess two levels of concentrate supplementation during summer grazing in alpine pastures. *Animal Feed Science and Technology*, 202: 100–105.

Peng, Y. K., Wang, W. X. (2015). Application of near-infrared spectroscopy for assessing meat quality and safety. In: Infrared Spectroscopy - Anharmonicity of Biomolecules, Crosslinking of Biopolymers, Food Quality and Medical Applications. InTech, London, UK.

Raab, V., Bruckner, S., Beierle, E., *et al.* (2008). Generic model for the prediction of remaining shelf life in support of cold chain management in pork and poultry supply chains. *Journal on Chain and Network Science*, 8: 59–73.

Rubingh, C. M., Bijlsma, S., Derks, E. P., *et al.* (2006). Assessing the performance of statistical validation tools for megavariate metabolomics data. *Metabolomics: Official Journal of the Metabolomic Society*, 2(2): 53–61.

Segato, S., Merlanti, R., Bisutti, V., *et al.* (2019). Multivariate and machine learning models to assess the heat effects on honey physicochemical, colour and NIR data. *European Food Research and Technology*, 245: 2269–2278.

Sivarajan, M., Lalithapriya, U., Mariajenita, P., *et al.* (2017). Synergistic effect of spice extracts and modified atmospheric packaging towards non-thermal preservation of chicken meat under refrigerated storage. *Poultry Science*, 96(8): 2839–2844.

Sujiwo, J., Kim, D., Jang, A. (2018). Relation among quality traits of chicken breast meat during cold storage: correlations between freshness traits and torrymeter values. *Poultry Science*, 97(8): 2887–2894.

Teixeira dos Santos, C. A., Lopo, M., Páscoa, R. N., *et al.* (2013). A review on the applications of portable near-infrared spectrometers in the agro-food industry. *Applied Spectroscopy*, 67(11): 1215–1233.

Tsenkova, R., Kovacs, Z., Kubota, Y. (2015). Aquaphotomics: near infrared spectroscopy and water states in biological systems. *Sub-Cellular Biochemistry*, 71: 189–211.

Xu, X., Xie, L. J., Ying, Y. B. (2019). Factors influencing near infrared spectroscopy analysis of agro-products: a review. *Frontiers of Agricultural Science and Engineering*, 6: 105–115.

Zareef, M., Chen, Q., Hassan, M. M., *et al.* (2020). An overview on the applications of typical non-linear algorithms coupled with NIR spectroscopy in food analysis. *Food Engineering Reviews*, 12: 173–190.

Zhao, G., Maclean, A. L. (2000). A comparison of canonical discriminant analysis and principal component analysis for spectral transformation. *Photogrammetric Engineering and Remote Sensing*, 66: 841–847.

CHAPTER 5

Spectroscopic Methods and Machine Learning Modelling to Differentiate Table Eggs from Quails Fed with Different Inclusion Levels of Silkworm Meal

---

Ilaria Lanza[1], Sarah Currò[2], Severino Segato[1§], Lorenzo Serva[1], Marco Cullere[1], Paolo Catellani[1], Luca Fasolato[2], Daniela Pasotto[1], Antonella Dalle Zotte[1]

[1] Department of Animal Medicine, Production and Health, University of Padova, University of Padova, 35020 Legnaro, PD, Italy

[2]Department of Comparative Biomedicine and Food Science, University of Padova, University of Padova, 35020 Legnaro, PD, Italy

Food Control 147 (2023) 109589

Food Control 147 (2023) 109589

Contents lists available at ScienceDirect

Food Control

journal homepage: www.elsevier.com/locate/foodcont

Spectroscopic methods and machine learning modelling to differentiate table eggs from quails fed with different inclusion levels of silkworm meal

Ilaria Lanza [a], Sarah Currò [b], Severino Segato [a,*], Lorenzo Serva [a], Marco Cullere [a], Paolo Catellani [a], Luca Fasolato [b], Daniela Pasotto [a], Antonella Dalle Zotte [a]

[a] Department of Animal Medicine, Production and Health, University of Padova, Viale dell'Università 16, 35020 Legnaro (PD), Italy
[b] Department of Comparative Biomedicine and Food Science, University of Padova, Viale dell'Università 35020 Legnaro (PD), Italy

ARTICLE INFO

Keywords:
Coturnix coturnix japonica
Silkworm meal
Table egg
NIR spectroscopy
NIR instruments
Random forest
Machine learning

ABSTRACT

The study aimed at evaluating the VIS/NIR and NIR instrument's capability to discriminate among table eggs from quails fed with different inclusion levels of silkworm (*Bombyx mori* L.) pupa meal (SWM). The trial consisted of four experimental groups of laying quails fed for 8 weeks with a 0%, 4%, 8% or 12% SWM inclusion levels. At week 7, 120 eggs (30 per experimental group) were sampled to form the training set used to perform the spectroscopy-based classification models, whereas at the end of the trial a second batch (n = 48) was used as an independent test set to assess the reliability of the classification models. Using a benchtop and two portable devices, VIS-NIR and NIR spectra were recorded from the training set and subsequently submitted to a random forest (RF) feature selection. The selected NIR informative wavelengths were used to perform the following supervised classification algorithms: partial least squares-discriminant analysis (PLS-DA), K-nearest neighbour (KNN) and support vector machine (SVM) linear and radial. The RF features predictive models were applied against the independent test set to assess the reliability by a set of confusion matrices. A moderate predictive capacity of the tested VIS/NIR and NIR devices in predicting the eggs feeding groups was observed probably due to the relative low difference in SWM amount among the classes. After a merging of the SWM4-12 experimental groups, both NIR benchtop and portable devices combined with the advanced machine learning models successfully showed capacity to recognize in the eggs the inclusion of insect meal in layers diet since an accuracy higher than 0.90 has been observed. Instead, the VIS-NIR portable tool recorded worse predictive capacity with an accuracy lower than 0.73. The most informative NIR wavelengths belonged to the 1350–1600 and 1850–2200 nm spectral regions. The achieved outcomes in terms of accuracy suggested that both KNN and SVM models provided more powerful machine learning algorithm than PLS-DA. The results showed that a portable NIR spectrometer had comparatively accurate classification to the benchtop instrument, highlighting the potential of hand-held NIR spectrometers in at-line monitoring eggs from SWM-fed layer quails.

1. Introduction

Currently, one of the main concerns in livestock systems is the limited availability of high biological value proteins for animal feeding as well as the shift towards a more sustainable production system which includes the utilisation of new feedstuffs with remarkable sustainability (Hawkey et al., 2021). Insects represent good candidates in this perspective, offering an alternative to conventional protein and lipid feedstuffs for monogastric animals, and therefore providing strategic solutions to address some environmental and ethical concerns linked to animal production and sustainability (Dalle Zotte, 2021). Many poultry species naturally consume insects as part of their diet, and available research on the inclusion of different insect species and derived products (i.e., protein meal and oil) in the diet of different poultry species provided positive outcomes in terms of animal performance and product quality (Dalle Zotte et al., 2019; Gasco et al., 2020). Furthermore, research on some insect species also highlighted that they could be used as feed ingredient for different food-producing animals, and it is even

Abbreviations: KNN, K-nearest neighbour; MCC, Matthew correlation coefficient; PLS-DA, partial least squares-discriminant analysis; ML, machine learning; NIR, near-infrared; PAPs, processed animal proteins; RF, random forest; SVM, support vector machine; SWM, silkworm meal.

* Corresponding author. Viale dell'Università 16, Legnaro, Padova, 35020, Italy.
E-mail address: severino.segato@unipd.it (S. Segato).

https://doi.org/10.1016/j.foodcont.2022.109589
Received 6 October 2022; Received in revised form 13 December 2022; Accepted 22 December 2022
Available online 27 December 2022

possible to achieve product improvements in terms of healthiness and/or sensory quality. In a study carried out on laying hens, eggs from the feeding group receiving a ration with insect meal (defatted meal from *Hermetia illucens* larvae) showed a redder yolks and a higher incidence of γ-tocopherol and carotenoids (lutein, β-carotene) compared to the soybean meal feeding group (Secci et al., 2018). The partial substitution of soybean meal and oil with full-fat silkworm (*Bombyx mori* L.) meal in the diet of growing chickens brought to an increase of polyunsaturated fatty acids (PUFA) n-3 on the breast meat, leading to a reduction of the n-6:n-3 PUFA ratio (Miah et al., 2020).

Together with the aforementioned positive research findings, the recent EU regulation 2021/1372 (European Commission, 2018) authorising the inclusion of processed animal proteins (PAPs) from insects in animal feeding boosted European companies who specialise in producing insects and stimulated conventional feeding companies to start considering insects as possible new livestock feedstuffs in their products range. On the consumer side, a recent UK-survey highlighted that consumers are keen to pay an extra amount of money to purchase eggs from insect-fed hens if animal welfare and sustainability are improved (Spartano & Grasso, 2021). Similarly, another study on Italian consumers showed that 85% of the surveyed people accept to consume eggs from insect-fed laying hens (Lippi et al., 2021).

Therefore, the inclusion of PAPs from insects in feed formulation for egg-producing poultry species could represent a premium value by declaring a highly-marketable labelling designation. With that said, the convenience of rearing livestock based on these insect-derived concentrates should be investigated also in terms of cost-benefit before promotion, in case of increased cost of production. To this regard, the need for rapid and accurate analytical methods and chemometric approaches for confirming specific quality features of the product, preferably exploiting real-time methods arises. Generally, the non-destructive characterisation tools based on the principles of light-matter interaction (such as VIS/NIR spectroscopy) could represent an end-step valuable screening of authentication providing a comprehensive overview of the productive and/or manufacturing process. A major challenge in the NIR spectroscopy-based analysis and authentication is the possibility of revealing the relationship between spectral data and cluster similarities among samples derived by proper development of predictive models that exploit the spectroscopic information for pursuing classification purposes.

Thus far, multivariate analysis techniques such as PLS-DA (Lin et al., 2011) and many machine learning (ML) approaches (Cruz-Tirado et al., 2021) have been widely used to process spectral data in order to estimate the freshness or quality traits of eggs (Coronel-Reyes et al., 2018; Loffredi et al., 2021). However, the use of algorithms based on ML models to distinguish among quality levels is still an ongoing topic as described in a recent study on the assessment of many egg's physical features (weight, size, colour), which highlighted different performance of classification among various classifier methods including LDA, SVM and KNN (Sehirli & Arslan, 2022).

Moreover, robust and ergonomic portable NIR spectrometers were also developed with similar spectral data recognition performance to the benchtop ones but offering more potential advantages in terms of wide applications in-field farm and/or on-site supply-chain control inspections (Zhu et al., 2022). However, to the best of our knowledge no research has been conducted to discriminate eggs obtained from insect-fed laying hens through NIR spectroscopic techniques. Thus, this study aimed to evaluate the feasibility of VIS/NIR and NIR spectroscopic techniques to segregate quail table eggs according to the dietary inclusion of an increasing percentage of silkworm meal (SWM). The evaluation of the predictive capability of VIS/NIR and NIR portable instruments compared to a NIR benchtop device was also performed according to four supervised pattern recognition models throughout a comparison between the consolidate approach based on PLS-DA and the more innovative SVM and KNN supervised classification models. An in-depth interpretation of the most predictive VIS/NIR and NIR features selected by a random forest (RF) algorithm was another challenge of the experimental trial.

2. Materials and methods

2.1. Experimental design and eggs sampling

The study was conducted during spring 2021 on an experimental farm (Veneto region, Italy) after the ethical approval (No 147882, December 2020) of the Ethical Committee for Animal Experimentation of the University of Padova. For the study, a total of 240 laying quails were allocated into 4 dietary groups with different inclusion levels of silkworm meal (SWM): SWM0 (control group with no SWM inclusion), SWM4, SWM8 and SWM12 corresponding to a dietary inclusion of 4%, 8% and 12%, SWM, respectively (Fig. 1). Quails received the experimental diets for 8 weeks. Feed and water were provided *ad libitum* throughout the study, temperature was kept in the range 20–25 °C and the photoperiod was 16L:8D. At the 7th week of feeding, eggs of each feeding group were collected in the morning (8 a.m.) in three sampling days to form the training set of eggs (n = 120) used to perform the classification models. At the end of the trial, the second batch of eggs was collected (n = 12 per treatment), and used as an independent test set (n = 48) to assess the reliability of the multivariate classification models. Collected eggs were analysed the day of sampling for NIR spectral data acquisition.

2.2. Spectra acquisition in transflectance mode

As reported in Fig. 1, the edible content (yolk and albumen mixture) of 168 eggs was individually homogenised by gentle mixing using a soft blender (Bonsenkitchen, Flowery Branch, Georgia, USA) and then the content of each egg (approx. 10 g) was submitted for NIR's spectra acquisition. To this purpose, the product was gently placed into a small ring cup, avoiding air bubbles, with a quartz window that allowed irradiation of an area of approximately 9.6 cm^2, and equipped with a 0.5 mm gold-reflector (1 mm of pathlength). The spectral data were collected in duplicate using: (i) a bench-top FOSS DS2500 analyser (FOSS Analytical A/S, Hillerød, Denmark), referred to in the study as NIR-benchtop, covering a range of 850–2500 nm at 0.5 nm intervals and each sample was scanned 32 times, placing the small ring cup in a rotating module; (ii) a NIR-portable Polispec (ITPhotonics, Fara Vicentina, Italy) covering a range of 902–1680 nm at 2.0 nm intervals; (iii) a VIS/NIR-portable Polispec (ITPhotonics, Fara Vicentina, Italy) covering a range of 700–1080 nm at 2.0 nm intervals. For both the portable tools, referred to as NIR portable and VIS-NIR portable, spectra were acquired through an embedded round scanning window (area of 3.2 cm^2) placed directly over the gold ring cup; each spectrum was obtained by averaging three scans of 5 s of data acquisition at 10 msec integration time each, by rotating the ring cup 120° after a scan. Spectral data were recorded in reflectance (R) and converted to absorbance (A) units as log (1/R) using WinISI 2 V1.05 (Infrasoft International Inc., Port. Matilda, USA) and poliDATA 3.0.1 (ITPhotonics, Fara Vicentina, Italy) software for benchtop and portable instruments, respectively. Spectra were subsequently exported in.csv format, and the two replicates were averaged prior to any manipulation. To reduce light scattering and to remove the baseline shift, all chemometric data analyses were performed after mathematical pre-treatment of the spectra with standard normal variate (SNV), detrend, first-order derivative and smoothing (Currò et al., 2021) (Figs. 1S, **2S**, **3S**, supplementary materials).

2.3. Chemometric modelling and machine learning algorithms

Chemometrics and data analyses were performed using R software version 3.2.5 (R Core Team, 2016). Based on the Boruta algorithm with a wrapper approach (Segato et al., 2019), RF feature selection procedure was applied to select the most informative bands and remove irrelevant

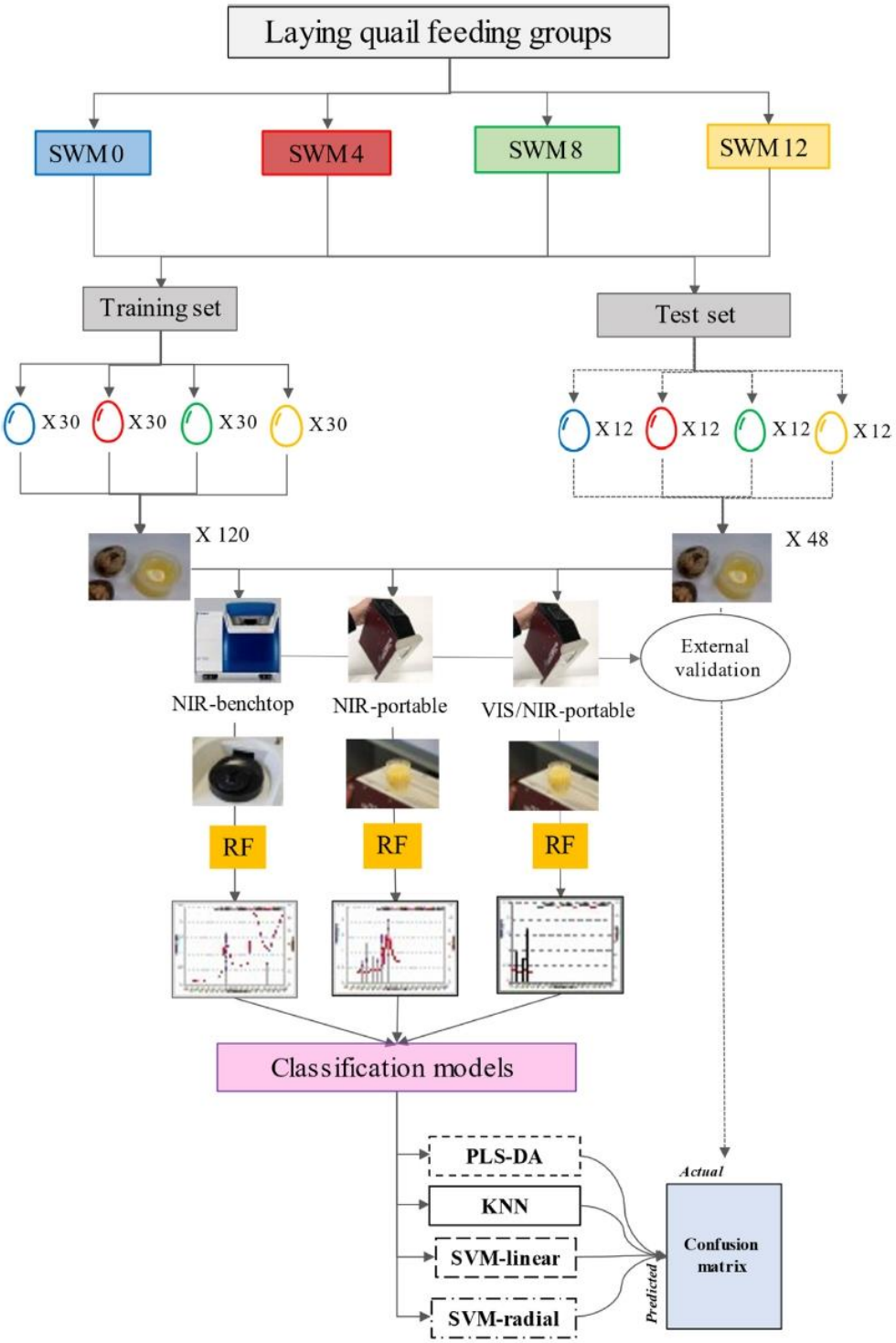

Fig. 1. Bench-top and portable NIR and VIS/NIR pre-treated data (training set, n = 120) of eggs (yolk and albumen) from laying quails fed 4 dietary levels of silkworm meal (SWM 0–12% inclusion) were submitted to random forest (RF) selection. Spectral RF features were used to build the supervised classification models. The predictive performance of classifying algorithms were evaluated by an external validation (test set, n = 48) by means of a set of confusion matrices.

and noisy data from the training set (120 samples). Choosing a short range of wavelengths to avoid irrelevant ones could be a strategy against the so-called minimal-optimal problem, improving the model's predictive ability and reducing complexity since many irrelevant variables may yield considerable variation in test set prediction (Mehmood et al., 2012). To segregate the feeding groups (SWM0, SWM4, SWM8 and SWM12) a set of independent classification models was performed and tested through a repeated K-folds cross-validation (setting number = 10 and repeats = 5) (Marcot & Hanea, 2021) applied on the RF selected VIS/NIR or NIR variables and then validated on the independent test set (n = 48 samples). The supervised classification models were performed through the PLS-DA, KNN and SVM algorithms. The PLS-DA is a

quantitative algorithm that involves performing a multivariate regression and classifying the samples into the pre-determined feeding classes (Bisutti et al., 2019). The KNN classification algorithm was assessed by using the 'caret' package in R; this classification algorithm predicts a class for a given test observed by attributing the class of the K-nearest observed sample and is optimised according to the CV accuracy (Currò et al., 2022). The SVM was modelled by the use of the 'caret' package, through both the linear and radial kernels and applied to the training dataset (Currò et al., 2022). In detail, the 'one-against-one' approach for multi-class (classes >3) classification was adopted, in which k (k − 1)/2 binary classifiers are trained, and a voting scheme to find the appropriate class; the C-value (Cost) in the linear classifier and the radial basis function sigma were customised, adopting a grid search.

The predictive models developed on the RF selected features of the training dataset were applied against the independent test set to assess their reliability. The predictions were arranged in a confusion matrix and a set of statistical measurements was calculated according to the following equations (1)–(4):

$$\text{Sensitivity} = \frac{TP}{TP + FN} \quad (1)$$

$$\text{Specificity} = \frac{TN}{TN + FP} \quad (2)$$

$$\text{Accuracy} = 1 - \left(\frac{FP + FN}{TP + TN + FP + FN}\right) \quad (3)$$

$$MCC = \frac{TP \cdot TN - FP \cdot FN}{\sqrt{(TP + FP) \cdot (TP + FN) \cdot (TN + FP) \cdot (TN + FN)}} \quad (4)$$

where, TP is true positive, FN is false negative, TN is true negative, and FP is false positive.

3. Results

3.1. Spectra patterns and NIR feature selection

The NIR and VIS/NIR spectral data of eggs were collected in transflectance mode and their overall spectra ranging between 700 and 2500 nm showed different absorption peaks across the level of SWM inclusion in the laying quails' diet. The eggs spectra pattern for NIR-benchtop

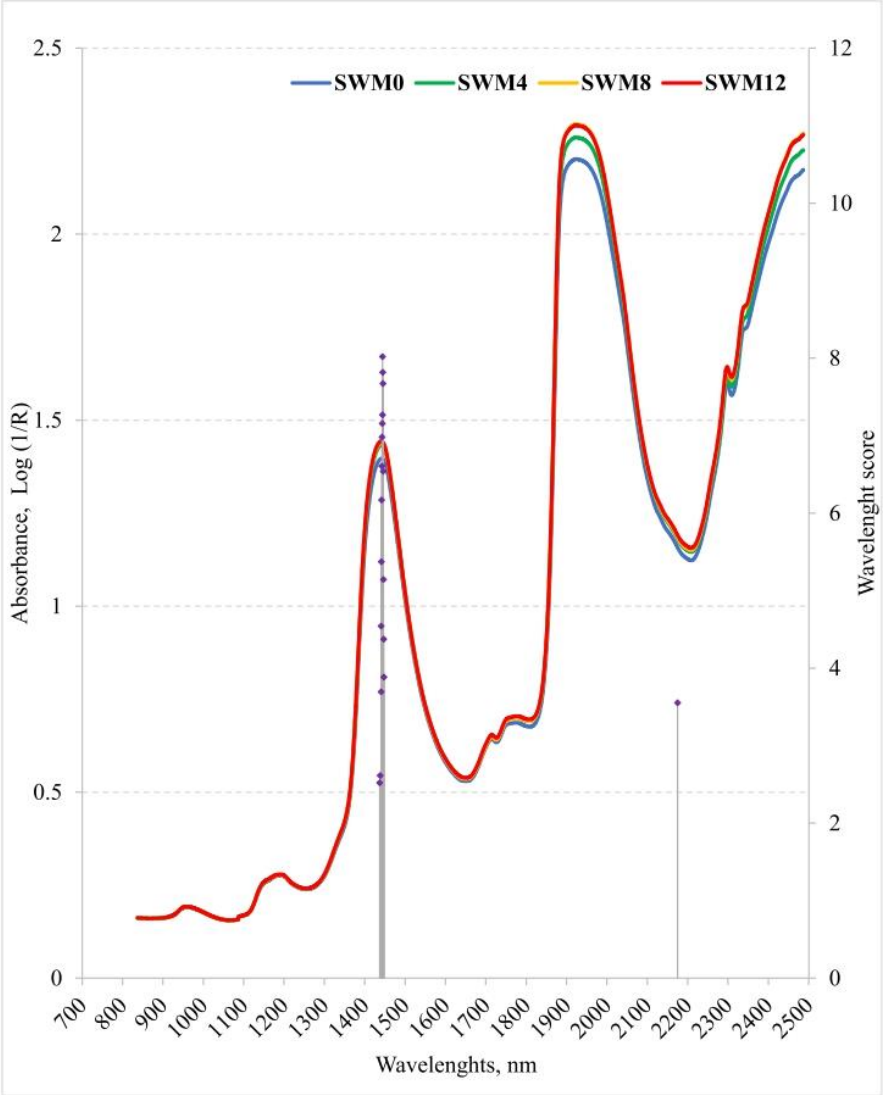

Fig. 2. NIR-benchtop. The mean NIR absorbance of the original spectra for eggs (yolk and albumen) of quails fed 4 dietary levels of silkworm meal (SWM 0–12% inclusion). Grey bars represent the informative wavelengths (wavelength score) selected by a random forest for predicting the SWM feeding groups.

device had three main absorption bands (1350–1600, 1850–2200 and 2300–2500 nm) and two slight bands (1150–1250 and 1700–1800 nm) with some differences in absorbance according to the four SWM dietary inclusion levels (Fig. 2). NIR spectral data collected using the portable device, an infrared technology with a limited range of investigation (from 900 to 1680 nm), showed a similar pattern of absorbance since the main peak was in the 1350–1600 nm region (Fig. 3). The use of the VIS/NIR spectrometer device evidenced a reduced absorbance by the edible portion of the egg with a marked absorption decrease from 700 to 900 nm and a main peak around the 950–1050 nm region where the SWM0 feeding group seemed to be lowest (Fig. 4). The consistency in the absorption peaks proves the feasibility of egg information extraction also in portable devices, especially in the case of the NIR-portable device. Among all the wavelengths investigated (3302, 389 and 192 for NIR-benchtop, NIR-portable and VIS/NIR-portable, respectively), the RF selection showed a lower percentage of significant wavelengths for benchtop (0.5%) than for the portable devices (7%); a relevant divergence due to the wide wavelength range referred to the NIR-benchtop instrument. Specifically, 28, 18 and 13 (for NIR-benchtop, NIR-portable and VIS/NIR-portable, respectively) of the selected RF wavelengths have been retained as significant in classifying quail table eggs according to the SWM feeding groups (Figs. 2–4).

3.2. NIR and VIS/NIR classification performance

A total of 120 quail eggs of the training set were subject to non-targeted profiling using NIR and VIS/NIR spectroscopy to identify the SWM level among four increasing levels of dietary inclusion of SWM (from 0 to 12% SWM). Based on the significative RF wavelengths of the training set, the results of the PLS-DA, KNN and SVM (linear and radial kernel) supervised models showed a limited predictive performance of spectroscopic instruments (Table S1, Table S2, Table S3 supplementary materials). With regard to feeding classes with the inclusion of SWM, MCC values lower than 0.52, 0.44 and 0.32 for NIR-benchtop, NIR-portable and VIS/NIR portable, respectively, were observed. To improve the NIR spectroscopy classification performance, a cut-off absence/presence of SWM in layers diet was performed. In detail, the predictive performance was calculated by comparing no (SWM0) vs. inclusion (SWM4-12), where the latter was a merged cluster of the rations formulated using SWM. Based on these premises, the NIR-benchtop instrument has proven to achieve the best classification performance along the algorithms (Table 1), meanwhile for the NIR-portable a slight reduction in the overall value of statistical indicators was observed (Table 2). The results for the VIS/NIR-portable spectrometer presented the lowest values of overall accuracy (0.70) and the lowest classification

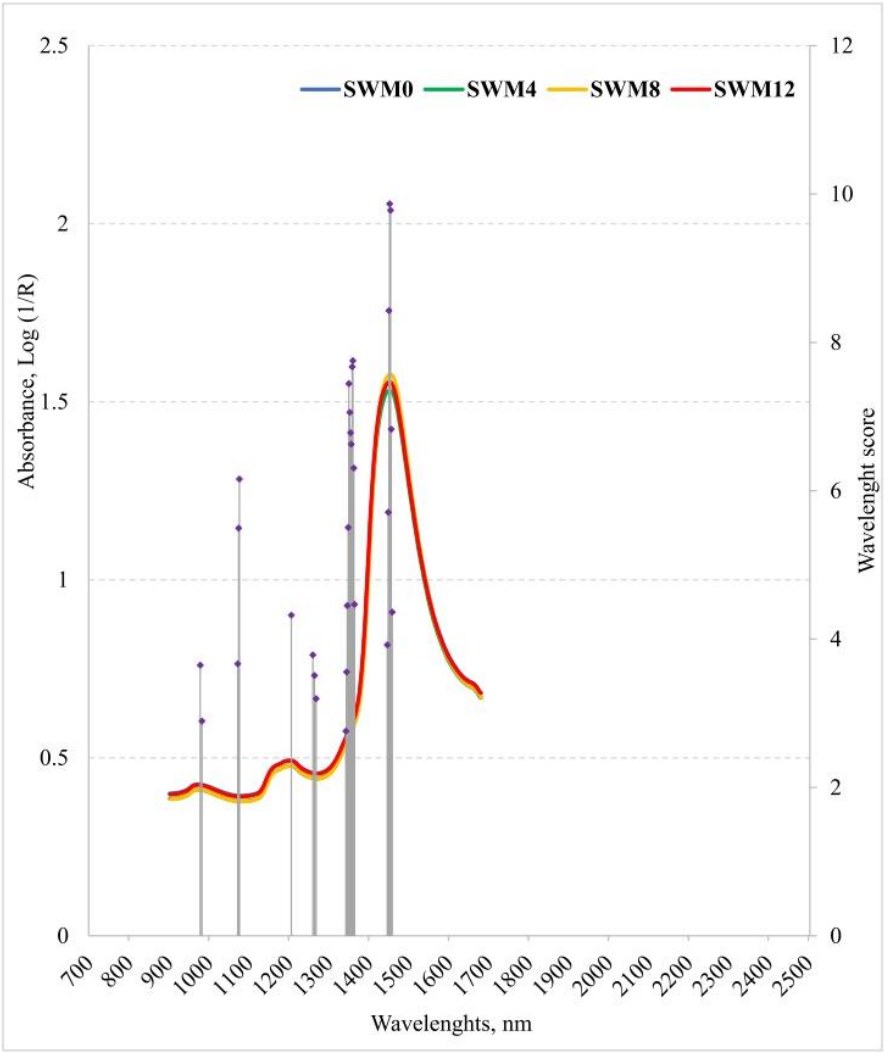

Fig. 3. NIR-portable. The mean NIR absorbance of the original spectra for eggs (yolk and albumen) of quails fed 4 dietary levels of silkworm meal (SWM 0–12% inclusion). Grey bars represent the informative wavelengths (wavelength score) selected by a random forest for predicting the SWM feeding groups.

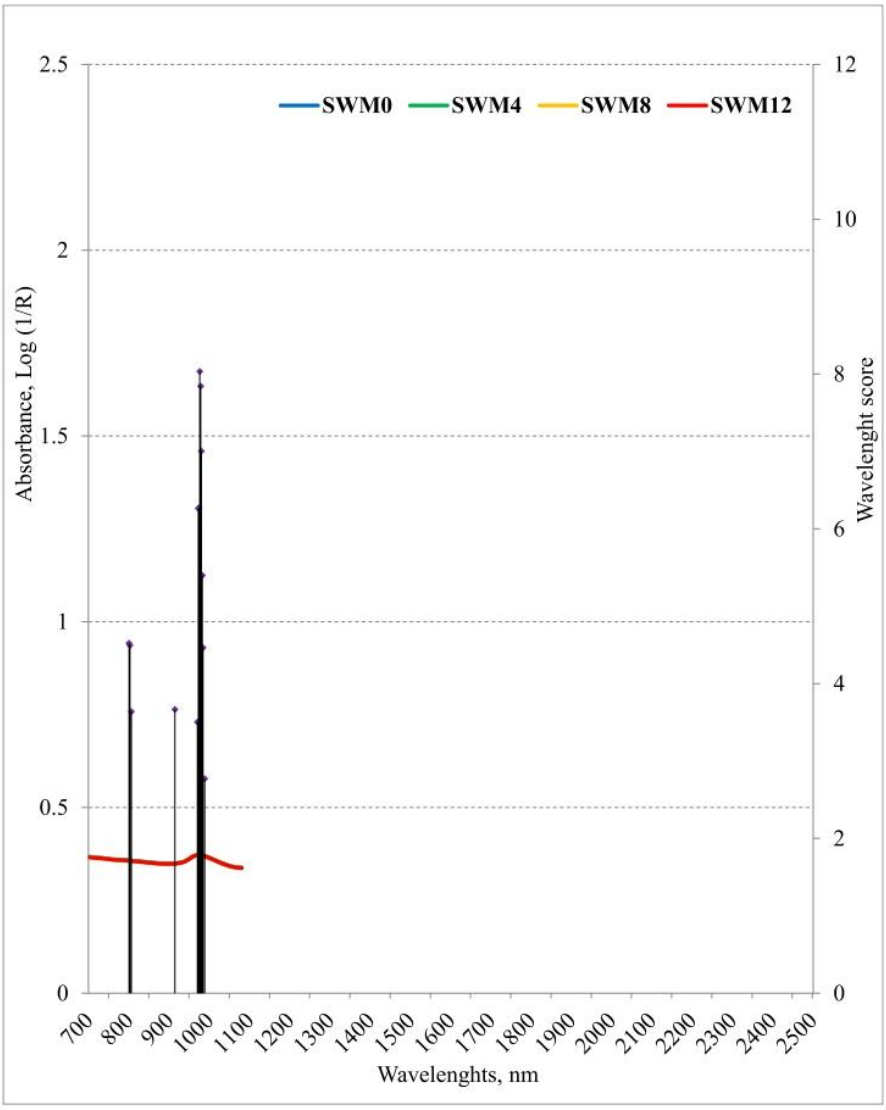

Fig. 4. VIS/NIR-portable. The mean NIR absorbance of the original spectra for eggs (yolk and albumen) of quails fed 4 dietary levels of silkworm meal (SWM 0–12% inclusion). Grey bars represent the informative wavelengths (wavelength score) selected by a random forest for predicting the SWM feeding groups.

capability (MCC <0.22) due to a high level of misclassification between samples indicating the combination of spectral and colour features did not improve the modelling results (Table S4, supplementary materials).

Among predictions obtained using the three machine learning methods on NIR and VIS/NIR data collected by the different devices on quail eggs, the absolute best classification performance was observed for the NIR-portable instrument coupled with a SVM-radial model. Indeed, this modelling combination was shown to be suitable as a fast and handheld screening approach reporting no misclassification of eggs from quail fed with or without the insect-derived protein source because the highest accuracy of prediction (accuracy and MCC of 1.00). However, the NIR-benchtop instrument coupled with the KNN algorithm was also proven to be accurate for egg feeding system detection since it provided a highly reliable prediction (accuracy of 0.98 and MCC of 0.94) with only one misclassified sample. The PLS-DA model showed the poorest predictive capabilities confirmed by high levels of misclassification among samples in both NIR-benchtop (MCC of 0.82) and NIR-portable (MCC of 0.60).

4. Discussion

The present research was designed to verify if increasing inclusion of SWM in quails' feed would be rapidly detected in eggs throughout an untargeted multivariate modelling approach based on NIR spectroscopy and chemometrics. To ensure a feasible at-line control of the productive process and a simultaneous fast qualitative characterisation of the end-product (egg and/or egg-derivatives), the effectiveness predictive capability of a handheld NIR instrument was also carried out. Despite a moderate sample size, as reported in literature (Nakaguchi & Ahamed, 2022), the investigated dataset could be considered suitable to prove the possibility of using ML coupled with VIS/NIR or NIR to solve a discriminant challenge related to the use of SWM as protein replacer in feeding quail's egg producer. Even thought, the inference capacity of ML methods to recognize patterns is generally proportional to the size of the dataset, intentional relative small collection focusing on a specific experimental factor could be able to produce appropriate standard statistical inferences (Faraway & Augustin, 2018). Among the more computational innovative ML algorithms, the study focused on SVM and KNN. SVM is proposed to separate multi-classes and try to find the best

Table 1
NIR-benchtop - Performance of the supervised models in classifying eggs from quails fed without (SWM0) or with SWM (SWM4-12) by external validation.

PLS-DA	Accuracy = 0.92			Actual	
Predicted	Sensitivity	Specificity	MCC	SWM0	SWM4-12
SWM0	1.00	0.89	0.82	12	4
SWM4-12	0.89	1.00	0.82	0	32
KNN	Accuracy = 0.98			Actual	
Predicted	Sensitivity	Specificity	MCC	SWM0	SWM4-12
SWM0	0.92	1.00	0.94	11	0
SWM4-12	1.00	0.92	0.94	1	36
SVM-linear	Accuracy = 0.96			Actual	
Predicted	Sensitivity	Specificity	MCC	SWM0	SWM4-12
SWM0	0.83	1.00	0.89	10	0
SWM4-12	1.00	0.83	0.89	2	36
SVM-radial	Accuracy = 0.94			Actual	
Predicted	Sensitivity	Specificity	MCC	SWM0	SWM4-12
SWM0	0.75	1.00	0.83	9	0
SWM4-12	1.00	0.75	0.83	3	36

Table 2
NIR-portable - Performance of the supervised models in classifying eggs from quails fed without (SWM0) or with SWM (SWM4-12) by external validation.

PLS-DA	Accuracy = 0.77			Actual	
Predicted	Sensitivity	Specificity	MCC	SWM0	SWM4-12
SWM0	1.00	0.69	0.60	12	11
SWM4-12	0.69	1.00	0.60	0	25
KNN	Accuracy = 0.90			Actual	
Predicted	Sensitivity	Specificity	MCC	SWM0	SWM4-12
SWM0	0.58	1.00	0.72	7	0
SWM4-12	1.00	0.58	0.72	5	36
SVM-linear	Accuracy = 0.98			Actual	
Predicted	Sensitivity	Specificity	MCC	SWM0	SWM4-12
SWM0	0.92	1.00	0.94	11	0
SWM4-12	1.00	0.92	0.94	1	36
SVM-radial	Accuracy = 1.00			Actual	
Predicted	Sensitivity	Specificity	MCC	SWM0	SWM4-12
SWM0	1.00	1.00	1.00	12	0
SWM4-12	1.00	1.00	1.00	0	36

line on hyper-planes for classification data for both classification and regression (Sehirli & Arslan, 2022). The KNN model does not require any assumption about the underlying data distribution and linearity between dependent/independent variables) and could be implemented at a low computational cost.

Portable NIR spectrometers demonstrated to be a low-cost and a

viable alternative to benchtop tools showing the advantage to be implemented on production lines and easily transported for *in situ* quality monitoring along the different steps of egg supply chain (Lanza et al., 2021). Even though NIR demonstrated a notable capability in the direct detection of insects in cereals (Biancolillo et al., 2019), the indirect assessment of insect presence (silkworm meal) in laying quails' diet throughout the spectroscopic analyses of eggs, showed a moderate capability of the tested VIS/NIR and NIR devices. This finding was probably due to the limited range of dietary SWM inclusion, which not induce relevant physical and chemical changes of the yolk and albumen mixture. Thus, the similarities among the spectral patterns for the SWM-classes resulted in poor predictive performance for all the spectroscopic devices and ML model's combinations. Therefore, the assessment of the prediction in external validation was performed also by a binary approach like SWM absence (SWM0) or presence (SWM4-12). Based on this fit-cut-off purpose, both NIR-benchtop and NIR-portable devices reported satisfactory classification performance in the external validation on the independent set, especially if combined with KNN and SVM models. The lower predictive accuracy of PLS-DA algorithm observed in this study might be due to the interference and overlapping of some uninformative spectral variables, even though a preliminary RF features selection was carried out. SVM and KNN are more complex and flexible supervised models reporting better classification performance due to the identification of the best numerical values to be assigned to building parameters (i.e., *C*, γ, and ε for SVM) of the classification algorithm, even with unbalanced experimental sample sets (Varrà et al., 2022). In advanced ML techniques such as SVM and KNN, the proper selection of wavelengths to obtain a small subset with lower sensitivity to non-linearities is usually effective in improving the performance of the models (Coronel-Reyes et al., 2018). As suggested from the literature (Zhang et al., 2022), the classifier models based on an SVM approach (linear or radial) seemed to be better than the KNN one at recognising a correct specimen assignment within the actual class, especially when predicting independent samples in test set. However, the choice of the more appropriate chemometric approach is still a topic of debate. A study on the application of a portable NIR reflective device focusing on the eggs' freshness prediction showed similar classification performance among the PLS-DA and SVM algorithms (Brasil et al., 2022).

Despite portable tools being comprised of comparatively basic spectroscopic components, which must be resized in order to miniaturise the device, the results highlighted a similar discriminative performance between the two devices based on NIR absorption (Zhu et al., 2022). Instead, for the VIS-NIR portable tool, a lower classification capacity was observed that might be explained by the size of the measuring head, the detector type, the distinctive optical properties of the VIS region and its lower absorption rate. Likely, the combination between the reduction in the spectral range (700–1080 nm) and lower sensors performances affected the prediction ability of the VIS/NIR-portable device (Lanza et al., 2021). Given the poor predictive capacity and to facilitate data interpretation, the results related to the latter instrument are available in the supplementary materials (Table S4) and the discussion below will focus only on the two NIR tools.

A preliminary feature selection based on a RF spectral NIR variable selection was made to reduce the intrinsic complexity of NIR spectra, an essential step for ML methods which can exhibit a decrease in accuracy when the number of variables is significantly higher than optimal. However, the interpretation of the interaction between infrared radiation and chemical traits of the investigated organic samples (eggs) still remained a limiting factor. The broad absorption trend for NIR or VIS-NIR spectra contain underneath a large number of overlapped bands making it a challenge to define a clear fingerprinting of the nominal chemical composition along the samples of the investigated classes. Based on spectra NIR line shape, peaks represent the result of vibrational transitions associated with chemical bonds (OH-, CH-, NH- and CO-) in most organic molecules; however, while most often the meaningful wavelengths for the classification models can be determined using various chemometric methods, their chemical attribution is not easy or directly interpretable in this infrared region (Beć et al., 2021).

In general, the devices showed similar trends among spectral patterns of eggs from laying quails fed with different SWM inclusion levels. However, eggs laid by quails fed the control diet yielded a spectrum with lower absorbance values, results more appreciable in spectra obtained in the NIR-benchtop (Fig. 2) and VIS/NIR-portable (Fig. 4). The most informative bands referred to 1150–1300 and 1350–1600 nm for both NIR instruments, and over 1850 nm in the case of benchtop, are related to the overtone and combination among the main functional groups such as OH-, CH-, NH- and CO-. These wavelength ranges were identified to exert the highest discriminative power between the feeding systems, probably due to the effect of the SWM on the molecular structure and spatial configuration of proteins and lipids stored in egg. Despite none RF was recorded at 1150 nm, the low peak characterizing these spectra region in both NIR devices has already been associated to the second overtone of C–H absorption of pure fatty acids containing cis double bonds (C═O and C–H) like in oleic acid (Kaufmann et al., 2019). This spectral outcome suggests that different levels of inclusion of SWM might interfere with the de-novo FA synthesis. Particularly for the benchtop-NIR instrument, more marketable differences in absorption levels among experimental groups were observed in the peak around 1400 nm associated with O–H elongation of water content, N–H (aromatic amines), and C–H combination tones (Torrico et al., 2022), which are light scattering dissimilarities not easily traceable to shift of specific molecules (i.e., proteins) and their water H-bonding with other molecules.

This hypothesis of changes in the egg nutrients chemical properties linked to the dietary inclusion of SWM might be supported by the relevant differences in absorption trends depicted for the benchtop-NIR (Fig. 2) over 1950 nm, a spectral region associated with many OH combination tone of water-absorbing bands and C–H combination of fatty acids (Prieto et al., 2009). Probably, the addition of SWM in the quails' diet caused changes in the water-holding capacity and protein functionality in the egg that should be carefully investigated. Considering the restricted pool of the selected RF informative wavelengths, for the NIR-portable, those recorded around 1340 nm may be associated with the second aromatic C–H elongation overtone, mainly related to CH_2 and CH_3 from the saturated fatty acids (Brasil et al., 2022; Cruz-Tirado et al., 2021), while the RF at 1205 nm might be associated with the C–H stretching second overtone of CH_2 and CH (Brasil et al., 2022). With both NIR instruments, the RF recorded around 1450 nm referred to the OH first overtone (1450 nm), while the benchtop-related RF at 2220 nm seemed to be linked to water-absorbing bands and C–H of specific fatty acids (Prieto et al., 2009). With regard to the VIS/NIR-portable, many RF are grouped in the water region around 970 nm generally associated with the O–H stretching.

The findings and tuned chemometric parameters cannot be considered the final endpoint but the applicability proof of the proposed spectroscopic methods coupled with SVM and KNN as pattern recognition models. Moreover, future studies should investigate additional variability sources as the breed, oviposition capability and layers management, which could affect the NIR or VIS/NIR spectra outcomes, to increase the robustness of classification through wider datasets. Additionally, the relationship between dietary insect-derived and chemical composition of eggs should be also explored. Furthermore, the application of other spectroscopic devices (e.g., MicroNIRS) should be tested to better design innovative specific analytical tools (e.g., monochromator, a sample holder, interferometer, photoelectric detector, etc.) for the at-line monitoring along the egg supply chain.

5. Conclusions

The study highlighted the feasibility of NIR spectroscopy combined with SVM or KNN algorithms as rapid and screening online approach to differentiate quail table eggs according to the inclusion of silkworm

meal into layers diet. Overall, the results demonstrated that a random forest (RF) spectral NIR variable selection improved the classification performance and provided reliable results for the insect-in-diet identification avoiding useless and interfering information. Results revealed an inconsistent predictive capacity of the VIS-NIR spectrometer to detect the use of insect meal into laying quails' diet, probably because at the visible wavelengths, accuracy of classification models is reduced. The NIR-portable tool showed comparable classification performance as its benchtop counterpart, but with the advantage of being an appealing alternative to benchtop units for its low cost, flexibility, ruggedness, compactness, robustness, and field applications. Summarising, the research highlights the potential of NIR data processed through a SVM or KNN machine learning methods to capture the spectroscopy fingerprinting linked to the dietary inclusion of SWM, suggesting that this fast chemometric evaluation may allow for the on-line inspection of insect-based feed along the egg supply chain.

Funding

This work was supported by University of Padova (call 2019, BIRD project number 193891 – OneHealth).

CRediT authorship contribution statement

Ilaria Lanza: Investigation, Data curation, Methodology, Writing – original draft, Writing – review & editing. **Sarah Currò:** Investigation, Writing – original draft, Writing – review & editing. **Severino Segato:** Supervision, Conceptualization, Visualization, Writing – original draft, Writing – review & editing. **Lorenzo Serva:** Software, Formal analysis, Data curation, Writing – review & editing. **Marco Cullere:** Investigation, Writing – original draft. **Paolo Catellani:** Investigation. **Luca Fasolato:** Investigation. **Daniela Pasotto:** Investigation. **Antonella Dalle Zotte:** Conceptualization, Resources, Funding acquisition, Project administration.

Declaration of competing interest

The authors declare that they have no known competing financial interests or personal relationships that could have appeared to influence the work reported in this paper.

Data availability

Data will be made available on request.

Appendix A. Supplementary data

Supplementary data to this article can be found online at https://doi.org/10.1016/j.foodcont.2022.109589.

References

Beć, K. B., Grabska, J., Plewka, N., & Huck, C. W. (2021). Insect protein content analysis in handcrafted fitness bars by nir spectroscopy. Gaussian process regression and data fusion for performance enhancement of miniaturized cost-effective consumer-grade sensors. *Molecules, 26*(21). https://doi.org/10.3390/molecules26216390

Biancolillo, A., Firmani, P., Bucci, R., Magrì, A., & Marini, F. (2019). NIR spectroscopy vs. food pests: The case of stored rice. *NIR News, 30*(5–6), 18–21. https://doi.org/10.1177/0960336019854284

Bisutti, V., Merlanti, R., Serva, L., Lucatello, L., Mirisola, M., Balzan, S., Tenti, S., Fontana, F., Trevisan, G., Montanucci, L., Contiero, B., Segato, S., & Capolongo, F. (2019). Multivariate and machine learning approaches for honey botanical origin authentication using near infrared spectroscopy. *Journal of Near Infrared Spectroscopy*. https://doi.org/10.1177/0967033518824765

Brasil, Y. L., Cruz-Tirado, J. P., & Barbin, D. F. (2022). Fast online estimation of quail eggs freshness using portable NIR spectrometer and machine learning. *Food Control, 131*(July 2021), Article 108418. https://doi.org/10.1016/j.foodcont.2021.108418

Coronel-Reyes, J., Ramirez-Morales, I., Fernandez-Blanco, E., Rivero, D., & Pazos, A. (2018). Determination of egg storage time at room temperature using a low-cost NIR spectrometer and machine learning techniques. *Computers and Electronics in Agriculture, 145*(September 2017), 1–10. https://doi.org/10.1016/j.compag.2017.12.030

Cruz-Tirado, J. P., Lucimar da Silva Medeiros, M., & Barbin, D. F. (2021). On-line monitoring of egg freshness using a portable NIR spectrometer in tandem with machine learning. *Journal of Food Engineering, 306*(October 2020), Article 110643. https://doi.org/10.1016/j.jfoodeng.2021.110643

Currò, S., Balzan, S., Serva, L., Boffo, L., Ferlito, J. C., Novelli, E., & Fasolato, L. (2021). Fast and green method to control frauds of geographical origin in traded cuttlefish using a portable infrared reflective instrument. *Foods, 10*(8). https://doi.org/10.3390/foods10081678

Currò, S., Fasolato, L., Serva, L., Boffo, L., Ferlito, J. C., Novelli, E., & Balzan, S. (2022). Use of a portable near-infrared tool for rapid on-site inspection of freezing and hydrogen peroxide treatment of cuttlefish (Sepia officinalis). *Food Control, 132*. https://doi.org/10.1016/j.foodcont.2021.108524. August 2021.

Dalle Zotte, A. (2021). Meat quality of poultry fed with diets supplemented with insects: A review. *IOP Conference Series: Earth and Environmental Science, 854*(1). https://doi.org/10.1088/1755-1315/854/1/012019

Dalle Zotte, A., Singh, Y., Michiels, J., & Cullere, M. (2019). Black soldier fly (Hermetia illucens) as dietary source for laying quails: Live performance, and egg physico-chemical quality, sensory profile and storage stability. *Animals, 9*(3). https://doi.org/10.3390/ani9030115

European Commission. (2018). *EU regulation 2021/1372*. 2016(68), 48–119.

Faraway, J. J., & Augustin, N. H. (2018). When small data beats big data. *Statistics & Probability Letters, 136*, 142–145. https://doi.org/10.1016/j.spl.2018.02.031

Gasco, L., Acuti, G., Bani, P., Dalle Zotte, A., Danieli, P. P., De Angelis, A., Fortina, R., Marino, R., Parisi, G., Piccolo, G., Pinotti, L., Prandini, A., Schiavone, A., Terova, G., Tulli, F., & Roncarati, A. (2020). Insect and fish by-products as sustainable alternatives to conventional animal proteins in animal nutrition. *Italian Journal of Animal Science, 19*(Issue 1). https://doi.org/10.1080/1828051X.2020.1743209

Hawkey, K. J., Lopez-Viso, C., Brameld, J. M., Parr, T., & Salter, A. M. (2021). Insects: A potential source of protein and other nutrients for feed and food. *In Annual Review of Animal Biosciences, 9*. https://doi.org/10.1146/annurev-animal-021419-083930

Kaufmann, K. C., Favero, F. de F., de Vasconcelos, M. A. M., Godoy, H. T., Sampaio, K. A., & Barbin, D. F. (2019). Portable NIR spectrometer for prediction of palm oil acidity. *Journal of Food Science, 84*(3). https://doi.org/10.1111/1750-3841.14467

Lanza, I., Conficoni, D., Balzan, S., Cullere, M., Fasolato, L., Serva, L., Contiero, B., Trocino, A., Marchesini, G., Xiccato, G., Novelli, E., & Segato, S. (2021). Assessment of chicken breast shelf life based on bench-top and portable near-infrared spectroscopy tools coupled with chemometrics. *Food Quality and Safety, 5*. https://doi.org/10.1093/fqsafe/fyaa032

Lin, H., Zhao, J., Sun, L., Chen, Q., & Zhou, F. (2011). Freshness measurement of eggs using near infrared (NIR) spectroscopy and multivariate data analysis. *Innovative Food Science & Emerging Technologies, 12*(2), 182–186. https://doi.org/10.1016/j.ifset.2011.01.008

Lippi, N., Predieri, S., Chieco, C., Daniele, G. M., Cianciabella, M., Magli, M., Maistrello, L., & Gatti, E. (2021). Italian consumers' readiness to adopt eggs from insect-fed hens. *Animals, 11*(11). https://doi.org/10.3390/ani11113278

Loffredi, E., Grassi, S., & Alamprese, C. (2021). Spectroscopic approaches for non-destructive shell egg quality and freshness evaluation: Opportunities and challenges. *Food Control, 129*. https://doi.org/10.1016/j.foodcont.2021.108255

Marcot, B. G., & Hanea, A. M. (2021). What is an optimal value of k in k-fold cross-validation in discrete Bayesian network analysis? *Computational Statistics, 36*(3), 2009–2031. https://doi.org/10.1007/s00180-020-00999-9

Mehmood, T., Liland, K. H., Snipen, L., & Sæbø, S. (2012). A review of variable selection methods in Partial Least Squares Regression. *Chemometrics and Intelligent Laboratory Systems, 118*, 62–69. https://doi.org/10.1016/j.chemolab.2012.07.010

Miah, M. Y., Singh, Y., Cullere, M., Tenti, S., & Dalle Zotte, A. (2020). Effect of dietary supplementation with full-fat silkworm (Bombyx mori L.) chrysalis meal on growth performance and meat quality of Rhode Island Red × Fayoumi crossbred chickens. *Italian Journal of Animal Science, 19*(1), 447–456. https://doi.org/10.1080/1828051X.2020.1752119

Nakaguchi, V. M., & Ahamed, T. (2022). Fast and non-destructive quail egg freshness assessment using a thermal camera and deep learning-based air cell detection algorithms for the revalidation of the expiration date of eggs. *Sensors, 22*(20). https://doi.org/10.3390/s22207703

Prieto, N., Roehe, R., Lavín, P., Batten, G., & Andrés, S. (2009). Application of near infrared reflectance spectroscopy to predict meat and meat products quality: A review. *Meat Science, 83*(Issue 2). https://doi.org/10.1016/j.meatsci.2009.04.016

Secci, G., Bovera, F., Nizza, S., Baronti, N., Gasco, L., Conte, G., Serra, A., Bonelli, A., & Parisi, G. (2018). Quality of eggs from Lohmann Brown Classic laying hens fed black soldier fly meal as substitute for soya bean. *Animal, 12*(10), 2191–2197. https://doi.org/10.1017/S1751731117003603

Segato, S., Merlanti, R., Bisutti, V., Montanucci, L., Serva, L., Lucatello, L., Mirisola, M., Contiero, B., Conficoni, D., Balzan, S., Marchesini, G., & Capolongo, F. (2019). Multivariate and machine learning models to assess the heat effects on honey physicochemical, colour and NIR data. *European Food Research and Technology, 245*(10), 2269–2278. https://doi.org/10.1007/s00217-019-03332-x

Sehirli, E., & Arslan, K. (2022). An application for the classification of egg quality and haugh unit based on characteristic egg features using machine learning models. *Expert Systems with Applications, 205*(February), Article 117692. https://doi.org/10.1016/j.eswa.2022.117692

Spartano, S., & Grasso, S. (2021). UK consumers' willingness to try and pay for eggs from insect-fed hens. *Future Foods, 3*. https://doi.org/10.1016/j.fufo.2021.100026

Torrico, D., Gonzalez Viejo, C., Christiaan Hoffman, L., Ni, D., Dayananda, B., Abdul Ghafar, N., & Cozzolino, D. (2022). *Unscrambling the Provenance of Eggs by Combining*

Chemometrics and Near-Infrared Reflectance Spectroscopy. https://doi.org/10.3390/s22134988

Varrà, M. O., Ghidini, S., Fabrile, M. P., Ianieri, A., & Zanardi, E. (2022). Country of origin label monitoring of musky and common octopuses (Eledone spp. and Octopus vulgaris) by means of a portable near-infrared spectroscopic device. *Food Control, 138*(April). https://doi.org/10.1016/j.foodcont.2022.109052

Zhang, X., Gao, Z., Yang, Y., Pan, S., Yin, J., & Yu, X. (2022). Rapid identification of the storage age of dried tangerine peel using a hand-held near infrared spectrometer and machine learning. *Journal of Near Infrared Spectroscopy, 30*(1), 31–39. https://doi.org/10.1177/09670335211057232

Zhu, C., Fu, X., Zhang, J., Qin, K., & Wu, C. (2022). Review of portable near infrared spectrometers: Current status and new techniques. *Journal of Near Infrared Spectroscopy, 30*(2), 51–66. https://doi.org/10.1177/09670335211030617

Appendix A.

Supplementary data

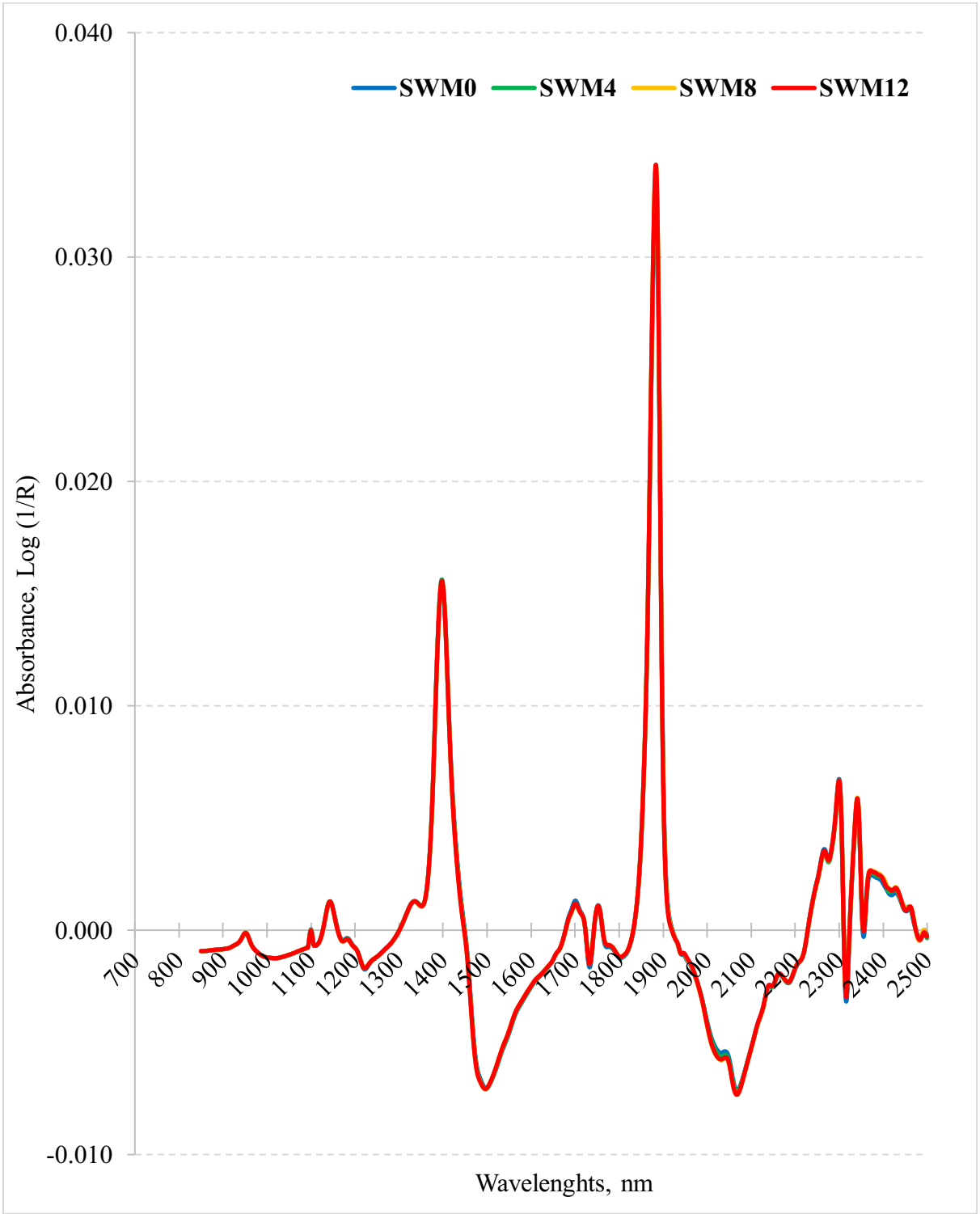

Fig. 1S. NIR-benchtop. The mean NIR absorbance curves after pre-treatment for eggs (yolk and albumen) of quails fed 4 dietary levels of silkworm meal (SWM 0-12% inclusion).

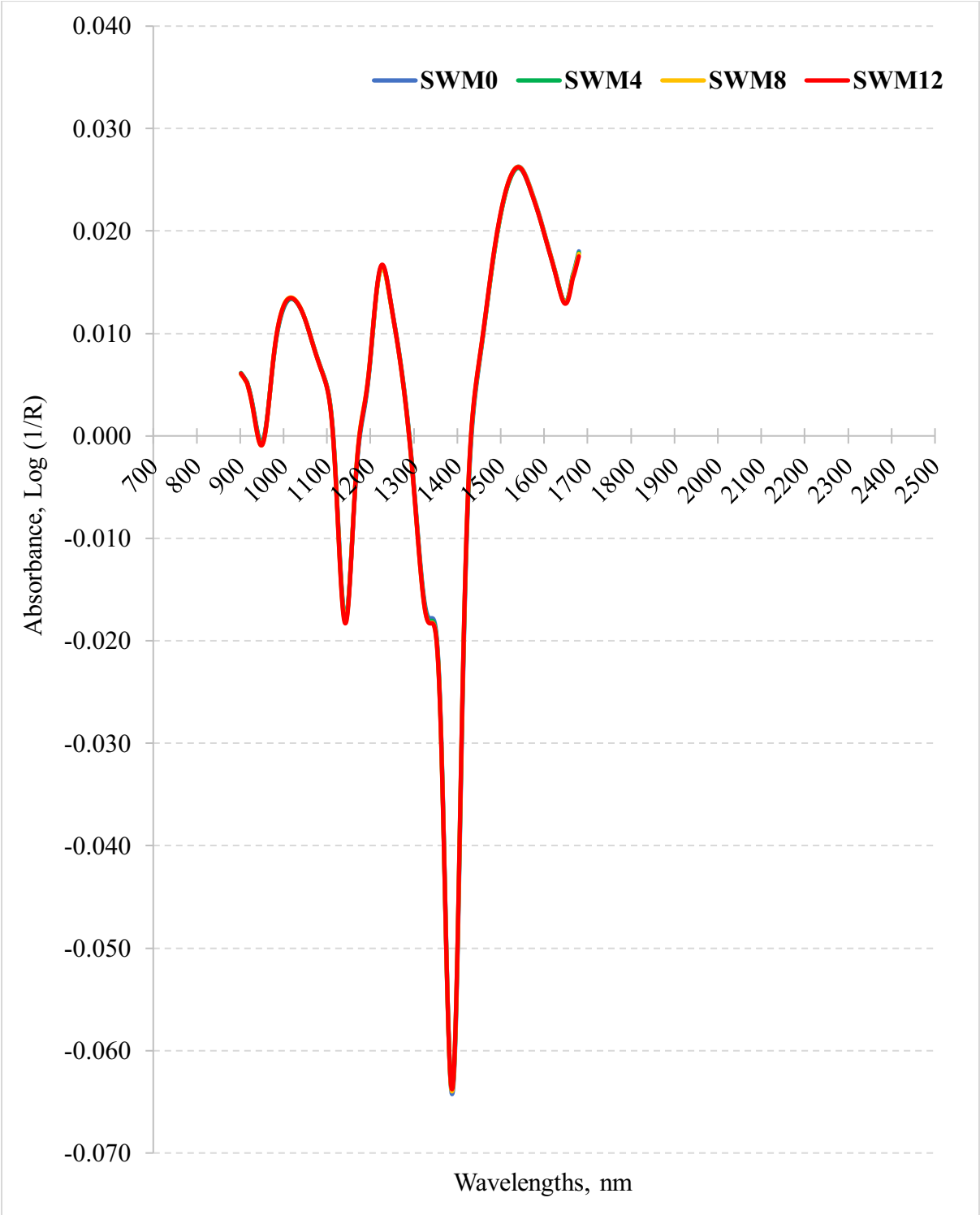

Fig. 2S. NIR-portable. The mean NIR absorbance curves after pre-treatment for eggs (yolk and albumen) of quails fed 4 dietary levels of silkworm meal (SWM 0-12% inclusion).

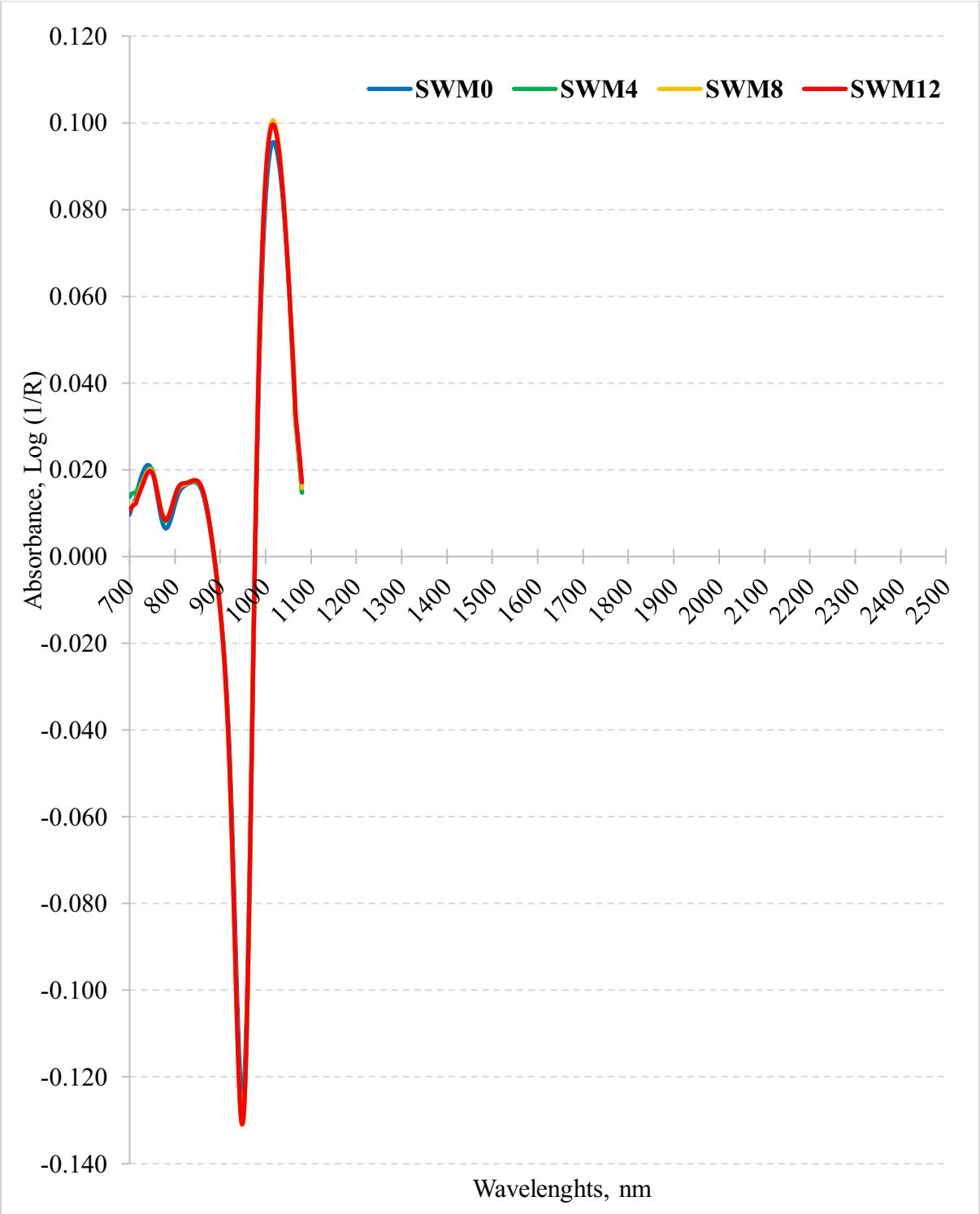

Fig. 3S. VIS/NIR-portable. The mean NIR absorbance curves after pre-treatment for eggs (yolk and albumen) of quails fed 4 dietary levels of silkworm meal (SWM 0-12% inclusion).

Table 1S. NIR-benchtop – Performance of the supervised models in classifying eggs from quails fed increasing levels of SWM by external validation.

PLS-DA	Accuracy = 0.76			Actual			
Predicted	Sensitivity	Specificity	MCC	SWM0	SWM4	SWM8	SWM12
SWM0	1.00	0.89	0.82	12	3	1	0
SWM4	0.17	0.83	0.00	0	2	5	1
SWM8	0.33	0.75	0.08	0	5	4	4
SWM12	0.58	0.89	0.49	0	2	2	7
KNN	Accuracy = 0.79			Actual			
Predicted	Sensitivity	Specificity	MCC	SWM0	SWM4	SWM8	SWM12
SWM0	0.92	1.00	0.94	11	0	0	0
SWM4	0.83	0.75	0.52	1	10	8	0
SWM8	0.17	0.78	-0.06	0	1	2	7
SWM12	0.42	0.92	0.39	0	1	2	5
SVM-linear	Accuracy = 0.79			Actual			
Predicted	Sensitivity	Specificity	MCC	SWM0	SWM4	SWM8	SWM12
SWM0	0.83	1.00	0.89	10	0	0	0
SWM4	0.83	0.67	0.43	2	10	9	1
SWM8	0.25	0.81	0.06	0	1	3	6
SWM12	0.42	0.97	0.51	0	1	0	5
SVM-radial	Accuracy = 0.77			Actual			
Predicted	Sensitivity	Specificity	MCC	SWM0	SWM4	SWM8	SWM12
SWM0	0.75	1.00	0.83	9	0	0	0
SWM4	0.83	0.64	0.41	3	10	9	1
SWM8	0.25	0.78	0.03	0	1	3	7
SWM12	0.33	0.97	0.43	0	1	0	4

PLS-DA, partial least squares-discriminant analysis; KNN, K-nearest neighbour; SVM-linear, support vector machine-linear; SVM-radial, support vector machine-radial; MCC, Matthew correlation coefficient; SWM0-SWM12, dietary inclusion (% on dry matter basis) of 0, 4, 8, 12 of silkworm meal (SWM).

Table 2S. NIR-portable – Performance of the supervised models in classifying eggs from quails fed increasing levels of SWM by external validation.

PLS-DA	Accuracy = 0.71			Actual			
Predicted	Sensitivity	Specificity	MCC	SWM0	SWM4	SWM8	SWM12
SWM0	1.00	0.69	0.60	12	5	6	0
SWM4	0.00	1.00	n.d.	0	0	0	0
SWM8	0.25	0.69	-0.05	0	4	3	7
SWM12	0.42	0.83	0.26	0	3	3	5
KNN	Accuracy = 0.75			Actual			
Predicted	Sensitivity	Specificity	MCC	SWM0	SWM4	SWM8	SWM12
SWM0	0.58	1.00	0.72	7	0	0	0
SWM4	0.58	0.75	0.31	5	7	4	0
SWM8	0.67	0.61	0.24	0	4	8	10
SWM12	0.17	0.97	0.25	0	1	0	2
SVM-linear	Accuracy = 0.75			Actual			
Predicted	Sensitivity	Specificity	MCC	SWM0	SWM4	SWM8	SWM12
SWM0	0.92	1.00	0.94	11	0	0	0
SWM4	0.58	0.78	0.34	1	7	7	0
SWM8	0.42	0.61	0.02	0	3	5	11
SWM12	0.08	0.94	0.05	0	2	0	1
SVM-radial	Accuracy = 0.76			Actual			
Predicted	Sensitivity	Specificity	MCC	SWM0	SWM4	SWM8	SWM12
SWM0	1.00	1.00	1.00	12	0	0	0
SWM4	0.67	0.81	0.44	0	8	7	0
SWM8	0.25	0.67	-0.08	0	2	3	10
SWM12	0.17	0.89	0.07	0	2	2	2

PLS-DA, partial least squares-discriminant analysis; KNN, K-nearest neighbour; SVM-linear, support vector machine-linear; SVM-radial, support vector machine-radial; MCC, Matthew correlation coefficient; SWM0-SWM12, dietary inclusion (% on dry matter basis) of 0, 4, 8, 12 of silkworm meal (SWM).

Table 3S. VIS/NIR-portable – Performance of the supervised models in classifying eggs from quails fed increasing levels of SWM by external validation.

PLS-DA	Accuracy = 0.65			Actual			
Predicted	Sensitivity	Specificity	MCC	SWM0	SWM4	SWM8	SWM12
SWM0	0.33	0.78	0.11	4	3	3	2
SWM4	0.08	0.72	-0.20	8	1	2	0
SWM8	0.00	0.97	-0.08	0	0	0	1
SWM12	0.75	0.58	0.29	0	8	7	9
KNN	Accuracy = 0.70			Actual			
Predicted	Sensitivity	Specificity	MCC	SWM0	SWM4	SWM8	SWM12
SWM0	0.17	0.89	0.07	2	0	1	3
SWM4	0.33	0.75	0.08	7	4	2	0
SWM8	0.67	0.69	0.32	3	4	8	4
SWM12	0.42	0.86	0.30	0	4	1	5
SVM-linear	Accuracy = 0.67			Actual			
Predicted	Sensitivity	Specificity	MCC	SWM0	SWM4	SWM8	SWM12
SWM0	0.33	0.86	0.22	4	0	2	3
SWM4	0.25	0.75	0.00	6	3	3	0
SWM8	0.25	0.81	0.06	0	4	3	3
SWM12	0.50	0.69	0.18	2	5	4	6
SVM-radial	Accuracy = 0.67			Actual			
Predicted	Sensitivity	Specificity	MCC	SWM0	SWM4	SWM8	SWM12
SWM0	0.17	0.83	0.00	2	1	1	4
SWM4	0.25	0.67	-0.08	8	3	4	0
SWM8	0.50	0.78	0.26	2	3	6	3
SWM12	0.42	0.83	0.26	0	5	1	5

PLS-DA, partial least squares-discriminant analysis; KNN, K-nearest neighbour; SVM-linear, support vector machine-linear; SVM-radial, support vector machine-radial; MCC, Matthew correlation coefficient; SWM0-SWM12, dietary inclusion (% on dry matter basis) of 0, 4, 8, 12 of silkworm meal (SWM).

Table 4S. VIS/NIR-portable – Performance of the supervised models in classifying eggs from quails fed without (SWM0) or with SWM (SWM4-12) by external validation.

PLSDA	Accuracy = 0.67			Actual	
Predicted	Sensitivity	Specificity	MCC	SWM0	SWM4-12
SWM0	0.33	0.78	0.11	4	8
SWM4-12	0.78	0.33	0.11	8	28
KNN	Accuracy = 0.71			Actual	
Predicted	Sensitivity	Specificity	MCC	SWM0	SWM4-12
SWM0	0.17	0.89	0.07	2	4
SWM4-12	0.89	0.17	0.07	10	32
SVM-linear	Accuracy = 0.73			Actual	
Predicted	Sensitivity	Specificity	MCC	SWM0	SWM4-12
SWM0	0.33	0.86	0.22	4	5
SWM4-12	0.86	0.33	0.22	8	31
SVM-radial	Accuracy = 0.67			Actual	
Predicted	Sensitivity	Specificity	MCC	SWM0	SWM4-12
SWM0	0.17	0.83	0.00	2	6
SWM4-12	0.83	0.17	0.00	10	30

PLS-DA, partial least squares-discriminant analysis; KNN, K-nearest neighbour; SVM-linear, support vector machine-linear; SVM-radial, support vector machine-radial; MCC, Matthew correlation coefficient; SWM0, no dietary inclusion of silkworm meal; SWM4-12, merging of feeding groups with dietary inclusion of silkworm meal.

CHAPTER 6

Use of GC-MS and ^{1}H NMR Low-Level Data Fusion as an Advanced and Comprehensive Metabolomic Approach to Discriminate Milk From Dairy Chains Based on Different Types of Forage

---

Ilaria Lanza[1], Veronica Lolli[2], Severino Segato[1], Augusta Caligiani[2], Barbara Contiero[1], Alessandro Lotto[3], Gianni Galaverna[2], Luisa Magrin[1], Giulio Cozzi[1]

[1] Department of Animal Medicine, Production and Health, University of Padova, Padova, Italy

[2] Department of Food and Drug, University of Parma, Parma, Italy

[3] Nutristar S.p.A., Reggio Emilia, Italy

International Dairy Journal 123 (2021) 105174

International Dairy Journal 123 (2021) 105174

Contents lists available at ScienceDirect

International Dairy Journal

journal homepage: www.elsevier.com/locate/idairyj

Use of GC–MS and ^{1}H NMR low-level data fusion as an advanced and comprehensive metabolomic approach to discriminate milk from dairy chains based on different types of forage

Ilaria Lanza [a], Veronica Lolli [b, *], Severino Segato [a], Augusta Caligiani [b], Barbara Contiero [a], Alessandro Lotto [c], Gianni Galaverna [b], Luisa Magrin [a], Giulio Cozzi [a]

[a] Department of Animal Medicine, Production and Health, University of Padova, Padova, Italy
[b] Department of Food and Drug, University of Parma, Parma, Italy
[c] Nutristar S.p.A., Reggio Emilia, Italy

ARTICLE INFO

Article history:
Received 4 May 2021
Received in revised form
22 July 2021
Accepted 26 July 2021
Available online 4 August 2021

ABSTRACT

As forage may affect the environmental sustainability of a given dairy chain, this study evaluated the discriminant capacity of fatty acids (FAs) and NMR metabolomic profiles of milk from three dairy chains, where forage components of cows diets were: maize silage (MS), grass-legume and maize silage (GMS), grass and lucerne hay (HAY). Canonical discriminant analysis (CDA) based on FAs and NMR metabolites highlighted a reliable discriminative performance for HAY samples that were correctly recognised, especially on the basis of C18:3n-3 and C17:0. The GMS samples were positively correlated with choline, C14:0 and C17:1 cis-9, while the MS ones were represented mainly by C16:1 cis-9. An overlap between MS and GMS samples was observed, even if a low-level fused CDA modelling improved their correct assignment. The footprint of maize silage on the milk metabolomic profile seemed not to be affected if partially replaced by a mix of legume and grass silages.

1. Introduction

Although several factors, such as breed, herd health status and seasonal variation, have been shown to affect milk yield and composition, the composition of the cows' feed is the key driver of the metabolic processes from nutrient intake to mammary gland synthesis (Borreani et al., 2013; Tenori et al., 2018).

In intensive dairy farming areas, maize is cultivated for silage production to maximise the amount of feed energy produced per unit of farmland (Borrelli, Catelli, Ceotto, Cabassi, & Tomasoni, 2014) and the inclusion of maize silage in dairy rations has increased progressively since the 1980s, replacing permanent meadow hay and/or other dried mixed grass-legume forages.

The impact of maize-related dairy rations on milk yield has been extremely positive (Lora, Zidi, Magrin, Prevedello, & Cozzi, 2020), but cow health status (i.e., lameness, loose faeces etc.) and reproductive efficiency have been noted to be sensitive to higher level of impairment, due to frequent aerobic deterioration during storage or to aflatoxin contamination of maize silage (Battilani et al., 2016).

Further concerns regarding the use of maize silage as the predominant forage source (FS) in dairy diets arise from the environmental sustainability of this cereal, which requires high fossil energy inputs in the face of high emissions of nitrous oxide into the atmosphere (Crutzen, Mosier, Smith, & Winiwarter, 2008).

To mitigate the negative effects of the cereal monoculture, the European common agricultural policy has recommended crop rotation and diversification to enhance soil fertility and the quality of underground microbial communities (Tiemann, Grandy, Atkinson, Marin-Spiotta, & Mcdaniel, 2015). For these reasons, several dairy chains are now evaluating the partial replacement of maize silage with alternative FS such as winter grass (e.g., Italian ryegrass) or cereals (e.g., wheat, oats and triticale) as well as mixtures of these cereals with legumes (e.g., lucerne, peas and vetch). Dairy systems based on alternative fodders could help increase overall farm sustainability by reducing leaching of soil nutrients, mitigating yield-scaled farm greenhouse gas emissions (increasing C sequestration in the soil organic matter) and limiting cows' enteric methane emissions (Tabacco, Comino, & Borreani, 2018).

* Corresponding author. Tel.: +39 0521 905407.
E-mail address: veronica.lolli@unipr.it (V. Lolli).

https://doi.org/10.1016/j.idairyj.2021.105174
0958-6946/

Consumers are now increasingly aware about sustainability issues in food production and recognise dairy chains that could couple milk quality with resource conservation and biodiversity issues (Schoof, Luick, Jürgens, & Jones, 2020). Therefore, milk quality authentication has become a topic of interest for regulatory authorities, food processors and dairy chains, especially when it comes to certified and high-value dairy products such as PDO-labelled cheeses (Coppa et al., 2015; Segato et al., 2017).

The effect of botanical origin and conservation processes of the forage on milk composition has been largely demonstrated. In addition to fatty acid (FA) detection by gas chromatography–mass spectrometry (GC–MS) (Capuano et al., 2014), high-resolution proton nuclear magnetic resonance (NMR) spectroscopy (^{1}H NMR) has become widespread for the screening of several metabolites in dairy products, providing information about the footprint of the feeding system used to produce them (Boiani et al., 2019; Segato et al., 2019a).

Both GC–MS and NMR are accurate metabolomic approaches for the authentication of dairy products, especially when applied in comparing low and high input systems (Tenori et al., 2018). However, a comprehensive metabolomic study is needed to better understand the influence of the dietary forage proportion (i.e., silages versus hays), especially in the case of intensive dairy systems (Rocchetti, Gallo, Nocetti, Lucini, & Masoero, 2020).

Findings of a study on olive oil adulteration proved that a low-level data fusion of the FA-nonpolar or NMR-polar fraction might enhance the discriminant performance of the model (Li, Xiong, & Min, 2019). The hypothesis that a low-level data fusion approach could provide a greater discriminating capacity for milk than those built on an FA-nonpolar or on NMR-polar dataset was tested in the present study by comparing samples from three dairy chains that differed in the main FS included in the cows' diets.

Two of these chains comply with cows feeding guidelines set by PDO requirements of Grana Padano cheese, allowing the use of the ensiled feeds. The third dairy chain identifies farms that follows the disciplinary of production of Parmigiano Reggiano PDO cheese, which forbids the detention and use of any ensiled feed for the cows rationing.

2. Material and methods

2.1. Experimental design and sampling

The study involved 45 Holstein dairy farms located in the central part of the Po Valley in Northern Italy. This is the core area of Italian dairy sector and it is the location of the main cheese chains such as Grana Padano PDO and Parmigiano Reggiano PDO cheeses.

As shown in Fig. 1, the experimental protocol of this study was aimed at assessing if a partial or a total replacement of maize silage with alternative ensiled or dried FS would significantly affect milk FAs and polar metabolomic profiles. Therefore, three dairy chains, based on different forages usually included in the diet of the lactating cows, were considered. Also, to provide a wide and comprehensive analysis, samples were taken from a relevant number of herds within each dairy chains.

The first dairy chain (MS group, 14 farms) use maize silage (34% of total DM) as the main forage component of the total mixed ration (TMR), while small amounts of grass silage and lucerne silage, lucerne hay, meadow hay and straw were the remaining ingredients of the forage portion of the TMR. The MS-diet was completed by energy and protein concentrates (23.1 and 19.3% of total DM, respectively) along with a residual of mineral-vitamin premix and additives (2.2% of total DM).

The second dairy chain identified dairy farms in which a relevant portion of maize silage was replaced by grass and lucerne silages (GMS group, 16 farms). In the mean composition of the TMRs used by 16 GMS farms, grass and legume silages counted for 35% of the total dietary DM, while maize silage only for 9% of it. The mean forage portion of GMS diets was completed by small amount of lucerne hay, meadow hay and straw, while energy and protein concentrates represented 34.1 and 14.7% of the total DM content of these rations, respectively.

The third dairy chain identified farms that use only dried forages as roughage components of cows TMR (HAY group, 15 farms).

The mean ingredient composition of the diets fed in the 15 HAY farms considered in this study showed lucerne hay (26.6% of total DM) and meadow hay (21.2% of total DM) as main FS and the mean diet was completed by energy (34.2% of total DM) and protein (13.1% of total DM) concentrates along with a residual percentage of mineral-vitamin premix and additives. Mean ingredients and proximate composition of the three different FS are provided as Supplementary material Table S1.

Regardless of the dairy chain, diets on all farms were formulated to fulfil the herd's nutritional requirements. To minimise the background noise on milk composition due to the other ingredients of the diets, the choice of the farms to be included in the study considered only dairy herds using similar energy and protein concentrates and mineral-vitamin premix, supplied by the same feed company. Diets were provided ad libitum as TMR in a single delivery after the morning milking.

Finally, raw bulk milk samples were collected on each farm in two different sessions (two replicates per farm): at the end of June and in the middle of July 2018. A total of 90 raw bulk milk samples were collected, including 28 (from 14 farms), 32 (from 16 farms) and 30 milk samples (from 15 farms) for MS, GMS and HAY dairy chains, respectively.

2.2. Diet and milk analysis

The experimental trial did not influence the farm activities or management strategies, nor involved any invasive procedure or manipulation of the lacating dairy cows. Therefore, there was no implication on the animals' welfare status.

Samples of TMR were collected in each farm at the two milk sampling sessions for further analysis. After collection, samples were kept frozen at −20 °C and, after thawing, they were assayed for DM, crude protein (CP), ether extract (EE), ash and starch by official chemical methods and for neutral detergent fibre (aNDF) and acid detergent fibre (ADF) contents using ANKOM methodology (De Nardi et al., 2014). The non-fibre carbohydrate content was calculated as [100 − (CP + EE + Ash + NDF)].

The levels of protein, casein, fat, lactose and urea in milk were recorded by a Fourier transform mid-infrared (FT-MIR) spectroscopy technique using a MilkoScan FT6000 (Foss Electric A/S, Hillerød, Denmark). The somatic cell count (SCC, cells mL^{-1} of milk) was determined by a Fossomatic 5000 (Foss Electric A/S) and reported as [$\log_2$ (SCC/100,000) + 3].

2.3. Fatty acid analysis

Lipid extraction of milk samples was carried out as described by Feng, Lock, and Garnsworthy (2004). Thirty millilitres of defrosted cows' milk in a 50-mL conical plastic tube was mixed for 2 min with 2 mL of 33% ammonia and centrifuged at 3900×*g* for 30 min at 4 °C. The entire the fat-cake layer was transferred to a 15-mL tube and mixed (by vortexing) with 5 mL of hexane. This was then centrifuged at 3900×*g* at room temperature (20 °C) for 20 min. After centrifugation, the sample had separated into three layers: a top layer of lipid; a middle layer of protein, fat and other water-

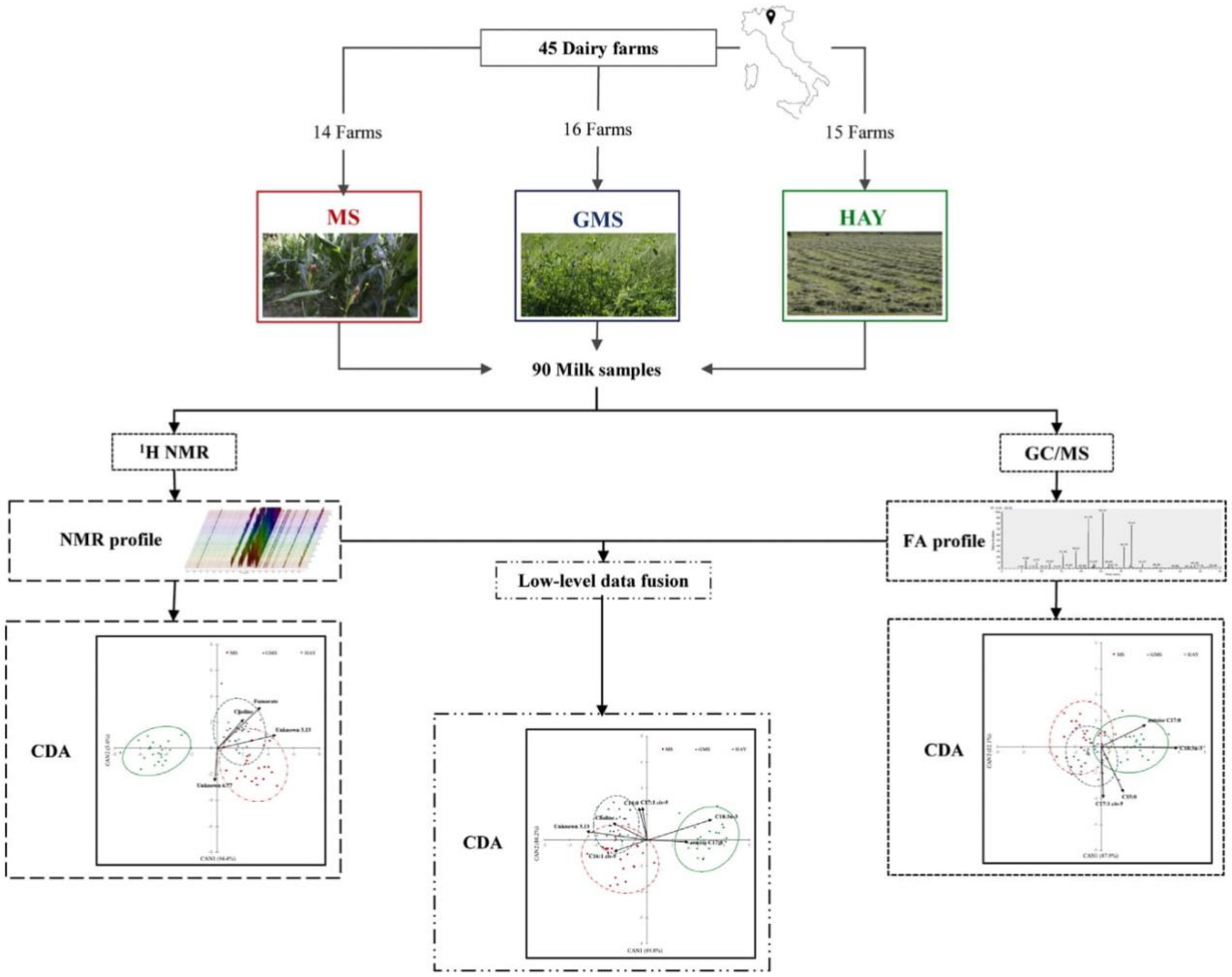

Fig. 1. Overall flowchart of the experiment. Ninety raw bulk milk samples were collected from dairy herds fed total mixed rations (TMR) based on three forage sources: maize silage (MS), grass-legume and maize silage (GMS) and lucerne and permanent meadow hay (HAY) in 45 intensive dairy farms of Northern Italy (top). Milk samples were analysed for fatty acid (right) and NMR (left) profiles and then submitted to canonical discriminant analysis (CDA) as illustrated in Fig. 2. After low-level FA and NMR fusion, a further CDA was performed on the merged dataset (bottom and Fig. 3). The CDA models were performed on the training set (80% of samples) and validated by a leave-one-out cross-validation on the test set (20% of samples), the results of which are reported in Table 3.

insoluble solids; and a bottom layer of water. The upper phase was recovered and evaporated to dryness under vacuum.

Milk fat for GC–MS fatty acid determination was subjected to basic transmethylation performed according to ISO 12966-2 (ISO, 2017), with slight modifications. Briefly, 20 mg of the extracted fat was dissolved in hexane (5 mL) containing tetracosane (Sigma Aldrich, Saint Louis, MO, USA; purity 99%) as an internal standard at 0.1 mg·· mL^{-1}, added to 0.2 mL of KOH 5% in methanol and mixed vigorously for 5 min. After phase separation, the upper organic phase was injected (1 μL, split mode 20:1, split flow 19.6 mL min^{-1}) on a Thermo Scientific Trace 1300 gas chromatograph (Thermo Scientific, Waltham, Massachusetts, USA) carrying a Supelcowax® 10 capillary column (30 m × 0.25 mm × 0.25 μm, Supelco, Bellafonte, USA) coupled to a Thermo Scientific Trace ISQ mass spectrometer (Thermo Scientific, Waltham, Massachusetts, USA). Helium was used as the carrier gas (1 mL min^{-1}). The injector and detector temperatures were set at 240 °C and 250 °C, respectively. The chromatogram was recorded in scan mode (40–500 *m/z*), and the column temperature was set at 80 °C for 2 min, increased to 280 °C (15 °C min^{-1}) and held at 280 °C for 20 min. The content of each single FA was calculated in relation to the concentration of the internal standard, following calculation of the response factors using the Supelco 37 Component FAME Mix® (Sigma Aldrich, Saint Louis, MO, USA) added to conjugated linoleic acid standard (as a mixture of isomers cis- and trans-9,11- and −10,12-octadecadienoic acids, Sigma Aldrich, Saint Louis, MO, USA) as a reference material. FA levels were expressed as g 100 g^{-1} total FAs.

2.4. NMR-based metabolomic analysis

The milk polar fraction was extracted according to the protocol described by Yanibada et al. (2018), with slight adaptations. Briefly, aliquots (400 μL) of milk samples were mixed with 600 μL of MeOD. First, the mixture was frozen at −20 °C for 30 min. Then, to ensure complete removal of the apolar component and to avoid possible chemical shift drifts due to pH effects (Yanibada et al., 2018), 400 μL of $CDCl_3$ and 200 μL of D_2O phosphate buffer (pH 7) solution containing 3-(trimethylsilyl)-propionate-d4 sodium salt, 98% atom D (TSP) (Sigma Aldrich, Saint Louis, MO, USA) at 1 mg min^{-1} as the internal standard were added to milk samples. After centrifugation

(at 4 °C for 30 min), 600 μL of the supernatant were removed for analysis.

^{1}H NMR spectra were recorded according to Segato et al. (2019b) on a VARIAN INOVA-600 MHz spectrometer (Varian, Palo Alto, CA, USA), equipped with a 5-mm triple resonance inverse probe. Spectra were acquired at 298 K, with 32 K complex points; using a 45° pulse length and 3 s of relaxation delay (d1). A total of 128 scans were acquired with a spectral width of 9595.8 Hz and an acquisition time of 1.707 s. Identification of ^{1}H NMR markers in milk samples was achieved through 1D and 2D spectra; TOCSY spectra were acquired at 298 K, with 2048 data points. A total of 32 scans were acquired for each of 256 increments, with an acquisition time of 0.155 s. Acquired ^{1}H NMR spectra were transferred to MestReNova software (release 6.0.2, Mestrelab Research, Spain) and referenced to TSP (0 ppm).

The assignment of ^{1}H NMR signals was supported using data available in the literature (Klein et al., 2010; Sundekilde, Larsen, & Bertram, 2013; Tenori et al., 2018; Yanibada et al., 2018) and the metabolomics data repository for NMR Metabolomics (bmrb.io).

An integration pattern was defined by choosing buckets manually in the range between 0 and 9 ppm on all considered spectra in the overlapped form (Supplementary material Fig. S1). This procedure permitted the choice of buckets sufficiently large as to compensate for the small chemical shift fluctuations in each spectrum and, for this reason, it was preferred to the standard automatic bucketing integration, which utilises a bin width of 0.04 ppm. Moreover, in this way, each bucket corresponds to a defined signal or to a group of signals, which simplifies the interpretation of statistical results. The defined pattern was used for automatic integration of all spectra and referred to TSP area.

2.5. Data and chemometric analyses

Data analyses were conducted using SAS software (release 9.4, SAS Institute Inc., Cary, NC, USA, 2018). The univariate step was conducted by performing ANOVA. Milk composition, FA and NMR data were analysed using a linear model (PROC GLM) based on the fixed effect of FS. Post-hoc pairwise comparisons among levels (MS, GMS and HAY) of the FS levels were performed using a Bonferroni correction and at $p < 0.05$ probalility level (a p-value threshold < 0.10 was set as a trend at the margin of statistical non-significance). The hypotheses of the linear model on the residuals were assessed graphically.

Prior to multivariate canonical discriminant analysis (CDA), both datasets (FA and NMR) were split into training (80% of the records) and test (20% of the records) sets. In each FA and NMR testing set, a preliminary stepwise feature selection (PROC STEPDISC) was conducted, and then the CDA (PROC CANDISC) was performed on the significant ($p < 0.05$) selected features using the FS groups (MS, GMS and HAY) as the prediction factor. After a low-level FA and NMR data fusion, the supervised CDA model was run on the jointed array (Fig. 1). Using the XLSTAT software (release 2016, Addinsoft, New York, NY, USA), the outcomes (loadings) of the CDA were plotted according to the two main canonical functions, named CAN1 and CAN2, and the degree of dissimilarity among FS groups was measured by D^2-Mahalanobis distances (Segato, Caligiani, et al., 2019). The total structure correlation coefficients between the FA and NMR original variables and the canonical functions (CAN1 and CAN2) were plotted (for absolute value greater than 0.30) in each CDA-scattergram to better understand the relationship among these most discriminant features and the CDA modelling classes.

The reliability of the CDA models was assessed by a leave-one-out cross-validation (SAS PROC DISCRIM) performed on the test set. A confusion matrix was built throughout the results of the procedure, and the classification performance was assessed by means of descriptive statistics such as accuracy, precision, sensitivity, specificity and the Matthews correlation coefficient (MCC), as reported by Bisutti et al. (2019).

3. Results and discussion

As consumers are now more aware in recognising dairy chains that could couple milk quality with resource conservation and biodiversity issues (Schoof et al., 2020), several dairy chains are now evaluating the footprint on milk and dairy products of different FS included in the rations of dairy cows as a way to discriminate and label products according to specific ecosystem services. For these reasons, the present study was designed to assess if partial or a total replacement of maize silage with alternative ensiled or dried forages sources would significantly affect milk metabolomic and FA profile.

3.1. Milk quality

Proximate composition data for milk from Holstein herds fed diets based on the three different FS are reported in Table 1. The FS did not affect the main quality traits, except for a significantly ($p < 0.05$) lower lactose content in HAY milk samples. According to Riuzzi et al. (2021), the slight decrease in the milk lactose content that occurred in HAY-fed cows was probably due to a lower level of propionate synthesis in the rumen.

3.2. Forage sources on fatty acid and NMR metabolomic profiles

As a first step, the FA and polar metabolite footprint of the different dietary forage types was assessed by GC–MS and ^{1}H NMR, to identify significant differences between hay- and ensiled-based milk samples. The 43 quantitatively determined milk FAs are provided as Supplementary material Table S2, while the significant ones are reported in Table 2. Milk from MS and GMS had greater concentrations of C14:1 *cis*-9 and C16:1 *cis*-9 than milk from the HAY system. The C17:1 *cis*-9 concentration was the highest in GMS. In contrast, milk from HAY had significant ($p < 0.05$) greater concentrations of *anteiso* C17:0, C17:0 and C18:3n-3, and a higher level of C18:2n-6 even if at the threshold of the significance ($p = 0.08$), which led to a significantly ($p < 0.05$) higher PUFA content. Overall, the main outcomes of the study showed a positive effect on some PUFAs and odd- and branched chain FAs (OBCFAs) in hay-compared with MS-milk. Particularly, consistent with the results of Bernardini et al. (2010) and Coppa et al. (2015), the hay-based TMR significantly increased both the C18:2n-6 and the C18:3n-3 concentrations as a result of high plant transfer and low ruminal biohydrogenation of these PUFAs from the rations to the milk. The higher content of *anteiso* C17:0, C17:0 and C17:1 *cis*-9, three odd-

Table 1
Proximate composition, somatic cell count (SCC) score and urea content of bulk milk samples from a Holstein herd fed diets based on different forage sources (FS).[a]

Component	MS	GMS	HAY	SEM	p-value
Protein (%)	3.23	3.25	3.31	0.24	0.081
Casein (%)	2.52	2.48	2.48	0.29	0.607
Fat (%)	3.64	3.71	3.52	0.06	0.080
Lactose (%)	4.80^a	4.82^a	4.77^b	0.01	0.013
SCC (units)	4.3	4.2	4.5	0.1	0.128
Urea (mg dL^{-1})	19.1	20.6	21.6	0.8	0.094

[a] Abbreviations are: MS, maize silage; GMS, grass-legume and maize silage; HAY, lucerne and permanent meadow hay; SCC, somatic cell count reported as [$\log_2$ (SCC/100,000) + 3]; SEM, standard error of the mean. Least squares-means in a row without a common superscript letter differ at $p < 0.05$.

Table 2
Holstein herd bulk milk fatty acid (% total FA) and NMR metabolite (relative %) levels significantly affected by the dietary forage source (FS).[a]

Component	Chemical shift (ppm)	MS	GMS	HAY	SEM	*p*-value
Fatty acid (FA)						
C14:1 *cis*-9		1.72^{a}	1.72^{a}	1.53^{b}	0.06	0.027
C16:1 *cis*-9		2.46^{a}	2.40^{a}	2.18^{b}	0.06	0.001
anteiso C17:0		0.60^{b}	0.60^{b}	0.68^{a}	0.01	0.001
C17:0		1.01^{b}	1.06^{ab}	1.14^{a}	0.03	0.004
C17:1 *cis*-9		0.39^{b}	0.44^{a}	0.41^{ab}	0.01	0.015
C18:2n-6		1.69^{AB}	1.66^{B}	1.89^{A}	0.08	0.076
C18:3n-3		0.47^{b}	0.59^{b}	0.92^{a}	0.04	0.001
C20:1		0.20^{b}	0.21^{b}	0.24^{a}	0.01	0.002
PUFA		3.57^{b}	3.58^{b}	4.30^{a}	0.19	0.009
Metabolite						
Valine	0.92	0.24^{A}	0.18^{B}	0.20^{AB}	0.02	0.076
Unknown	2.95	0.005^{b}	0.005^{ab}	0.006^{a}	0.000	0.022
Unknown	3.13	0.045^{a}	0.047^{a}	0.031^{b}	0.002	0.001
Choline	3.22	0.33^{ab}	0.35^{a}	0.29^{b}	0.02	0.026
Lactose	3.65	1.19^{b}	1.32^{a}	1.17^{b}	0.05	0.045
Unknown	5.85	0.009	0.009	0.007	0.001	0.090
Unknown	5.97	0.010^{a}	0.010^{a}	0.008^{b}	0.001	0.018
Fumarate	6.58	0.003^{a}	0.004^{a}	0.001^{b}	0.000	0.001
Hippurate	7.52	0.015^{a}	0.014^{a}	0.010^{b}	0.001	0.001

[a] Abbreviations are: MS, maize silage; GMS, grass-legume and maize silage; HAY, lucerne and permanent meadow hay; SEM, standard error of the mean. Least squares-means in a row without a common superscript lowercase or uppercase letter differ at $p < 0.05$ and at $p < 0.10$, respectively.

chain FAs, observed in HAY- and GMS-milk, compared with that in MS milk, was probably due to increased ruminal fibre degradation of their forage source (Patel, Wredle, & Bertilsson, 2013).

For each ^{1}H NMR spectrum, 92 different integrating areas of all signals were obtained and are reported as Supplementary material Table S3 and Fig. S1 together with their ^{1}H chemical shift (ppm range) and relative levels. Among these, 43 signals (corresponding to 27 metabolites) were correctly assigned in milk polar fraction spectra (Supplementary material Table S3).

Overall, the ^{1}H NMR spectra of the analysed samples were dominated by resonances from lactose and a wide range of metabolites belonging to amino acids, sugars (monosaccharides and disaccharides), nucleotides, organic acids and other secondary metabolites, such as choline, creatine and creatinine.

The three different feeding regimens under investigation had a limited influence on this polar fraction, as only nine NMR variables (of which five were identified) were significantly affected by the FS (Table 2). The four unknown metabolites reported in Table 2 could not be definitively assigned to any corresponding molecules. Among these, the unknown compound at 3.13 ppm was suggested to belong to the trimethylamine group of lecithin by Tenori et al. (2018), even if they unsuccessfully attempted to assign this signal too.

Compared with both MS and GMS, HAY milk samples showed a significantly lower content of choline, lactose, fumarate and hippurate. Moreover, the highest concentration of choline was found in the GMS samples. The MS milk tended ($p = 0.08$) to have the greatest concentration of free valine, an essential branched-chain amino acid involved in the physiology of lactation (Maher et al., 2013). Thus, the milk NMR polar fraction seemed to be less sensitive to forage dietary manipulation than FA profile.

In accordance with these findings, O'Callaghan et al. (2018) also found that the replacement of TMR based on maize silage with perennial ryegrass and/or white clover pasture-based feeding systems significantly increased the milk choline content. However, Buccioni, Decandia, Minieri, Molle, and Cabiddu (2012) reported a relationship between the forage botanical origin and the content of phospholipids, which may include phosphatidylcholine, with implications for the transfer of choline from the diet to the milk. Moreover, in lactating dairy cows, choline traces in milk were suggested as a biomarker of FA release from animal phospholipid break-down, as a response to higher energetic requirements (Klein et al., 2012). Consistent with our findings, Besle et al. (2010) found a higher content of hippuric acid in MS based-diets compared with HAY based-TMR; therefore, this organic acid could be considered a biomarker of dairy products obtained from the use of ensiled forages. However, the highest levels of hippurate were also recorded in milk from outdoor feeding regimes (i.e., cows grazing on perennial ryegrass and legumes), highlighting how the variability in these secondary metabolites is related to multifactorial metabolic pathways (Boiani et al., 2019). On the other side, the higher content of valine found in MS samples is in contrast with the literature, where it has been reported that this amino acid is a potential limiting amino acid for milk protein synthesis, especially in dairy cows fed grass silage-based diets (Korhonen, Vanthalo, & Huhtanen, 2002).

3.3. Forage dairy chains discrimination

Based on the outcomes of univariate statistical analysis, it is a challenging task to clarify the relationship between milk NMR spectral data and the dietary FS. Indeed, great focus has been placed on describing the changes that feeding systems can impose on milk fatty acid composition (Borreani et al., 2013; Coppa et al., 2015; O'Callaghan et al., 2016; Werteker, Huber, Kuchling, Rossmann, & Schreiner, 2017); however, information is lacking on the interpretation of dietary effects on the NMR milk metabolome (Boiani et al., 2019; Tenori et al., 2018).

3.3.1. Discriminant analysis based on fatty acid and NMR datasets

The CDA carried out on the FA-nonpolar dataset (Wilks' $\lambda = 0.198$, approx. F value $= 13.1$, df1 $= 12$ df2 $= 126$, $p < 0.001$) had a moderate discriminative capacity because of low D^2-Mahalanobis values, which ranged from 2.7 to 14.6 ($p < 0.001$). This exploratory targeting model attributed a significant discriminant role to C15:0, C16:1 *cis-9*, *anteiso* C17:0, C17:1 *cis-9*, C18:3n-3 and C22:0. Considering the plot of CDA for FAs, it appeared that milk samples tended to cluster in two classes, mostly separated along the first canonical function, CAN1 (Fig. 2a). The HAY sample group was shifted on the right side of the scattergram and positively correlated with *anteiso* C17:0 and C18:3n-3. The GMS- and MS-groups overlapped on the centre-left of the plot, and only the GMS one

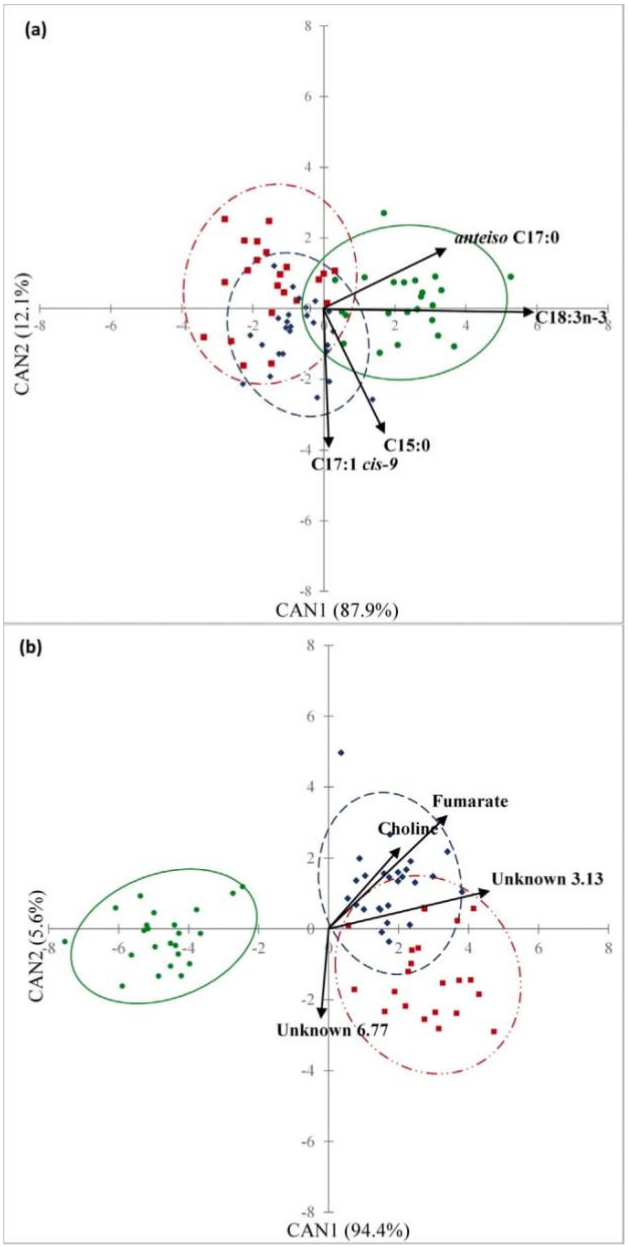

Fig. 2. Canonical discriminant analysis scatterplot of milk samples according to the three forage groups based on (a) fatty acid and (b) NMR variables. The 0.95 confidence ellipses are drawn around each centroid of groupings. MS (maize silage), red-dotted-pointed line and ■; GMS (grass-legume and maize silage), blue-dotted line and ◆; HAY (lucerne and permanent meadow hay), green solid line and ●. The vectors (black arrows) represent the FA with a total structure correlation coefficient higher than 0.30 in absolute values, for at least one of the two canonical functions (for graphical plotting, the correlation coefficients were multiplied eight times according to the maximum value of the axes). (For interpretation of the references to colour in this figure legend, the reader is referred to the Web version of this article.)

seemed to be positively correlated with C17:1 *cis*-9 and C15:0, while no FA was correlated with MS. As explained above, PUFA (i.e., C18:3n-3) and OBCFA (i.e., *anteiso* C:17:0) levels are increased in milk by hay feeding due to both high plant transfer and enhanced ruminal cellulolytic bacterial activity (Werteker et al., 2017). The lack of separation between the MS and GMS groups confirmed that the partial replacement of maize silage (MS group) with a mix of grass and legume silages (GMS group) had a reduced influence on the FA profile (Borreani et al., 2013), especially when the TMR is formulated with high-density energy concentrates mainly from maize products (Paredes et al., 2018).

The CDA performed with the NMR dataset (Wilks' $\lambda = 0.090$, approx. F value = 20.7, df1 = 14 df2 = 124, $p < 0.001$) also had a limited discriminant capacity (D^2-Mahalanobis values ranged from 2.6 to 31.7; $p < 0.001$) and sorted a restricted pool of seven informative integrated ^{1}H NMR signals from the large dataset: creatine, choline, fumarate, and the four unknown metabolites mentioned above. The CDA-plot based on NMR data showed a distinguishable separation of the HAY group on the left side according to the score of the main CAN1 function, even though no nonpolar compounds were correlated with this FS group, except for a weak but significant positive relationship with creatine that was consistent with the outcomes of Tenori et al. (2018) in a previous study (Fig. 2b). As for FAs, the NMR-CDA-targeting model did not result in a separation between MS and GMS, both converging on the centre-right scattergram and correlating positively with choline, fumarate and the unknown compound at 3.13 ppm; instead, the unknown one at 6.77 ppm seemed to be a marker of MS samples.

The outcomes of the validation procedure (leave-one-out cross validation) based on the test set confirmed that the use of both datasets (FA- and NMR-) made it possible to correctly separate HAY milk samples from those of the two silage groups, that were instead misclassified among them.

3.3.2. *Discriminant analysis based on low-level fatty acid and NMR fusion*

The capacity of the FA-nonpolar or NMR-polar datasets to discriminate milk samples according to the main FS was enhanced by performing a low-level data fusion, which resulted in a better predictive performance of the CDA algorithm. In fact, the outcomes reported lower value of Wilks' λ (Wilks' $\lambda = 0.037$, approx. F value = 19.9, df1 = 24 df2 = 114, $p < 0.001$) and higher D^2-Mahalanobis values, which ranged from 7.2 to 51.2 ($p < 0.001$). The foreword stepwise procedure within the multivariate model selected six FAs (C4:0, C14:0, C16:1 *cis*-9, *anteiso* C17:0, C17:1 *cis*-9, C18:3n-3) and six NMR variables (choline, N-acetylglucosamine, orotate, three unknown signals centred at 3.13, 3.15, and 3.19 ppm). However, only the original FA and NMR variables that had a total structure correlation coefficient with at least CAN1 or CAN2 higher than 0.30 were also plotted within the biplot-scattergram to explain the magnitude (length and direction of the vector) of the relationship between the metabolites and the feeding regimens.

The HAY samples migrated alone toward the right side of CAN1 and were characterised by higher contents of *anteiso* C17:0 and C18:3n-3 (Fig. 3). The GMS samples tended to aggregate in the upper-left side and were mainly correlated with C14:0, C17:1 *cis*-9, choline and unknown at 3.13 ppm. On the lower-left side of the plot, MS samples were partially separated from GMS ones due to a higher correlation with C16:1 *cis*-9.

A noticeable role in explaining the effect of FS by the NMR metabolome was also played by four unknown compounds, which cannot be clearly assigned because of low intensities and overlapping signals.

Through the outcomes of the cross-validation procedure, the fused-CDA algorithm built in this trial could be deemed a robust and reliable discriminative model to authenticate HAY milk samples (Table 3). The discriminant capacity of the CDA carried out on the merged dataset was also improved both for MS (MCC = 0.32) and GMS (MCC = 0.51) groups due to the higher values of specificity and sensitivity, respectively. However, there is still a moderate misclassification rate between the two ensiled-based FS groups, specifically a 33.3% bias for the MS samples.

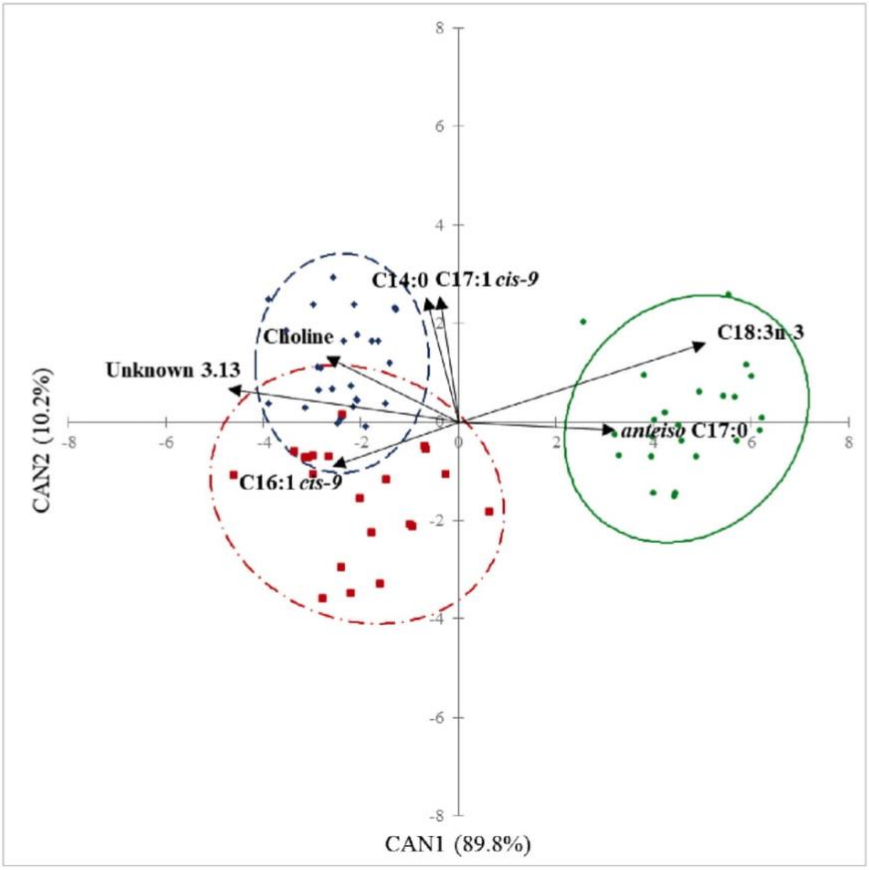

Fig. 3. Canonical discriminant analysis scatterplot of milk samples according to the three forage groups (MS, GMS and HAY) based on FA and NMR low-level fusion. See Fig. 2 for details of the 0.95 confidence ellipses, vectors and forage groups.

Table 3
Classification performance of canonical discriminant analysis (CDA) by leave-one-out cross-validation performed on the fused FA and NMR test set.[a]

Predicted	Actual		
	MS	GMS	HAY
MS	2	1	0
GMS	4	5	0
HAY	0	0	6
Total	6	6	6
Sensitivity	0.33	0.83	1.00
Specificity	0.92	0.67	1.00
Accuracy	0.72	0.72	1.00
Precision	0.67	0.56	1.00
MCC	0.32	0.51	1.00

[a] Abbreviations are: MS, maize silage; GMS, grass-legume and maize silage; HAY, lucerne and permanent meadow hay; MCC, Matthews correlation coefficient.

Compared with the MS group, the partial substitution of maize silage with a mix of ensiled grass and legumes significantly increased the C14:0 content, in accordance with the findings of Borreani et al. (2013), even though it is a medium-chain FAs mainly originating from de novo synthesis in the mammary gland. With regard to MS, a high amount of C16:1 *cis*-9 has already been indicated as a reliable biomarker of the use of a high maize silage proportion in lactating dairy cows' diets, compared with hay-based rations (Khiaosa-Ard, Klevenhusen, Soliva, Kreuzer, & Leiber, 2010) or alpine pasture (Segato et al., 2017).

Furthermore, a moderate discriminant capacity was provided by C4:0, orotate and N-acetylglucosamine along the main function CAN2, as their correlation coefficient (r) values resulted 0.19, 0.23 and 0.21, respectively (vectors not graphically reported because $r < 0.30$).

The short chain-FA C4:0 was related to both GMS and HAY samples, as confirmed by the literature that highlighted the lowest value of this SFA in milk from a maize silage-based diet (Borreani et al., 2013; Segato et al., 2017). Moreover, a tiny but significant correlation between C4:0 and the amount of grass silage was found by Coppa et al. (2015), even if they stated that differences may be related to the analytical detection, due to the volatility of this short-chain FAs. The two NMR variables seemed to be associated with GMS samples.

Orotate is synthesised by the mammary gland and takes part as an intermediate in the biosynthesis of pyrimidine nucleotides, required for the regulation of genes involved in the development of cell, tissues and organisms (O'Callaghan et al., 2021).

N-acetylglucosamine is an amide derivative of glucose belonging to the oligosaccharides fraction of cow milk. To the best of our knowledge, changes in this organic acid and sugar-like compound were not ascribed to the FS but to other husbandry factors such as breed, stage of lactation and cow health status (Sundekilde et al., 2015; Rysova et al., 2021).

Indeed, the outcomes of this study supported the hypothesis that only the total replacement of maize silage (MS) with hay would

lead to relevant variations in ruminal and mammary metabolism with changes in the milk FA and NMR profiles (Akbaridoust et al., 2014; Eisenstecken, Stanstrup, Robatscher, Huck, & Oberhuber, 2021). However, the low-level data fusion performed in this study provided a more comprehensive selection of metabolomic features, thus improving the detection accuracy.

4. Conclusions

A comparison among milk samples from different forage based dairy chains showed that a only total replacement of maize silage with legume and grass hays in the cows' diet led to a significant change in the milk metabolomic profile. The footprint of maize silage on the milk metabolomic profile was not significantly modified when the forage was only partially replaced by a mix of legume and grass silages. From a methodological point of view, a low-level FA and NMR data fusion coupled with a CDA chemometric approach has been shown to empower the predictive performance of the supervised CDA discriminant model of bulk milk samples from diverse ensiled or dried forage-based feeding systems.

CRediT authorship contribution statement

Ilaria Lanza: Writing - original draft, Writing - review & editing, Visualization. **Veronica Lolli:** Methodology, Formal analysis, Investigation, Writing - review & editing, Validation. **Severino Segato:** Data analysis, Writing - review & editing. **Augusta Ca-li-gia-ni:** Conceptualization, Methodology, Writing - review & editing, Supervision. **Barbara Contiero:** Data analysis, Writing - review & editing. **Alessandro Lotto:** Conceptualization, Review & editing. **Gianni Galaverna:** Resources, Conceptualization, Visualization. **Luisa Magrin:** Writing - review & editing. **Giulio Cozzi:** Conceptualization, Writing - review & editing, Visualization, Supervision.

Declaration of competing interest

The authors declare that they have no known competing financial interests or personal relationships that could have appeared to influence the work reported in this paper.

Acknowledgement

This work was supported by a research grant of Nutristar SpA. Viale del Paracadutista 9, 42122, Reggio Emilia, Italy.

Appendix A. Supplementary data

Supplementary data to this article can be found online at https://doi.org/10.1016/j.idairyj.2021.105174.

References

Akbaridoust, G., Plozza, T., Trenerry, V. C., Wales, W. J., Auldist, M. J., Dunshea, F. R., et al. (2014). Influence of different systems for feeding supplements to grazing dairy cows on milk fatty acid composition. *Journal of Dairy Research, 81*, 156–163.

Battilani, P., Toscano, P., Van Der Fels-Klerx, H. J., Moretti, A., Camardo Leggieri, M., Brera, C., et al. (2016). Aflatoxin B 1 contamination in maize in Europe increases due to climate change. *Scientific Reports, 6*. Article 24328.

Bernardini, D., Gerardi, G., Elia, C. A., Marchesini, G., Tenti, S., & Segato, S. (2010). Relationship between milk fatty acid composition and dietary roughage source in dairy cows. *Veterinary Research Communications, 34*, 135–138.

Besle, J. M., Viala, D., Martin, B., Pradel, P., Meunier, B., Berdagué, J. L., et al. (2010). Ultraviolet-absorbing compounds in milk are related to forage polyphenols. *Journal of Dairy Science, 93*, 2846–2856.

Bisutti, V., Merlanti, R., Serva, L., Lucatello, L., Mirisola, M., Balzan, S., et al. (2019). Multivariate and machine learning approaches for honey botanical origin authentication using near infrared spectroscopy. *Journal of Near Infrared Spectroscopy, 27*, 65–74.

Boiani, M., Sundekilde, U. K., Bateman, L. M., McCarthy, D. G., Maguire, A. R., Gulati, A., et al. (2019). Integration of high and low field 1 H NMR to analyse the effects of bovine dietary regime on milk metabolomics and protein-bound moisture characterisation of the resulting mozzarella cheeses during ripening. *International Dairy Journal, 91*, 155–164.

Borreani, G., Coppa, M., Revello-Chion, A., Comino, L., Giaccone, D., Ferlay, A., et al. (2013). Effect of different feeding strategies in intensive dairy farming systems on milk fatty acid profiles, and implications on feeding costs in Italy. *Journal of Dairy Science, 100*, 8705–8721.

Borrelli, L., Castelli, F., Ceotto, E., Cabassi, G., & Tomasoni, C. (2014). Maize grain and silage yield and yield stability in a long-term cropping system experiment in northern Italy. *European Journal of Agronomy, 55*, 12–19.

Buccioni, A., Decandia, M., Minieri, S., Molle, G., & Cabiddu, A. (2012). Lipid metabolism in the rumen: New insights on lipolysis and biohydrogenation with an emphasis on the role of endogenous plant factors. *Animal Feed Science and Technology, 174*, 1–25.

Capuano, E., Van Der Veer, G., Boerrigter-Eenling, R., Elgersma, A., Rademaker, J., Sterian, A., et al. (2014). Verification of fresh grass feeding, pasture grazing and organic farming by cows farm milk fatty acid profile. *Food Chemistry, 164*, 234–241.

Coppa, M., Chassaing, C., Ferlay, A., Agabriel, C., Laurent, C., Borreani, G., et al. (2015). Potential of milk fatty acid composition to predict diet composition and authenticate feeding systems and altitude origin of European bulk milk. *Journal of Dairy Science, 98*, 1539–1551.

Crutzen, P. J., Mosier, A. R., Smith, K. A., & Winiwarter, W. (2008). N_2O release from agro-biofuel production negates global warming reduction by replacing fossil fuels. *Atmospheric Chemistry and Physics, 8*, 389–395.

De Nardi, R., Marchesini, G., Stefani, A. L., Barberio, A., Andrighetto, I., & Segato, S. (2014). Effect of feeding fine maize particles on the reticular pH, milk yield and composition of dairy cows. *Journal of Animal Physiology and Animal Nutrition, 98*, 504–510.

Eisenstecken, D., Stanstrup, J., Robatscher, P., Huck, C. W., & Oberhuber, M. (2021). Fatty acid profiling of bovine milk and cheese from six European areas by GC-FID and GC-MS. *International Journal of Dairy Technology, 74*, 215–224.

Feng, S., Lock, A. L., & Garnsworthy, P. C. (2004). Technical note: A rapid lipid separation method for determining fatty acid composition of milk. *Journal of Dairy Science, 87*, 3785–3788.

ISO. (2017). *ISO 12966–2: Animal and vegetable fats and oils-gas chromatography of fatty acid methyl esters-Part 2: Preparation of methyl esters of fatty acids*. Geneva, Switzerland: International Standardisation Organisation.

Khiaosa-Ard, R., Klevenhusen, F., Soliva, C. R., Kreuzer, M., & Leiber, F. (2010). Transfer of linoleic and linolenic acid from feed to milk in cows fed isoenergetic diets differing in proportion and origin of concentrates and roughages. *Journal of Dairy Research, 77*, 331–336.

Klein, M. S., Almstetter, M. F., Schlamberger, G., Nürnberger, N., Dettmer, K., Oefner, P. J., et al. (2010). Nuclear magnetic resonance and mass spectrometry-based milk metabolomics in dairy cows during early and late lactation. *Journal of Dairy Science, 93*, 1539–1550.

Klein, M. S., Buttchereit, N., Miemczyk, S. P., Immervoll, A. K., Louis, C., Wiedemann, S., et al. (2012). NMR metabolomic analysis of dairy cows reveals milk glycerophosphocholine to phosphocholine ratio as prognostic biomarker for risk of ketosis. *Journal of Proteome Research, 11*, 1373–1381.

Korhonen, M., Vanhatalo, A., & Huhtanen, P. (2002). Evaluation of isoleucine, leucine, and valine as a second-limiting amino acid for milk production in dairy cows fed grass silage diet. *Journal of Dairy Science, 85*, 1533–1545.

Li, Y., Xiong, Y., & Min, S. (2019). Data fusion strategy in quantitative analysis of spectroscopy relevant to olive oil adulteration. *Vibrational Spectroscopy, 101*, 20–27.

Lora, I., Zidi, A., Magrin, L., Prevedello, P., & Cozzi, G. (2020). An insight into the dairy chain of a Protected Designation of Origin cheese: The case study of Asiago cheese. *Journal of Dairy Science, 103*, 9116–9123.

Maher, A. D., Hayes, B., Cocks, B., Marett, L., Wales, W. J., & Rochfort, S. J. (2013). Latent biochemical relationships in the blood-milk metabolic axis of dairy cows revealed by statistical integration of 1H NMR spectroscopic data. *Journal of Proteome Research, 12*, 1428–1435.

O'Callaghan, T. F., O'Donovan, M., Murphy, J. P., Sugrue, K., Tobin, J. T., McNamara, A. E., et al. (2021). The bovine colostrum and milk metabolome at the onset of lactation as determined by ^{1}H-NMR. *International Dairy Journal, 113*. Article 104881.

O'Callaghan, T. F., Vázquez-Fresno, R., Serra-Cayuela, A., Dong, E., Mandal, R., Hennessy, D., et al. (2018). Pasture feeding changes the bovine rumen and milk metabolome. *Metabolites, 8*. Article 27.

O'Callaghan, T. F., Hennessy, D., McAuliffe, S., Kilcawley, K. N., O'Donovan, M., Dillon, P., et al. (2016). Effect of pasture versus indoor feeding systems on raw milk composition and quality over an entire lactation. *Journal of Dairy Science, 99*, 9424–9440.

Paredes, C. L. L., Werteker, M., Rossmann, B., Keplinger, J., Olschewski, I. L., & Schreiner, M. (2018). Discrimination of haymilk and conventional milk via fatty acid profiles. *Journal of Food Measurement and Characterization, 12*, 1391–1398.

Patel, M., Wredle, E., & Bertilsson, J. (2013). Effect of dietary proportion of grass silage on milk fat with emphasis on odd- and branched-chain fatty acids in dairy cows. *Journal of Dairy Science, 96*, 390–397.

Riuzzi, G., Tata, A., Massaro, A., Bisutti, V., Lanza, I., Contiero, B., et al. (2021). Authentication of forage-based milk by mid-level data fusion of (+/−) DART-HRMS signatures. *International Dairy Journal, 112*. Article 104859.

Rocchetti, G., Gallo, A., Nocetti, M., Lucini, L., & Masoero, F. (2020). Milk metabolomics based on ultra-high-performance liquid chromatography coupled with quadrupole time-of-flight mass spectrometry to discriminate different cows feeding regimens. *Food Research International, 134*. Article 109279.

Rysova, L., Legarova, V., Pacakova, Z., Hanus, O., Nemeckova, I., Klimesova, M., et al. (2021). Detection of bovine milk adulteration in caprine milk with N-acetyl carbohydrate biomarkers by using ^{1}H nuclear magnetic resonance spectroscopy. *Journal of Dairy Science, 104*. Article 9.

Schoof, N., Luick, R., Jürgens, K., & Jones, G. (2020). Dairies in Germany: Key factors for grassland conservation? *Sustainability, 12*. Article 4139.

Segato, S., Caligiani, A., Contiero, B., Galaverna, G., Bisutti, V., & Cozzi, G. (2019b). 1H NMR metabolic profile to discriminate pasture based alpine asiago PDO cheeses. *Animals, 9*. Article 722.

Segato, S., Galaverna, G., Contiero, B., Berzaghi, P., Caligiani, A., Marseglia, A., et al. (2017). Identification of lipid biomarkers to discriminate between the different production systems for Asiago PDO cheese. *Journal of Agricultural and Food Chemistry, 65*, 9887–9892.

Segato, S., Merlanti, R., Bisutti, V., Montanucci, L., Serva, L., Lucatello, L., et al. (2019a). Multivariate and machine learning models to assess the heat effects on honey physicochemical, colour and NIR data. *European Food Research and Technology, 245*, 2269–2278.

Sundekilde, U. K., Clausen, M. R., Lejonklev, J., Weisbjerg, M. R., Larsen, M. K., & Bertram, H. C. S. (2015). Addition of essential oils to cows' feed alters the milk metabolome-NMR spectroscopic studies of "Nature's perfect food". In F. Capozzi, L. Laghi, & P. S. Belton (Eds.), *Magnetic resonance in food science: Defining food by magnetic resonance* (pp. 161–170). Cambridge, UK: Royal Society of Chemistry.

Sundekilde, U. K., Larsen, L. B., & Bertram, H. C. (2013). NMR-based milk metabolomics. *Metabolites, 3*, 204–222.

Tabacco, E., Comino, L., & Borreani, G. (2018). Production efficiency, costs and environmental impacts of conventional and dynamic forage systems for dairy farms in Italy. *European Journal of Agronomy, 99*, 1–12.

Tenori, L., Santucci, C., Meoni, G., Morrocchi, V., Matteucci, G., & Luchinat, C. (2018). NMR metabolomic fingerprinting distinguishes milk from different farms. *Food Research International, 113*, 131–139.

Tiemann, L. K., Grandy, A. S., Atkinson, E. E., Marin-Spiotta, E., & Mcdaniel, M. D. (2015). Crop rotational diversity enhances belowground communities and functions in an agroecosystem. *Ecology Letters, 18*, 761–771.

Werteker, M., Huber, S., Kuchling, S., Rossmann, B., & Schreiner, M. (2017). Differentiation of milk by fatty acid spectra and principal component analysis. *Measurement: Journal of the International Measurement Confederation, 98*, 311–320.

Yanibada, B., Boudra, H., Debrauwer, L., Martin, C., Morgavi, D. P., & Canlet, C. (2018). Evaluation of sample preparation methods for NMR-based metabolomics of cow milk. *Heliyon, 4*. Article 00856.

Appendix A.

Supplementary data

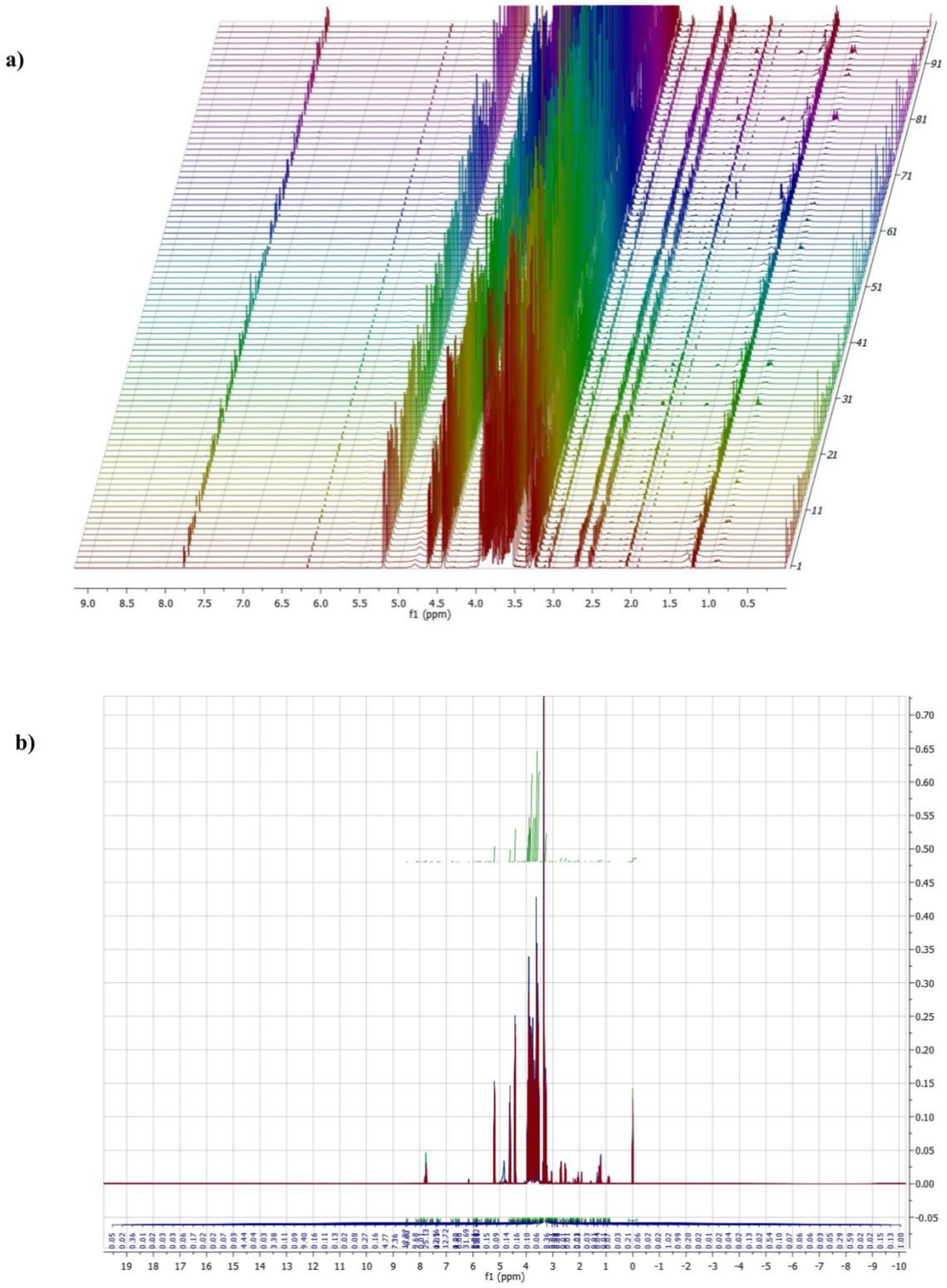

Fig 1S. Overlapping of the total 90 NMR spectra of milk samples from the three different forage sources (a) and the integration zone of all 92 detected signals in the range between 0 and 9 ppm (b).

Table S1. Mean ingredients and proximate composition (average ± standard deviation) of total mixed rations based on different forage sources (FS).

	MS	GMS	HAY
Ingredients (% DM)			
Maize silage	34.0 (±7.1)	8.9 (±6.3)	
Grass silage	8.4 (±7.0)	26.5 (±10.7)	
Lucerne silage	2.9 (±4.9)	8.0 (±6.9)	
Lucerne hay	3.6 (±5.0)	3.5 (±5.2)	26.6 (±4.8)
Meadow hay	4.7 (±5.5)	2.2 (±3.1)	21.2 (±5.9)
Straw	1.8 (±1.9)	0.4 (±0.8)	2.6 (±3.0)
Energy concentrates[a]	23.1 (±4.3)	34.1 (±6.8)	34.2 (±2.7)
Protein concentrates[b]	19.3 (±3.0)	14.7 (±7.3)	13.1 (±3.9)
Residual[c]	2.2 (±2.6)	1.7 (±2.2)	2.2 (±1.8)
Proximate composition (% DM)			
DM (%)	52.9 (±3.7)	49.4 (±6.6)	75.6 (±5.8)
Crude protein	15.2 (±0.8)	15.6 (±0.9)	15.1 (±1.1)
Ether extract	3.7 (±0.4)	3.6 (±0.5)	3.2 (±0.4)
Ash	8.0 (±0.7)	8.4 (±1.3)	7.9 (±1.3)
aNDF	34.8 (±3.1)	34.7 (±3.0)	37.2 (±5.0)
ADF	22.9 (±2.2)	22.2 (±2.0)	26.4 (±3.8)
Non-fibre carbohydrates	38.3 (±2.6)	37.7 (±2.3)	36.6 (±5.1)
Starch	25.4 (±2.0)	23.6 (±2.5)	20.9 (±4.8)

MS, maize silage; GMS, grass-legume and maize silage; HAY, lucerne and permanent meadow hay.
[a]Mainly maize products. [b] Mainly soybean and sunflower products. [c] Molasses, vit-mineral premix.

Table 2S. List of the fatty acids (FA) quali-quantitatively determined by GC-MS in milk samples from three different forage sources of cows' diets, their relative mean concentrations (g 100 g-1 total FA), standard error (SEM) and P-value resulting from the ANOVA.

Fatty acids (g/100 g total FA)	**MS**	**GS**	**HAY**	**SEM**	***P* value**
C4:0	3.68	3.89	3.87	0.09	0.24
C6:0	3.38	3.39	3.13	0.14	0.35
C8:0	2.49	2.58	2.22	0.15	0.20
C10:0	5.29	5.67	5.03	0.29	0.28
C10:1	0.54	0.46	0.39	0.05	0.16
C11:0	0.24	0.13	0.12	0.06	0.30
C12:0	5.71	6.15	5.61	0.23	0.22
C12:1 *trans*	0.23	0.14	0.11	0.06	0.34
C12:1 *cis*	0.25	0.16	0.13	0.06	0.31
C13:0	0.32	0.22	0.21	0.05	0.34
C14:0 *iso*	0.29	0.19	0.20	0.06	0.45
C14:0	13.36	14.23	13.91	0.31	0.14
C14:1 *cis-9*	1.72	1.72	1.53	0.06	0.03
C15:0 *anteiso*	0.53	0.47	0.47	0.05	0.58
C15:0 *iso*	0.85	0.77	0.83	0.05	0.44
C15:0	1.83	1.90	1.91	0.05	0.48
C15:1	0.24	0.07	0.14	0.06	0.20
C16:0 *iso*	0.35	0.36	0.36	0.01	0.92
C16:0	24.16	23.59	23.84	0.49	0.71
C16:1 *trans*	0.33	0.32	0.31	0.01	0.56
C16:1 *cis-9*	2.46	2.40	2.18	0.06	<0.001
C17:0 *anteiso*	0.60	0.60	0.68	0.01	<0.001
C17:0 *iso*	0.82	0.82	0.87	0.02	0.19
C17:0	1.01	1.06	1.14	0.03	<0.001
C17:1 *cis-9*	0.39	0.44	0.41	0.01	0.01
C18:0	10.65	10.34	10.90	0.34	0.50
C18:1 *cis-9* (Oleic Acid)	12.58	12.31	13.08	0.28	0.14
C18:1 *isomer* 1	0.59	0.51	0.53	0.05	0.47
C18:1 *isomer* 2	0.64	0.65	0.68	0.05	0.81
C18:1 *isomer* 3	0.23	0.22	0.24	0.02	0.67

C18:2 *cis-9, cis-12* (LA)	1.69	1.66	1.89	0.08	0.08
C18:2 *isomer* 1	0.13	0.12	0.14	0.01	0.60
C19:0	0.08	0.09	0.09	0.01	0.60
C18:3 *isomer* 1	0.11	0.11	0.12	0.01	0.57
C19:1	0.09	0.10	0.10	0.00	0.24
C18:3 n-3 (linolenic)	0.47	0.59	0.92	0.04	<0.001
C18:2 *cis-9 trans-11* (rumenic)	0.71	0.67	0.76	0.04	0.40
C20:0	0.15	0.16	0.17	0.01	0.38
C20:1	0.20	0.21	0.24	0.01	<0.001
C20:3 n-6	0.17	0.16	0.19	0.01	0.26
C20:4 n-6	0.29	0.27	0.29	0.02	0.75
C22:0	0.05	0.05	0.06	0.01	0.74
Total SFA	75.92	76.72	75.62	0.48	0.25
Total MUFA	20.47	19.70	20.08	0.35	0.31
Total PUFA	3.57	3.58	4.30	0.19	0.01

Table 3S. List of 1H NMR compounds, chemical shift values (ppm range), relative levels and proton assignments determined in milk samples from three different forage sources of cows' diets, standard error (SEM) and P-value resulting from the ANOVA.

Variable	[1]H Chemical shift (range ppm)	MS	GS	HAY	SEM	*P* value	[2]Identification
v1	0.90 - 0.87	0.23	0.18	0.19	0.02	0.24	Leucine/Isoleucine
v2	0.94 - 0.90	0.24	0.18	0.20	0.02	0.08	Valine
v3	1.02 - 1.01	0.03	0.02	0.03	0.00	0.13	
v4	1.08 - 1.06	0.02	0.02	0.02	0.00	0.13	
v5	1.10 - 1.09	0.01	0.01	0.01	0.00	0.73	
v6	1.22 - 1.18	0.66	0.69	0.62	0.02	0.11	
v7	1.32 - 1.23	0.75	0.54	0.54	0.13	0.44	
v8	1.34 - 1.32	0.10	0.08	0.14	0.03	0.31	Lactate
v9	1.45 - 1.45	0.01	0.01	0.01	0.00	0.19	Alanine
v10	1.50 - 1.47	0.04	0.04	0.04	0.00	0.38	Butyrate
v11	1.61 - 1.56	0.14	0.09	0.10	0.02	0.12	
v12	1.81 - 1.76	0.06	0.06	0.07	0.00	0.93	
v13	1.92 - 1.90	0.06	0.06	0.07	0.01	0.65	Acetate
v14	2.04 - 1.99	0.13	0.12	0.12	0.01	0.48	
v15	2.07 - 2.04	0.55	0.57	0.56	0.02	0.74	N-acetylglucosamine
v16	2.09 - 2.09	0.01	0.01	0.01	0.00	0.73	
v17	2.10 - 2.09	0.02	0.02	0.02	0.00	0.26	
v18	2.18 - 2.13	0.22	0.18	0.18	0.02	0.20	Glutamate + Methionine
v19	2.23 - 2.22	0.03	0.03	0.03	0.00	0.69	Succinate
v20	2.27 - 2.24	0.04	0.04	0.04	0.00	0.34	
v21	2.31 - 2.30	0.03	0.03	0.03	0.00	0.82	
v22	2.34 - 2.33	0.01	0.01	0.01	0.00	0.74	

v23	2.35 - 2.35	0.02	0.02	0.02	0.00	0.33	
v24	2.45 - 2.36	0.23	0.24	0.23	0.01	0.88	Creatine/phosphocreatine
v25	2.57 - 2.49	1.09	1.17	1.04	0.04	0.13	Citrate
v26	2.61 - 2.60	0.01	0.01	0.01	0.00	0.27	
v27	2.74 - 2.66	1.14	1.20	1.09	0.05	0.26	Citrate
v28	2.83 - 2.83	0.01	0.01	0.01	0.00	0.26	
v29	2.89 - 2.87	0.03	0.02	0.03	0.00	0.26	Creatine
v30	2.92 - 2.90	0.02	0.02	0.03	0.00	0.34	
v31	2.95 - 2.94	0.01	0.01	0.01	0.00	0.02	
v32	3.01 - 2.98	0.06	0.06	0.06	0.00	0.94	Alpha-ketoglutarate
v33	3.03 - 3.03	0.01	0.01	0.02	0.00	0.34	Creatine/Phosphocreatine
v34	3.06 - 3.04	0.21	0.22	0.21	0.01	0.43	Creatinine
v35	3.07 - 3.06	0.03	0.03	0.03	0.00	0.46	
v36	3.12 - 3.10	0.07	0.07	0.07	0.00	0.83	
v37	3.14 - 3.12	0.04	0.05	0.03	0.00	<0.001	
v38	3.15 - 3.14	0.03	0.03	0.03	0.00	0.38	
v39	3.16 - 3.15	0.03	0.03	0.03	0.00	0.50	
v40	3.19 - 3.19	0.01	0.02	0.01	0.00	0.12	
v41	3.23 - 3.22	0.33	0.35	0.30	0.02	0.03	Choline/Phosphocoline
v42	3.29 - 3.24	8.61	9.03	8.79	0.30	0.61	Lactose + Betaine
v43	3.38 - 3.36	0.14	0.14	0.13	0.02	0.86	
v44	3.42 - 3.40	0.09	0.10	0.10	0.00	0.57	
v45	3.44 - 3.42	0.15	0.16	0.16	0.01	0.46	
v46	3.46 - 3.44	0.18	0.18	0.16	0.02	0.52	
v47	3.47 - 3.46	0.10	0.10	0.10	0.00	0.81	
v48	3.49 - 3.47	0.16	0.16	0.17	0.01	0.50	
v49	3.58 - 3.50	26.84	28.10	27.08	0.95	0.60	Lactose

v50	3.64 - 3.58	32.77	34.37	33.20	1.18	0.60	Lactose
v51	3.66 - 3.64	1.19	1.32	1.17	0.05	0.04	Lactose
v52	3.71 - 3.66	13.03	13.74	13.24	0.47	0.54	Lactose
v53	3.77 - 3.72	12.96	13.57	13.17	0.48	0.65	Lactose
v54	3.85 - 3.77	25.88	27.19	26.18	0.92	0.56	Lactose
v55	3.88 - 3.85	9.86	10.32	10.04	0.35	0.64	Lactose
v56	3.92 - 3.88	13.19	13.85	13.31	0.46	0.55	Lactose
v57	3.94 - 3.92	7.71	8.03	7.76	0.28	0.67	Lactose
v58	3.97 - 3.94	4.71	5.07	4.83	0.17	0.31	Lactose
v59	4.03 - 4.00	0.16	0.16	0.15	0.01	0.63	
v60	4.08 - 4.03	0.30	0.30	0.29	0.01	0.83	
v61	4.11 - 4.08	0.08	0.08	0.08	0.00	0.69	
v62	4.15 - 4.13	0.02	0.02	0.02	0.00	0.38	
v63	4.22 - 4.15	0.13	0.13	0.12	0.01	0.67	
v64	4.30 - 4.26	0.11	0.12	0.11	0.00	0.58	
v65	4.35 - 4.30	0.17	0.16	0.18	0.01	0.22	
v66	4.46 - 4.38	9.69	10.18	9.81	0.34	0.57	Lactose
v67	4.50 - 4.46	0.10	0.10	0.09	0.00	0.38	
v68	4.57 - 4.51	0.11	0.11	0.11	0.01	0.90	Galactose
v69	4.66 - 4.57	3.53	3.68	3.56	0.12	0.62	Lactose
v70	5.07 - 5.04	0.05	0.07	0.05	0.01	0.14	
v71	5.17 - 5.16	0.05	0.05	0.05	0.00	0.40	Mannose
v72	5.24 - 5.17	4.63	4.88	4.67	0.16	0.52	Lactose + Galactose
v73	5.35 - 5.31	0.03	0.03	0.03	0.00	0.37	
v74	5.42 - 5.35	0.08	0.08	0.07	0.01	0.50	
v75	5.46 - 5.42	0.02	0.02	0.02	0.00	0.46	Glucose-1-phosphate
v76	5.56 - 5.50	0.02	0.02	0.01	0.00	0.14	UDP-N-acetylglucosammine

v77	5.82 - 5.68	0.19	0.20	0.18	0.01	0.33	Cis-aconitate
v78	5.87 - 5.83	0.01	0.01	0.01	0.00	0.09	
v79	5.91 - 5.88	0.00	0.00	0.00	0.00	0.34	Uridine
v80	5.99 - 5.95	0.01	0.01	0.01	0.00	0.02	
v81	6.19 - 6.15	0.05	0.05	0.05	0.00	0.11	Orotate
v82	6.56 - 6.51	0.00	0.00	0.00	0.00	<0.001	Fumarate
v83	6.65 - 6.61	0.00	0.00	0.00	0.00	0.47	
v84	6.82 - 6.73	0.03	0.02	0.03	0.00	0.17	
v85	7.32 - 7.22	0.03	0.03	0.03	0.00	0.13	
v86	7.36 - 7.32	0.01	0.01	0.01	0.00	0.19	
v87	7.54 - 7.50	0.02	0.01	0.01	0.00	<0.001	Hippurate
v88	7.62 - 7.56	0.01	0.01	0.01	0.00	0.01	Hippurate
v89	7.83 - 7.73	0.32	0.29	0.32	0.02	0.43	
v90	7.88 - 7.83	0.02	0.02	0.01	0.00	<0.001	Hippurate
v91	7.96 - 7.93	0.01	0.01	0.01	0.00	0.92	
v92	8.14 - 8.02	0.05	0.05	0.05	0.00	0.89	Adenine

[1] Values are reported as relative abundance

[2] Identification of NMR signals was performed according to Klein et al., 2010; Sundekilde, Larsen, & Bertram, 2013, Tenori et al., 2018; Yanibada et al., 2018.

CHAPTER 7
Conclusions

With the increasing complexity of food chains and hidden food fraud, the authentication of agri-food products has become a crucial task in recent times. Increasing interest and awareness about food product quality in the general public has necessitated accurate and precise analytical methods in order to guarantee the quality of food. Thus, there is a requirement to introduce modern, affordable and rapid food control methods (when compared to traditional methods) to ensure product quality.

In this doctoral thesis, NIR and NMR spectroscopy are used across four studies in an effort to determine the viability of those techniques when it comes to food authentication. Specifically, in **Chapter 3** benchtop and portable NIR tools are used with chemometric techniques to determine the presence of pyrrolizidine alkaloids (PAs) and their N-oxides (PANOs) (which have been reported to cause toxicity in humans) in bee pollen. Here the need, as suggested from the EFSA, to develop new methods to detect PAs/PANOs in food. The combination of NIR with a statistical modelling approach have been demonstrated to have the potential to be applied for rapid and reliable identification of contaminated bee pollen in large-scale screening in the food supply chain by also using a portable-at-line operating system.

In **Chapter 4**, NIRS classification and modelling abilities were also tested on chicken breasts, which were classified according to their freshness. Preservation of quality during refrigerated storage represents one of the main challenges for the poultry industry especially if poultry meat's relatively short shelf life is considered. NIR spectroscopy coupled with a multivariate model provided deep insight into the physicochemical processes occurring during storage of fresh chicken meat cuts. Spectroscopy showed reliable effectiveness to recognise a 7-day shelf life threshold of breasts, suitable for routine at-line application for screening of meat quality. The bench-top instrument provided a wide range of spectral information suitable for the in-depth interpretation of biochemical and spoilage phenomena causing meat deterioration.

The inclusion of PAPs from insects in feed formulation for egg-producing poultry species could represent a premium value by declaring a highly-marketable labelling designation and a shift towards a more sustainable production system which includes the

utilisation of new feedstuffs with remarkable sustainability. Therefore, in **Chapter 5**, a study on table eggs from quails highlighted the feasibility of NIR spectroscopy combined with multivariate statistical models as rapid screening approach to differentiate eggs according to the inclusion of silkworm meal in quails' diet. The results demonstrated that a random forest (RF) spectral NIR variable selection improved the classification performance and provided reliable results for the insect-in-diet identification avoiding useless and interfering information. However, the similarities among the spectral patterns for the SWM-classes resulted in poor predictive performance for all the spectroscopic devices and ML models combinations. Therefore, the assessment of the prediction in external validation was performed also by a binary approach - SWM absence or presence. According to this, both NIR-benchtop and NIR-portable devices reported satisfactory classification performance, especially if combined with KNN and SVM models. Moreover, the main outcomes of this study revealed that the classification performances of NIR instruments varies according to the statistical model applied. Among the different tested techniques, SVM or KNN have shown the best predictive performances.

Based on the experimental findings of **Chapters 3, 4** & **5**, non-destructive NIR spectroscopy could represent an end-step valuable screening authentication approach providing a comprehensive overview of the analysed sample. In all NIR-related studies, the bench-top instrument provided satisfactory accuracy and it might be considered the more feasible NIR tool to achieve the purpose of the studies. Considering an operative scenario, the challenge of portable NIR instruments could be its suitability for rapid at-line screening along the supply chain in a real time scenario. In fact, despite worse optical properties and negative interference of the field, the advantages of portable NIR tools (simple hardware, low-power consumption, and small size) allow it to be an at/in-line flexible, efficient, fast, and reliable alternative to food matrices.

NIR cannot replace conventional techniques, but it can be combined with them to reduce the number of wet-chemistry analyses and improve the efficiency of the testing process. The speed of analysis and response of NIR technology suits the inspection of perishable products that have a short supply chain.

In **Chapter 6**, comparison of milk samples from different forage-based dairy chains was conducted. Forage type affects the environmental sustainability of a given dairy chain and has considerable impact on the quality of the milk and its suitability for specific cheese such as those having PDO trademark, often subjected to fraudulent actions. ^{1}H NMR combined with multivariate statistical analysis showed that only total replacement of maize

silage with dried forages (hays) in the cows' diet led to significant variations in ruminal and mammary metabolism with relevant changes in the milk fatty acids and NMR profiles. The milk metabolomic profile was not significantly modified when the ensiled whole-plant maize was only partially replaced by a mix of legume and grass silages. From a methodological point of view, a low-level FA and NMR data fusion coupled with a CDA chemometric approach was shown to enhance the predictive performance of the supervised CDA discriminant model for bulk milk samples from the different feeding systems. ^{1}H NMR was shown to be an a very responsive and high-performance technology effective in the assessment the existence of milk non-target metabolites quickly.

In summary, both NIR and NMR spectroscopic techniques have been shown to be accurate and effective analytical methods for inspection to control food authentication and/or safety on a real operative scenario based on rapid, eco-friendly and non-destructive assessment. Indeed, for the animal food supply chain one of the main challenges still remaining is the ability to implement simple but reliable routinary authentication methods while keeping the costs low and the performance level high, which is currently a gap in research that can be further explored and improved. A further goal is to have a better understanding of the interaction between infrared radiation and molecular functional groups of given food to improve the understanding of NIR spectra for the meaningful interpretation of spectra from molecules ranging from single compounds to polymers.